ATC
AUTOMOBILE TECHNOLOGY CENTER

帝京大学
自動車技術センター

年報

第2巻
2024年8月

Annual Report of Automobile Technology Center Teikyo University

Vol.2 Aug,2024

ATC
AUTOMOBILE TECHNOLOGY CENTER

帝京大学
自動車技術センター

年報

第2巻
2024年8月

Annual Report of Automobile Technology Center Teikyo University

Vol.2 Aug,2024

巻　頭　言

帝京大学自動車技術センター
センター長　加　藤　　彰

帝京大学自動車技術センターは2020年4月に発足し、今年で5年目を迎えました。新型コロナの感染拡大も昨年5月に「5類」に移行したことに伴い、ほぼコロナ前の日常に戻ったと感じていますが、まだまだ感染は継続しているようです。

コロナの感染によって世界が一変したのと時を同じく、自動車産業も「100年に一度の大変革期」を迎えています。100年に一度といっても米国にてT型フォードが1908年に大量生産されてから約 100 年ですから、自動車産業にとっては初めての大変革といっても過言ではありません。いままで自動車は1970年に米国の大気汚染を抑制するための排出ガス規制基準を定めたマスキー法への対応や、1970～1980年代の石油危機によるエネルギー価格の高騰に対応した省エネルギー化を目指した燃費規制など、幾度も大きな変革を乗り越えてきました。上記の変革に対して排ガス規制にはCVCC（ホンダ）、燃費規制にはハイブリッド車（トヨタ）などの新技術を生み出して世界の自動車技術を大きくリードしてきました。

さて、昨今の自動車業界を見渡すと EV が世界の環境車としての地位を確立し、米国で2003年に創業した投資家イーロン・マスク氏がCEOのテスラ社や中国のバッテリー製造メーカーだったBYD社など、今まで自動車を製造していなかった新興自動車メーカーが世界市場にて大きな存在感を示しているのは皆さんもご存じの通りです。

しかしながら今年に入ってテスラ社が 2 期連続減益との報道や、日本国内においては上半期のEV車の販売台数が38.8%減と大きく低下しており、EV車の販売もこれまでの予測とは異なる可能性も考えられます。これまで世界の自動車市場にエンジンの燃焼技術やハイブリッドなどの革新的技術で世界をリードしてきた日本の自動車メーカーですが、EV技術のみならず製造技術や、昨今のSDVと呼ばれる次世代車の分野においても後塵を拝しているのではないかと心配されています。日本の基幹産業である国内自動車各社の世界市場での地位の変化が無いことを心から祈っています。

最後になりますが、帝京大学自動車技術センターの2023年ですが、昨年度に引き続き栃木県産業労働観光部工業振興課から中小企業支援のための EV 車の分解委託事業を行いました。本事業は社会的な関心が非常に高く、NHKからの取材を受けてEV車の解体の難しさが「解体キングダム」で2024年1月に本センターのスタッフが出演し全国放映されました。変化の大きい自動車業界ですが、所属教員による自動車における研究活動のみならず、センターの使命である社会貢献や情報発信を目指して、センターの特定整備の認証を有する優れた設備と、高い技術力を持ったスタッフで皆様の自動車に関するニーズ・課題に対応してまいりますので、いつでもお声がけいただきたく何卒よろしくお願いします。

帝京大学自動車技術センター年報

目　　次

第一部

活　動　報　告

2023年度講演会 開催報告書

報告書作成日 2023年6月9日

帝京大学自動車技術センター　簾内 将景

＜趣旨＞

自動車技術センターの活動目的である人材育成、情報発信の一貫として、2023年度講演会「2050年カーボンニュートラルに向けた Honda の取り組みと未来づくり」を本学の教職員と学生をはじめ、栃木県内企業の技術者に向けて開催した。

様々な場面で話題となる「カーボンニュートラル（CN）」について、株式会社本田技術研究所執行役員の武石様をお招きし、宇都宮キャンパス内自動車技術センターの講義室にて対面で実施した。

＜開催日＞

2023年 6月 1日 木曜日　16:40~18:10

＜コンテンツ＞

・講師　株式会社本田技術研究所 執行役員 先進パワーユニット・エネルギー研究所　　武石 伊久雄 様

・講演タイトル　「2050年カーボンニュートラルに向けたHondaの取り組みと未来づくり」

・講演概要

Hondaの原点は、「世のため人のために、自分達が何かできることはないか」という思いです。Hondaはこれまでも、低公害エンジンの開発や、F1レースでのチャンピオン獲得など、数々のチャレンジをしてきましたが、今「全製品、企業活動を通じたカーボンニュートラル」という最大の難問に挑んでいます。またその先には、もっとワクワクする世界が待っていると信じて、「未来づくり」にもチャレンジしています。今回の講演では、こうしたHondaの取り組みについてご紹介いたします。

＜イベントの様子＞

当日参加者数　計80名　内訳（本学学生・教職員 58名、一般・企業 22名）

今回の講演会は、機械・精密システム工学科2年生「機械セミナー」と同3年生「機械工学特別講義」を併催したが、他学科や講義受講者以外の学生の参加も見られ、予定を上回る人数での開催となった。一般申し込み者は企業技術者が多く、CNに対する関心の高さが伺えた。

講演では、一部の解説で動画が使用されており、Hondaが取り組む新たなチャレンジについて理解しやすく、夢がありワクワクする内容であり、講演内容を必死にメモを取る学生や、質疑応答において学生が質問し、武石様と意見交換をしている姿が印象的であった。

また、終了時に実施した参加者アンケートでは、Hondaの新たなチャレンジに対する感想や、「CNは他人事ではないことが分かった」「高度な技術や研究の話を聞けた貴重な講義だった」「CNに向けた企業努力の一端を見られて参考になった」などのコメントが寄せられ、本セミナーの満足度調査では、参加者の87%から満足との評価をいただくなど、高評価をいただいた。

今後も学生や企業人のニーズに合った情報発信を行っていきたい。

以上

ギャラリー

↑講演会の様子①

↑講演会の様子②

教室の前から後ろまでほぼ満席であった。

↑講演会の様子③

↑記念品贈呈

宇都宮大学コラボレーション・フェア参加報告書

報告書作成日 2023 年 10 月 10 日

帝京大学自動車技術センター　簾内 将景

帝京大学自動車技術センターは宇都宮大学主催「第 4 回宇都宮大学コラボレーション・フェア」のポスター・セッションに参加した。

＜イベント趣旨＞

宇都宮大学は、企業や自治体など各団体のシーズ(研究成果、技術等)と、ニーズ(社会・企業課題等)の出会いを加速し、産学官金連携の場としてコラボレーション・フェアを開催している。

帝京大学自動車技術センターが参加したポスター・セッションでは、産学官金それぞれの立場から、各企業・団体の紹介のほか、シーズ・ニーズ、連携の取組事例など、多様な情報を共有し、新たな出会いと交流の場として位置づけられている。本イベントへの参加を通して、ATC の活動の県内産学官金への情報発信と、ATC 所属教員研究への新たなコラボレーション先発見を目的とした。

＜開催日、場所＞

2023 年 9 月 22 日 金曜日　13:00~17:00　マロニエプラザ大展示場（栃木県宇都宮市）

＜コンテンツ＞

今回のフェアは 2 部構成であり、帝京大学自動車技術センターは第 II 部に参加した。

・第 I 部　講演会＆パネルディスカッション
　急速にデジタル化が進む中で、データ駆動型社会の実現に向けて、新たな産学官金連携の在り方について考える。

・第 II 部　ポスター・セッション
　産学官金のそれぞれの立場から、各団体の紹介のほか、シーズやニーズ、連携の取組等の情報を共有し、新たな連携の契機とする。

＜イベントの様子＞

ポスター・セッションには展示参加 283 件、一般参加者 595 名が参加し、各ブースでポスターによる説明や、質疑応答が行われた。企業自治体の参加件数も多く、終始活発なコミュニケーションがとられていた。帝京大学自動車技術センターもセンターの紹介を主として、パンフレットを渡しながらコミュニケーションを図り、大変有意義な時間であった。

＜まとめ＞

今回のコラボレーション・フェアでの新たなコラボレーション発見には至らなかったが、センターの活動や施設設備に関心を示す来場者とコミュニケーションを取ることができた。このような情報発信の機会も利用しつつ、今後の活動推進に役立てていきたい。

以上

ギャラリー


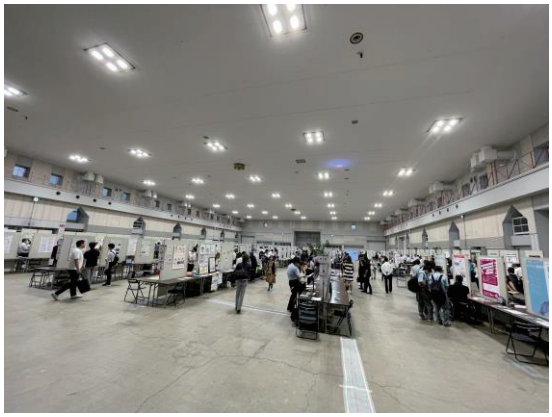

会場の様子

帝京大学自動車技術センターのポスター・セッションの様子

自動車技術センターツアー 2023 開催報告書

報告書作成日 2023 年 11 月 16 日
帝京大学自動車技術センター　簾内 将景

＜趣旨＞

宇都宮キャンパス学園祭「帝祭」のイベントとして、本学学生や地域の一般来場者を対象に、車を通して交流し親睦を深める場として開催した。

自動車技術センター保有の施設設備を見学できる場とすることで、センターを多くの人に知っていただける内容とするとともに、学園祭を盛り上げる一助となることを目的とする。

＜開催日＞

2023 年 11 月 4 日 土曜日　13:00~16:00

＜コンテンツ＞

施設設備の展示

・4 輪アライメントテスター、シャシダイナモメーター、エンジンベンチなど

車両の展示（以下展示車両一覧）

・1993 年式日産スカイライン GT-R（R32 型）
・1998 年式 BMW　R100GS
・2007 年式スバル レガシィツーリングワゴン（BP9 型）
・2002 年式日産フェアレディ Z（Z32 型）※実習車両
・2023 年式日産サクラ（分解後の状態）

＜イベントの様子＞

来場者数　計 89 名（一般来場者と本学学生）

多くの方にご来場いただき、各々が気になる設備や車両の見学をしていた。中には車両の持ち主と談話する様子も見られた。学生からの関心も高く、出展者と共にボンネットを開けて車両の構造や機能について説明を受けている場面も見られた。自動車技術センターに初めて訪れた方は、充実した設備に驚いていた。

＜まとめ＞

昨年実施した帝京モーターショーの好評を受け、車両の展示は引き継ぎつつ、多くの方に自動車技術センターを知っていただくため、代表的な施設設備の紹介や EV 分解活動の紹介を実施し、こちらも関心が高いことが分かった。

来年以降も開催し、学園祭の盛り上げや宇都宮キャンパスのアピールに寄与できるようなイベントにしていきたいと思う。

以上

ギャラリー

車両展示の様子

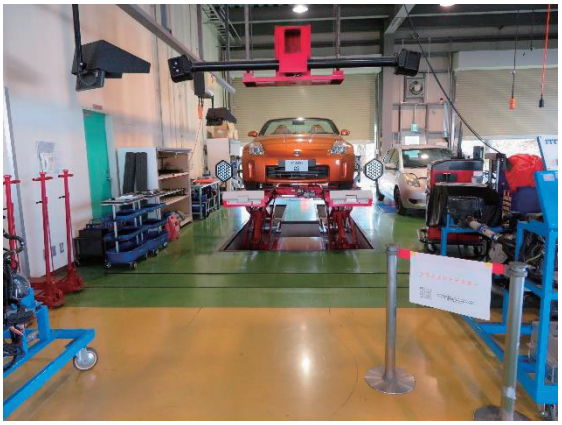

アライメントテスターの展示

シャシダイナモメーターの展示

ATC の取り組み紹介（EV 分解）

令和５（2023）年度次世代自動車研究開発ワークショップ事業
栃木県主催「日産サクラ事前見学会」開催報告書

報告書作成日 2023 年 11 月 7 日

帝京大学自動車技術センター　簾内 将景

＜趣旨＞

栃木県は県内自動車部品サプライヤーの電動化等の対応に向けた開発力と提案力の向上を支援するため、次世代自動車研究開発ワークショップ事業を展開している。この事業は今年度で 2 年目であり、今回は「日産サクラ」の実車を分解・解析する。

帝京大学自動車技術センターは、本事業における車両分解の委託を受け作業を進めており、この度の事前見学会では、参加者が分解の途中経過を見学できるよう部品の展示を行うとともに、質疑への対応も行った。

＜開催日＞

2023 年 10 月 31 日 火曜日　14:00~16:00

＜開催場所＞

帝京大学自動車技術センター　1F 実習場

＜コンテンツ＞

・開会の挨拶

・分解過程解説（PU 降ろし編）　解説担当 帝京大学自動車技術センター　小柳出敏弘

・自由見学　質疑対応担当 小柳出敏弘、白沢洋一

＜イベントの様子＞

参加者数　計 68 名　参加企業数 27 社

分解過程解説（PU 降ろし編）では、スクリーンを使用して実際に部品の取り外しを行う動画を上映した。また、動画に合わせて小柳出助手が口頭で解説を行い、参加者も熱心に聞いていた。自由見学では、取り外された部品や日産サクラの実車に触れながら、材質や構造を熱心に確認する参加者が多く、昨年以上の関心の高さを感じた。小柳出、白沢両名は参加者からの質疑に丁寧に対応していた。

＜まとめ＞

今年度から新たに途中経過を見学する場を設けたことで、部品の組み付き方を把握することができ、日産サクラに対してより理解を深めていただく機会となったと考える。

自動車技術センターとしては 11 月 21 日に開催される分解過程解説・部品見学会において、分解過程解説と部品の展示作業を行うため、更なる貢献ができるよう準備を行いたい。

以上

ギャラリー

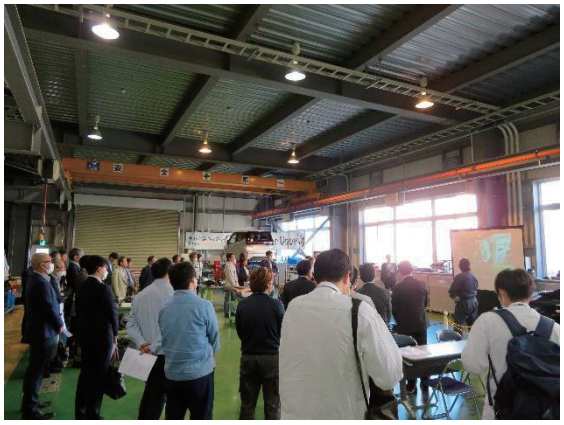

分解説明の様子

説明をする小柳出助手

部品見学会の様子

令和５（2023）年度次世代自動車研究開発ワークショップ事業
栃木県主催「日産サクラ分解過程解説・部品見学会」開催報告書

報告書作成日 2023 年 11 月 28 日
帝京大学自動車技術センター　簾内 将景

＜趣旨＞

栃木県は県内自動車部品サプライヤーの電動化等の対応に向けた開発力と提案力の向上を支援するため、次世代自動車研究開発ワークショップ事業を展開している。この事業は今年度で 2 年目であり、今回は「日産サクラ」の実車を分解・解析する。

自動車技術センターは、本事業における車両分解の委託を受け作業を行い、この度の分解過程解説・部品見学会では、分解を担当した自動車技術センター小柳出助手と白沢助手がセンター2F 教室にて解説講演を行った。また、講演後の見学会のために部品の配列を行うとともに、質疑への対応も行った。

＜開催日＞

2023 年 11 月 21 日 火曜日　13:30~16:00

＜開催場所＞

帝京大学自動車技術センター　2F 教室(分解過程解説)、1F 実習場(部品見学会)

＜コンテンツ＞

・開会あいさつ
・解析ワークショップについて
　栃木県産業振興センター担当者
・日産サクラ分解過程解説
　帝京大学自動車技術センター　小柳出敏弘、白沢洋一
・部品見学会

＜イベントの様子＞

参加者数　計 85 名　参加企業数 35 社

分解過程解説では、昨年度に分解をした「Honda e」と「日産サクラ」を比較しながら、EV の特徴的な部品や機能等について、スクリーンを使用して解説した。EV への理解を深めるとともに、メーカーによる違いや、EV の技術的な進歩について小柳出、白沢両名が解説を行った。参加者からは分かりやすかったとのお声をいただくなど、大変有意義な時間となった。見学会では、10/30 に開催した事前見学会時より部品点数が増えたこともあり、より多くの参加者からの質疑が寄せられ、小柳出、白沢両名は常に対応する形となった。参加者は部品の撮影や、手に取って確認をするなど、大盛況であった。

＜まとめ＞

本事業が 2 年目ということもあり、参加者の EV に対する知識の向上がうかがえた。また、昨年度と比較することでメーカーの違いによる設計思想の違いを知ることができた点は、自動車技術センターとしても大きな収穫となったと考える。ここで得たことを、今後の講義や自動車技術センターとしての地域貢献、情報発信活動に活かしていきたい。

以上

ギャラリー

分解過程解説会

解説をする小柳出助手

解説をする白沢助手

部品見学会の様子

部品見学にて解説をする小柳出助手

部品見学にて解説をする白沢助手

モビリティリゾートもてぎ安全運転講習会開催報告書

報告書作成日 2023 年 12 月 15 日
帝京大学自動車技術センター　簾内 将景

＜趣旨＞

モビリティリゾートもてぎ内、交通教育センターもてぎにおいて、急ブレーキやスピン等、一般道路では起きてはいけない体験をもとに、実路での安全運転を目指す。

また、ホンダコレクションホール見学を通してモビリティの歴史と将来について考える場とする。

＜開催日＞

2023 年 12 月 2 日 土曜日　10:00~15:00

＜コンテンツ＞

・モビリティリゾートもてぎ交通教育センター

1.スキットリカバリー

車がスピン状態になることを回避するトレーニング

2.スリパリーコーナリング

雪道を想定したコースを走行し、適切なペダルワーク、ステアワークを身に付けます

・ホンダコレクションホールの見学

＜費用＞

講習費（8000 円）は個人負担とし、バス代金のみ学校負担

＜イベントの様子＞

当日参加者数　計 8 名　学生 7 名（機械科 7 名）　引率 1 名

申込学生数は 8 名であったが、1 名は当日欠席であった。

安全運転講習会では、学生は 2 人一組に分かれて乗車し、インストラクターの指導の下、トレーニングメニューをこなしていた。途中インストラクターからの質問に答える学生の姿もあり、安全運転の意識向上だけでなく、車両運動性能に対しても理解を深めた。

ホンダコレクションホール見学では、自由見学の時間とし、学生は各々の興味の引かれた展示車両について、談話や記念撮影を行っていた。国内レース車両や F1 車両も展示されており、形状の意味や部品の働きについて話し合う学生の姿もあった。

＜まとめ＞

今回の参加学生は全員が機械・精密システム工学科自動車工学コース選択者であり、インストラクターとの対話において、講義の内容が生かされていることを実感した。PC 上でシミュレーションを行った事象を実体験することができ、とても充実した講習であったとの声も聞こえた。

今後も実施していくとともに、機械科以外の参加者も募るべく工夫をしたい。

以上

ギャラリー


インストラクターによる説明と、デモンストレーションの様子


トレーニング（実車走行）の様子

ホンダコレクションホール見学の様子

NHK 解体キングダム取材に関する報告書

報告書作成日 2024 年 1 月 19 日

帝京大学自動車技術センター　簾内 将景

＜番組趣旨と受託の経緯＞

解体キングダムは、ふだん見ることのできない解体現場に潜入し、知られざる日本の超絶技術を紹介する、NHK 総合で放送されているテレビ番組である。今回は、「自動車解体ニッポンの技ここにあり」の題目の元、ガソリン自動車の解体についてと、電気自動車解体の課題について放送された。自動車技術センターでは、栃木県からの委託を受け EV 分解を行っていることから、栃木県工業振興課を通して、取材撮影依頼を受けた。

＜取材日＞

2023 年 12 月 17 日 日曜日　10:00~13:00　撮影下見日

2023 年 12 月 18 日 月曜日　9:00~17:00　撮影日

＜出演番組＞

解体キングダム　自動車解体 ニッポンの技ここにあり

「百年に一度の大変革期」にある自動車業界。ガソリン車から電気自動車へ大きなシフトが予測される今、自動車解体の最前線を魔裟斗と千賀健永が取材する！日本最大級の自動車解体工場では、ガソリン車解体リサイクル率 99%を成し遂げる、日本の技に出会う。さらに電気自動車解体に立ちはだかる難関を研究機関に取材。このままでは持続可能ではなくなるという世界的課題とは！？

＜放映日＞

2024 年 1 月 10 日 月曜日　19:57~20:42　NHK 総合

＜取材の様子＞

自動車技術センターで所有している、日産リーフの実車やパワーユニット、及び栃木県からの EV 分解事業で分解した日産サクラのバッテリー等を使用した。主に、番組キャストの Kis-My-Ft2 千賀健永さんに対して、小柳出助手が解説をする形で撮影が進められた。解説では、EV の仕組みやバッテリーに使用されるコバルト等の希少金属のリサイクルに関する課題にもふれた。また、撮影の助手として技術職員簾内も参加した。

＜まとめ＞

この度の撮影は、EV の問題点に関する視点について考えるきっかけとなり、大変貴重な経験であった。放送終了後には全国からの多くの問い合わせが来るなど、新たな交流が生まれた。また、この度の放送において、解体キングダム番組最高視聴率を記録したと担当者から報告があり、全国的に関心の高い内容であったことが分かった。

今後も取材等に可能な限り応じることで当センター活動を発信する機会を大切にしつつ、センター主催のイベントによる情報発信、社会貢献をより活発化したいと考える。

以上

ギャラリー

第二部

研 究 ノ ー ト

研 究 ノ ー ト

井上秀明

白線追従機能を有する電動車椅子による歩行支援効果

Effectiveness of Walking Assistance by Electric Wheelchair
with White Line Tracking Function

○井上秀明（帝京大），高橋直也（帝京大）

Tsutomu Ozaki（帝京大），曾梓傑（帝京大）

Hideaki INOUE, Teikyo University, 1-1 Toyosatodai, Utsunomiya-shi, Tochigi
Naoya TAKAHASHI, Teikyo University, 1-1 Toyosatodai, Utsunomiya-shi, Tochigi
Tsutomu OZAKI, Teikyo University, 1-1 Toyosatodai, Utsunomiya-shi, Tochigi
Shiketsu SOU, Teikyo University, 1-1 Toyosatodai, Utsunomiya-shi, Tochigi

Key Words : Wheelchair, White line tracking, Walking assist, Stumbling, Elderly people

１．緒　言

高齢者の歩行支援を目的に，歩行車やシルバーカーにセンサやアクチュエータを付加して自動運転技術による支援効果の拡大を目指す研究が進んでいる(1)～(3)が，その自動化率（機械に任せる割合）は低いのが現状である．自動化率を高めると操作によらず歩行支援が行われるため、高齢者の多様な歩行ニーズに応えることができる一方、装置の不具合による万が一の状況に備える安全技術の確立が必要となる．

自動化率を高めるための安全性確保を装置のみに負わせるのは多くのセンサを必要とするなどコスト面で問題が多いため，使用環境を整備することで装置の負担を減らす方が合理的である．本研究では，床面や歩道面に専用の白線を引き，これを跨ぐように自動で動く装置を試作して，その装置の自動走行機能と，高齢者への歩行支援効果を検証した．なお、歩行支援効果としては，通常歩行の支援効果と，躓き後の転倒抑止効果について検証した．

２．歩行支援装置

２．１ 装置構成概要と白線追従性能

本研究で開発した歩行支援装置は，市販の電動車椅子（Whill 社製 Model CR）をベースに，WEB カメラ，LiDAR 等の各センサ，およびノート PC を搭載したものである（図１）．各センサからの情報を基にノート PC 内のプログラムにて電動車椅子の後２輪のモーターを独立に駆動することで電動車椅子の動き（速度とヨーレイト）を制御する．

Fig.1.　Configuration of walking assist device

図２に白線追従結果の一例を示す．白線が角形状の部分においても旋回を先行させながら滑らかに追従できている．

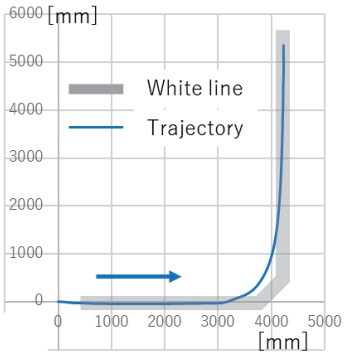

Fig.2.　Example of white line following experiment results

２．２ 安全対策

本装置は人による入力が無くても白線に沿って動き続ける機能を有しており自動化率が高い．そのためとっさの場合に正しい判断と行動を期待できない高齢者を意識した十分な安全対策が必要となる．

２．２．１ 立ち止まり検出と自動停止

本装置には追加で手元レバーを設け，操作者が止まりたいと思えばこれを引けば装置は停止するようにした．しかしながら，この手元レバーを上手く操作できないときは，装置は動き続けてしまう．そこで，装置と操作者との距離を計測し，通常使用の場合より距離が長い場合は，操作者が立ち止まったと判断して自動停止することとした．

２．２．２ 障害物検出と自動停止

前方に障害物があれば手元の操作レバーで止まることが基本であるが，これを上手く操作できない場合は LiDAR が障害物を検出し自動停止するようにした．

３．歩行実験

３．１ 実験参加者

実験参加者は高齢者施設に居住する高齢者６名（男３名，女３名，86～95 歳）と若年者６名（男６名，21～24 歳）である．実験は大学の倫理委員会の承認を得た内容で，実験参加者には事前に実験内容を説明し，同意を得た上で実験を行った．

３．２ 実験方法

高齢者施設または大学校舎内の廊下で，直線約 10m を普通の速さで歩くように指示した．以下これを自由歩行と称する．これを合計 4 回行った．同じ要領で，一定速度で動く電動車椅子につかまって歩くように指示した．以下これを支援歩行と称する．本研究においてはインソール型の足底力計を用いて上下床反力を計測し，計測結果と歩行距離から歩幅，歩調，歩行速度等の歩容データを算出した．

また，若年者には高齢者疑似体験キットを装着させて，後述する疑似的な「躓き実験」を行い，歩行支援装置の「躓き」後の転倒抑止効果について評価した．

なお，安全のため，電動車椅子を動かす全ての実験では，各人の自由歩行での速度に制御するよう電動車椅子の速度を設定した上で，白線への自動追従ではなく，別の操縦者が電動車椅子に乗って操縦した．

３．２ 実験結果

３．２．１ 歩行負荷と安定性

高齢者の歩容が，従来研究が示している特徴[(5)]を捉えていることを確認した．その上で，自由歩行と支援歩行の床反力の一歩毎のピーク荷重を読み取り比較した．高齢者１名の結果を例として図３に示す．明らかに歩行支援によって荷重が減少していることが分かる．その平均値と標準偏差を算出したところ，それぞれが６名中５名で有意に減少していた．即ち，歩行支援装置につかまって歩くと脚への負荷が下がると共に，変動が小さく安定して歩けるようになっていた．

３．２．２ 転倒抑止

前述の高齢者による支援歩行の実験中に，偶然軽く躓くことがあり，その足底力データを記録することができた．特徴が分かるようにピーク値をプロットしたのが図４(a)である（4 秒付近で躓きが発生した）．これより，躓きは本来発生すべき床反力が十分に発生しないことをきっかけとして生じる一連の現象とも言える．これを参考に，疑似的に躓きを再現することを試みた．自由歩行中に，ある地点に差し掛かったら意識的に一方の足（遊脚）を前に出さずに他方の足（接地足）に揃えるよう，また，その後は転倒しないよう十分な余裕をもっていずれかの足を前に出すよう指示した．実験参加者は高齢者疑似体験キット[(4)]を装着した若年者（6 名)とし，歩行支援装置有無で比較した．

結果の一例を図４(b),(c)に示す．歩行支援装置につかまって歩いている方が躓き前後の荷重変動が小さい．これは躓きによる前後の動的荷重変動を歩行支援装置が受け止めるからである．この傾向は実験を実施した6名全員に見られた．このことから歩行支援装置は躓きによる転倒抑止に効果があることが示唆された．

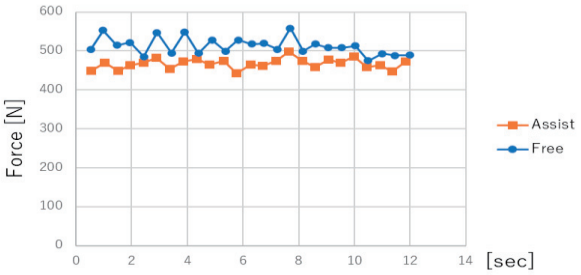

Fig. 3.　Comparison of peak floor reaction force

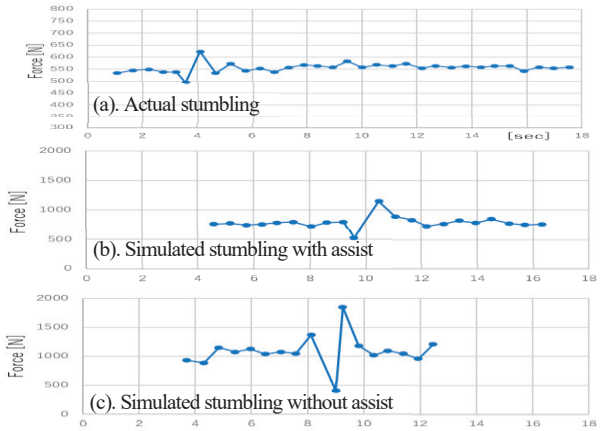

Fig. 4.　Peak floor reaction force during stumbling

６．結　言

自動停止機能などの安全機能を付加することで，高い自動化率と安全性を両立する高齢者向けの歩行支援装置を開発した．

本歩行支援装置につかまって歩くと，歩行負荷が低減し，安定性が増すことを確認した．また，躓き後の転倒抑止効果の可能性を検証した．

今後は装置改良とより多くの高齢者での検証を行う．

最後に，実験に協力いただいたケアハウスジョイナス長岡の入居者と職員の皆様に心より感謝致します．

参考文献

(1) 宮脇和人・ほか６名，電動歩行機を用いた高齢者歩行の評価，日本機械学会論文集(C 編), 64-640 (1999)，pp. 171-178.
(2) 高野倉雅人・ほか３名，ロボット技術搭載歩行車による歩行アシスト効果,日本経営工学会論文誌, 67-3 (2016), pp.261-271.
(3) 新田収，起立・歩行をアシストし要介護者を自立へ導くインテリジェントシュルバーカー，バイオメカニクス学会誌, 39-3 (2015), pp.135-141.
(4) 小林陽子・ほか３名，高齢者疑似体験装具装着による歩行への影響，Yamanashi Nursing Journal, 1-1 (2002) pp.33-36.
(5) 伊藤将円・ほか２名，高齢者における歩行器・歩行車を使用した際の歩行分析，理学療法学，47-5 (2020), pp.450-458.

日本福祉工学会 第 27 回学術講演会において発表
日本福祉工学会の承認を得て掲載

研 究 ノ ー ト

加藤　彰

講演番号	285

文献番号	20235285

Study of Actual Road Power Consumption Improvement Method for Electric Vehicle using Traffic Flow Simulation

Michael Melkior Kanugroho[1)] Yuta Nakane[2)] Taizo Otsuki[2)] Akira Kato[2)]

1) Teikyo University, Graduate School of Science and Engineering, Division of Integrated Science and Engineering
Toyosatodai 1-1, Utsunomiya City, Tochigi Prefecture 320-8551, Japan
2) Teikyo University, Department of Mechanical Precision Systems Engineering, Faculty of Science and Engineering
Toyosatodai 1-1, Utsunomiya City, Tochigi Prefecture 320-8551, Japan

ABSTRACT: CO_2 and exhaust emissions regulations are becoming stricter year by year. Passenger cars are shifting from ICE Vehicles to BEV (Battery-Electric Vehicles). Concerning the range of BEV that will not have enough battery charge to reach their destination, the purpose of this study is to make a propose for an improved method of energy efficiency of a BEV using traffic flow simulation (SUMO). The vehicle numerical model was created using Matlab based on the vehicle used in test cycles and real driving tests. The vehicle numerical model will be connected with SUMO and the eco-driving of BEV will be presented as an energy efficiency improvement method.

KEY WORDS: **EV and HV Systems, Electric Mileage,** Energy Consumption, Real Driving Emission, WLTC, Numerical Modeling, Traffic Flow Simulation (A3)

1. INTRODUCTION

Nowadays, the world has to deal with three matters such as air pollution, global warming, and the energy crisis(1). Concerning global warming, to reduce the harmful effect of climate change, COP26 (2021)(2) agreed to maintain the Earth's temperature rise below 1.5°C, and to achieve it, the realization of Carbon Neutral in 2050 is necessary, and one of the ways is the CO_2 reduction in the transportation sector such as automobiles(3). Passenger cars are shifting from ICE vehicles to BEV (Battery-Electric Vehicles), intending to become carbon-neutral by 2050.

In a previous study, we proposed a fuel efficiency improvement method for gasoline vehicles(4) and HEV (Hybrid Electric Vehicles)(5) on real roads using vehicle numerical modeling and traffic flow simulations (SUMO, Simulation of Urban Mobility)(6).

In this study, concerning the range of the BEV that will not have enough battery charge to reach their destination, the purpose of this study is to make a propose for an improved method of energy efficiency of a BEV using SUMO. The vehicle numerical model was created using Matlab based on the vehicle used in test cycles and real driving tests. The vehicle numerical model will be connected with SUMO and the eco-driving of BEV will be presented as an energy efficiency improvement method.

2. EXPERIMENT AND SIMULATION METHOD

2.1. Test Cycles and Real Driving Test

BEV as the specifications in Table 1 is chosen to use in the experiment. The chosen test vehicle (Nissan LEAF ZE1) has sold approximately 167,000 units in Japan since December 2010 and is representative of domestic BEVs.

The test cycles used in experiment on the chassis dynamometer are steady speed tests (40, 60, 80, 100, and 120 km/h) and WLTC (Urban, Rural, and Highway). WLTC cycle starts with the SOC (State of Charge) of the HV (High Voltage) battery being 80%. Experiment on the chassis dynamometer was conducted at room temperatures of 5°C, 20°C, and 35°C with the AC (Air Conditioner) system is ON (set to 25°C) and OFF at each room temperature. In the chassis dynamometer experiment, the running resistance value is set based on EPA (Environmental Protection Agency) data of the used test vehicle. The test vehicle's weight is 1530 kg and 110 kg (weight assuming two passengers) was added in order to match the weight of the test vehicle in a real driving test.

The real driving tests were conducted on three different driving roads such as urban, rural, and highway around Utsunomiya City (shown in Fig. 1) with two different drivers (Driver A and B). The real driving test was conducted in summer, autumn, and winter. In the summer and winter, the AC system is used and the target temperature is 25°C, the vehicle will adjust the temperature inside the cabin automatically. In autumn, the AC system is not used. The real driving test starts with the SOC of the HV battery being 80%.

For the steady speed, WLTC, and real driving test, the external diagnosis tool (HDM9000 made by Hitachi Astemo) is used for the real-time measurement method, it is connected to the OBD port of the test vehicle. We calculate the energy consumption

of the BEV by using the HV battery electric power divided by the travel distances of the vehicle[7].

Table 1 Vehicle specifications

Vehicle	Nissan LEAF (ZE1)
Motor Type	AC Synchronous Permanent Magnet Motor
Motor Model Code	EM57
Maximum Motor Speed (RPM)	9795
Drive Wheels	Front Wheel Drive
Torque (Nm)	320
Power (PS)	150
DriveTrain	2WD
Battery Type	Lithium-ion Battery
Battery Cells	98
Battery Capacity (kWh)	40
Battery Voltage (V)	350
WLTC Energy Consumption (Wh/km)	155
JC08 Energy Consumption (Wh/km)	120
Weight (kg)	1530
Full length (mm)	4,480
Full width (mm)	1,790
Overall height (mm)	1,540
Wheelbase (mm)	2,700
Number of passengers	5

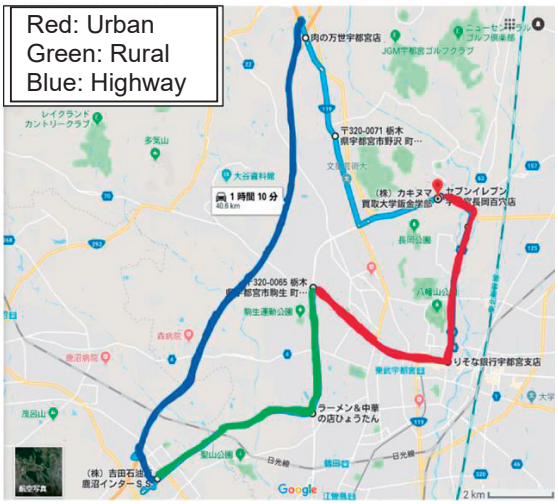

Fig. 1 Real Driving Road Test in Utsunomiya City

2.2. Vehicle Numerical Modeling

A vehicle numerical modeling is constructed using Matlab, which can perform vehicle modeling, simulation, and analysis in a multi-domain environment[8]. The constructed vehicle model using the Powertrain Blockset from Matlab as we can see in Fig. 2, is a model of the automobile powertrain system. BEV model is selected as a reference model for the test vehicle model. BEV model parameters are adjusted based on the test vehicle used in the experiment (shown in Table 2). Therefore, the aim of energy consumption differences between experiment and simulation is below 5%. We set a 5% target value because of the chassis dynamo test accuracy.

The experiment energy consumption results which are used to compare the simulation results are the steady speed test, WLTC during the temperature of 20°C, and the real driving test conducted in autumn with two different drivers. Regarding the vehicle weight for the simulation parameter of the BEV, in the steady speed test and WLTC, the vehicle weight was set to 1640 kg, and in the real driving test, the vehicle weight of Driver A was set to 1710 kg and Driver B set to 1699 kg to match the driver and passenger weight.

Table 3 is a calibrated motor efficiency map. By using the steady speed test motor torque and motor speed data, we calibrated the motor efficiency map in the simulation. The colored columns in Table 3 are the calibrated motor efficiency in percentage. Because we only use the steady speed test to calibrate the motor efficiency map, we can't calibrate all the columns.

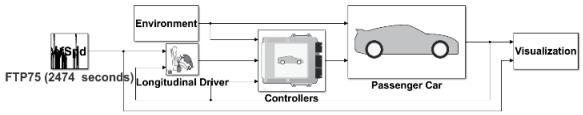

Fig. 2 Powertrain Blockset

Table 2 Adjustment of BEV model parameters

	Parameter		Default	Adjustment	Information
Longitudinal Driver	Control Type		Predictive	Scheduled PI	Adjust the dynamic response of the driver
Passenger Car	Motor	Torque (Nm)	254	320	Adjustments to match the specification of Test Vehicle (ZE1)
		Power (W)	80000	110000	
	Battery	Maximum Capacity (Ah)	66.7	114.29	
		Initial Capacity (Ah)	66.7	80	
	Wheels & Brakes	Disc Type	Front&Rear: Disc	Front&Rear: Disc	
		Wheel Diameter (mm)	530	631.9	
		Running Resistance	Pressure & Velocity	Rolling Resistance + Air Resistance	
	Vehicle	Gear Reduction Ratio	7.9:1	8.520:1	
		Mass (kg)	1200	1640	Adjustment for Steady Vehicle Speed Test and WLTC Cycles
				1710 (Driver A) 1699 (Driver B)	Adjustment for RDE Test
		Frontal Area (m^2)	2.53	2.585	Adjustments to match the experiment condition
		Air Temperature (K)	298	293.15	

Table 3 Motor efficiency map

		Motor Torque (Nm)														
		0	10	15	20	50	100	120	140	160	180	200	220	240	260	320
Motor Speed (RPM)	0	71.8	71.8	71.8	78.4	85	85	85	85	85	85	85	85	85	85	85
	1000	71.8	71.8	71.8	78.4	85	85	85	85	85	85	85	85	85	85	85
	2000	71.8	71.8	71.8	79.7	87.5	87.5	87.5	87.5	87.5	87.5	87.5	87.5	87.5	86.5	86.5
	3000	71.8	71.8	71.8	80.9	90	90	90	90	90	90	90	90	88	88	88
	4000	77.2	77.2	80.9	84.6	92	92	92	92	92	92	92	92	90	90	90
	4500	82.8	82.8	82.8	82.8	87.9	93	93	93	93	92	92	92	90	90	90
	5000	82.8	82.8	82.8	82.8	87.9	94	94	94	94	94	94	94	94	94	94
	6000	85	89.2	89.2	89.2	91.6	94	95	95	95	95	95	95	95	95	95
	7000	85	89.2	90.1	90.9	92.7	93.9	95	95	95	95	95	95	95	95	95
	8000	85	88.8	90.8	92.7	92.7	93.9	95	95	95	95	95	95	95	95	95
	9000	85	88.5	90.2	91.9	91.9	93.5	95	95	95	95	95	95	95	95	95
	9500	85	85	87.5	90	92	93	93	93	93	93	93	93	93	93	93

2.3. Traffic Flow Simulation (SUMO)

SUMO is an open-source, microscopic multimodal traffic flow simulation. As a feature of SUMO, the vehicle can be modeled explicitly, has its own route, and can move individually through the network. By using SUMO, it is possible to model intermodal transportation systems such as road vehicles, public transportation, and pedestrians. It also includes support tools for

route search, visualization, network import, emissions calculation, etc.

The Utsunomiya City map downloaded from OpenStreetMap (OSM) was used in this study as the driving route of the simulation. In order to reproduce the real driving environment on the simulation, the data “2015 National Road and Street Survey Schedule”[9] of the Ministry of Land, Infrastructure, Transport, and Tourism was used for traffic volume by road and time zone.

The speed limit in SUMO was set according to the legal speed of the real driving condition. Using one vehicle as a test vehicle, the designated test route was run and the vehicle speed data was recorded. The acceleration and deceleration of the vehicle are adjusted to match the vehicle speed results of the real driving experiment. In addition, the SpeedFactor was adjusted with the target of vehicle speed result by SUMO is matched the vehicle speed result (average vehicle speed) in real driving (urban, rural, and highway). The adjusted acceleration, deceleration, and SpeedFactor parameters can be seen in Table 4. The SpeedDev parameter was adjusted from 0.1 to 0 in order to decrease oscillation in vehicle speed results.

Table 4 SUMO parameters

Parameter	Description	Default	Adjusted Value
Depart [s]	The time step which the vehicle shall enter the network	0	0
Arrival Speed [m/s]	The speed with which the vehicle shall leave the network	current	0
Accel [m/s^2]	The acceleration ability of vehicles of this type	2.6	1.25
Decel [m/s^2]	The deceleration ability of vehicles of this type	4.5	1.32
SpeedFactor	The vehicle expected multiplicator for lane speed limits	1.0	Adjusted the SpeedFactor to match the average vehicle speed Urban: 0.80, Rural: 1.15, Highway: 0.97
SpeedDev	The deviation of the SpeedFactor	0.1	0

2.4. Combination of MATLAB/Simulink and SUMO

In this study, energy consumption is calculated by connecting SUMO with the vehicle numerical model built in Matlab (as shown in Fig. 3). The vehicle speed generated by SUMO is input to the vehicle model of Matlab as the target speed command. The vehicle model can drive according to the target speed and calculate the energy consumption[10].

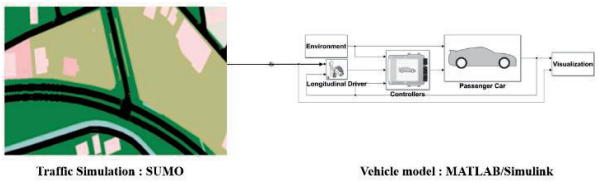

Fig. 3 Connection of SUMO and Matlab/Simulink

3. RESULT & DISCUSSION

3.1. Simulation Accuracy of Steady Speed Test

The accuracy of the vehicle model built using adjusted parameters of the simulation was verified by comparing the energy consumption from experiment and simulation results. Table 5 is a result of energy consumption on the steady speed test. After adjusting the motor efficiency map in simulation, the steady speed test energy consumption shows good results and accuracy as the differences between experiment and simulation are below 5%.

Table 5 Energy consumption comparison of steady speed test between experiment and simulation

Speed km/h	Experiment Wh/km	Simulation Wh/km	difference %
40	81.04	81.93	1.08%
60	106.48	106.60	0.11%
80	137.03	137.19	0.12%
100	181.16	181.28	0.07%
120	241.20	241.84	0.26%

3.2. Simulation Accuracy of WLTC

For the WLTC energy consumption results, by using adjusted parameters, we run the WLTC class 3b simulation in urban, rural, and highway. Table 6 is the WLTC result of energy consumption between experiment and simulation in urban, rural, highway, and combination. Table 6 shows good results and accuracy as a good calculation was obtained. In the WLTC, the regeneration braking process can be seen in Fig. 4, Fig. 5, and Fig. 6. The HV battery electric power shows negative results at certain points, it can be understood as the regenerative braking process of the BEV.

Table 6 Energy consumption comparison of WLTC between experiment and simulation

WLTC Mode	Experiment Wh/km	Simulation Wh/km	Difference %
Urban	118.21	111.84	-5.69%
Rural	114.91	117.01	1.80%
Highway	136.13	139.16	2.17%
Combine	125.71	126.49	0.61%

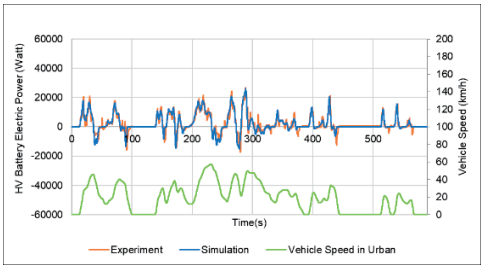

Fig. 4 HV Battery Electric Power Comparison Between Experiment and Simulation in Urban of WLTC

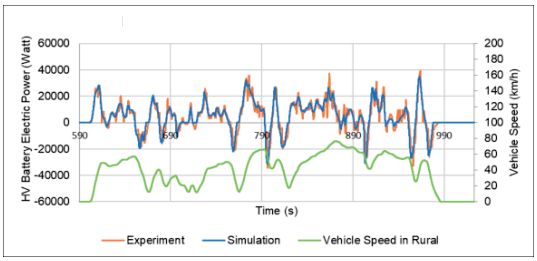

Fig. 5 HV Battery Electric Power Comparison Between Experiment and Simulation in Rural of WLTC

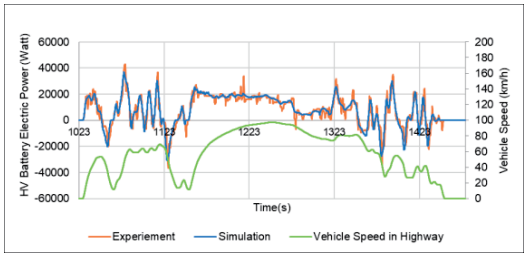

Fig. 6 HV Battery Electric Power Comparison Between Experiment and Simulation in Highway of WLTC

3.3. Simulation Accuracy of the Real Driving Test

For the real driving test energy consumption results, by using adjusted parameters, we run the real driving simulation using vehicle speed data from experiment. The real driving test is performed by two different drivers (Driver A and B). The energy consumption and HV battery electric power of real driving test results can be seen in Table 7 and Table 8 of Driver A and Table 9 and Table 10 of Driver B.

The results of energy consumption in a rural area of both Driver A and Driver B show a good result since the difference between the experiment and simulation is below 5%. However, the results of energy consumption differences between the experiment and simulation from urban, highway, and combination of all phases are above 5%.

For an urban area, the HV battery electric power result of simulation is lower than experiment. For the HV battery electric power in the urban area of Driver A, as we can see in Table 8, the simulation has a difference of -15.12% compared to the experiment. For the HV battery electric power in the urban area of Driver B, as we can see in Table 10, the simulation has a difference of -11.42% compared to the experiment. The concern comes from the motor efficiency map. Because we use the steady speed test data of motor speed and torque to calibrate the motor efficiency map, only the colored columns in Table 3 can be calibrated. We can't calibrate all columns in the motor efficiency map.

There is also a possibility in the highway area, the simulation was run using only vehicle speed data from the experiment and doesn't encounter the hill and slope (gradient resistance) in the real driving condition. The gradient resistance can affect the amount of electric power used by the electric motor to run the vehicle. As can be seen in Table 8 of Driver A and Table 10 of Driver B, in the highway area, the vehicle model in simulation consumes less electric power compared to the experiment result.

For the highway area (From Kanuma IC to Utsunomiya IC), the slope has a height of 54.9 m, with a distance of 10,791 m, and an angle of 0.29°. By using Eq. 4.1 and 4.2, for Driver A, the gradient resistance result is 85.345 N and the energy from the gradient resistance is 255.82 Wh. For Driver B, the gradient resistance result is 84.796 N and the energy from the gradient resistance is 254.18 Wh.

If the increased energy from gradient resistance is added to the simulation electric power result, as can be seen in Table 11, the difference between experiment and simulation in the highway area of Driver A is 1.55% and Driver B is 3.06%. Table 11 shows a good result since the difference between experiment and simulation is below 5%.

Since the vehicle numerical model of simulation shows good results and accuracy in rural and highway areas, we conclude the vehicle numerical model created this time can be used in our research work.

Table 7 Real driving test energy consumption comparison between experiment and simulation of Driver A

Phases	Experiment Wh/km	Simulation Wh/km	Difference %
Urban	123.86	107.92	-14.77%
Rural	105.08	106.01	0.88%
Highway	142.50	123.06	-15.80%
Combine	127.50	114.23	-11.62%

Table 8 Real driving test HV battery electric power comparison between experiment and simulation of Driver A

Phases	Experiment Wh	Simulation Wh	Difference %
Urban	977.19	848.88	-15.12%
Rural	729.98	737.83	1.06%
Highway	1717.49	1488.75	-15.36%
Combine	3427.04	3075.46	-11.43%

Table 9 Real driving test energy consumption comparison between experiment and simulation of Driver B

Phases	Experiment Wh/km	Simulation Wh/km	Difference %
Urban	127.82	114.47	-11.66%
Rural	102.25	104.06	1.74%
Highway	181.43	166.10	-9.23%
Combine	145.13	134.81	-7.66%

Table 10 Real driving test HV battery electric power comparison between experiment and simulation Driver B

Phases	Experiment Wh	Simulation Wh	Difference %
Urban	1008.44	905.06	-11.42%
Rural	713.04	726.94	1.91%
Highway	2179.86	1994.41	-9.30%
Combine	3900.82	3626.41	-7.57%

Table 11 Fixed Value using Gradient Resistance of HV Battery Electric Power in Highway of Real Driving Test

Phases	Driver A			Driver B		
	Experiment Wh	Simulation Wh	Difference %	Experiment Wh	Simulation Wh	Difference %
Highway	1717.49	1744.57	1.55%	2179.86	2248.588	3.06%

$$F_{gradient\ resistance}(N) = m \times g \times sin\theta \quad (4.1)$$

$$Energy\ (J) = F_{gradient\ resistance} A \times Distance \quad (4.2)$$

3.4. Influence of Acceleration on Energy Consumption

In order to analyze the effect of acceleration on energy consumption using simulation. The acceleration parameter of SUMO, which the base is 1.25 m/s^2, decreased by 50% to 0.625 m/s^2 and increased by 50% to 1.875 m/s^2. After changing the acceleration parameter, the simulation was run and the energy consumption was calculated and shown in Fig. 7 to Fig. 9. The average speed, time, idle time ratio, etc of each area from the simulation results can be seen in Table 12 to Table 14.

In urban, as can be seen in Fig. 7, decreasing acceleration by 50% from 1.25 m/s^2 to 0.625 m/s^2 increased energy consumption by 2.29%. The reason for this difference is because during low acceleration, the adjusted motor efficiency map showed low efficiency, and the electric motor needs to consume higher electric power to overcome the acceleration resistance. The total electric power consumption of HV battery is increased, as can be seen in Table 15, the total electric power consumption is increased by 2.14%. When acceleration is increased by 50%, the energy consumption increased by 2.91%. The reason for this difference is because the vehicle needs to overcome higher acceleration resistance, and the electric motor consumes higher electric power to run the vehicle as can be seen in Table 15, the total electric power consumption is increased by 3.02%.

In rural, as can be seen in Fig. 8, decreasing acceleration by 50%, increased energy consumption by 3.33%. The reason for this difference is because during low acceleration, the adjusted motor efficiency map showed low efficiency, which the electric motor need to consume higher electric power overcome acceleration resistance. The total electric power consumption of HV battery is increased, as can be seen in Table 15, the total electric power consumption is increased by 3.23%. Increased acceleration by 50%, the energy consumption improved by 5.57%. Even though, the vehicle needs to overcome acceleration resistance, the motor efficiency shows higher efficiency during high acceleration. As can be seen in Table 15, the total electric power consume by electric motor decreased by 5.80%.

In highways, as can be seen in Fig. 9, decreasing acceleration by 50% improved energy consumption by 0.23%, and increasing by 50% improved energy consumption by 0.37%. The change in energy consumption is small. The reason for small energy consumption difference is due to there are no traffic lights on the highway which cause less acceleration and deceleration.

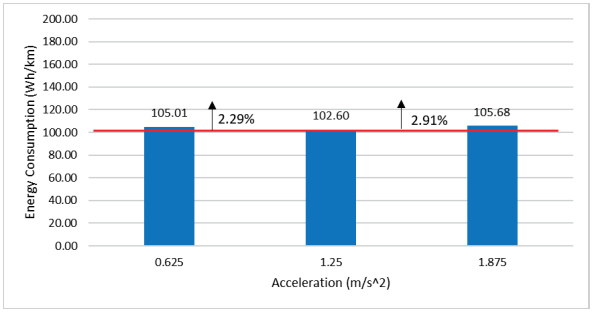

Fig. 7 Influence of Acceleration on Energy Consumption in Real Driving Urban

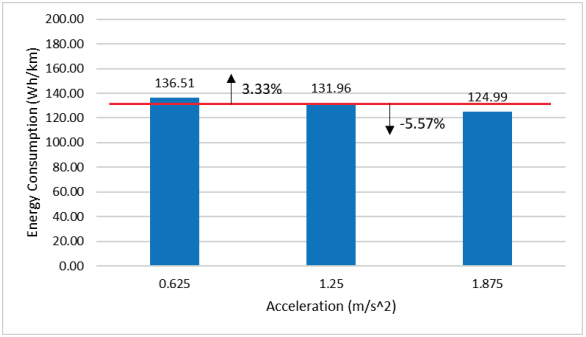

Fig. 8 Influence of Acceleration on Energy Consumption in Real Driving Rural

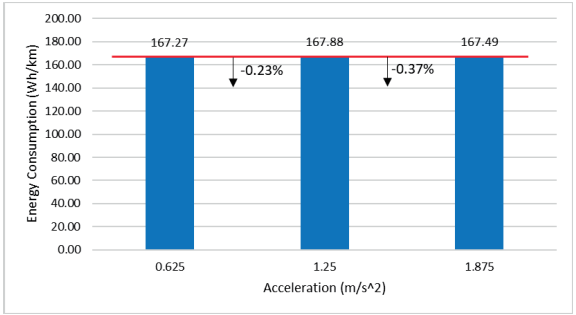

Fig. 9 Influence of Acceleration on Energy Consumption in Real Driving Highway

Table 12 Real driving urban simulation results in different acceleration

	Accel 0.625 (m/s^2)		Accel 1.25 (m/s^2)	Accel 1.875 (m/s^2)	
Energy Consumption (Wh/km)	105.01	2.29%	102.60	105.68	2.91%
Average Vehicle Speed (km/h)	18.80	-14.41%	21.51	21.68	0.77%
Time (Sec)	1475.00	13.29%	1279.00	1279.00	0.00%
Stop amount at traffic light	11		11	11	
Idle time ratio	25.50%		21.00%	23.00%	
Cruise time ratio	63.80%		59.10%	52.00%	
Acceleration time ratio	1.70%		10.90%	12.30%	
Deceleration time ratio	8.90%		9.10%	12.70%	

Table 13 Real driving rural simulation results in different acceleration

	Accel 0.625 (m/s^2)		Accel 1.25 (m/s^2)	Accel 1.875 (m/s^2)	
Energy Consumption (Wh/km)	136.51	3.33%	131.96	124.99	-5.57%
Average Vehicle Speed (km/h)	29.11	-24.01%	36.10	39.50	8.60%
Time (Sec)	858.00	23.89%	653.00	591.00	-10.49%
Stop amount at traffic light	7		6	5	
Idle time ratio	20.50%		11.47%	8.30%	
Cruise time ratio	60.50%		45.72%	48.80%	
Acceleration time ratio	3.60%		24.30%	20.10%	
Deceleration time ratio	15.40%		18.50%	22.80%	

Table 14 Real driving highway simulation results in different acceleration

	Accel 0.625 (m/s^2)		Accel 1.25 (m/s^2)	Accel 1.875 (m/s^2)	
Energy Consumption (Wh/km)	167.27	-0.37%	167.88	167.49	-0.23%
Average Vehicle Speed (km/h)	80.75	-3.68%	83.72	84.63	1.08%
Time (Sec)	526.00	3.23%	509.00	506.00	-0.59%
Idle time ratio	0.20%		0.20%	0.20%	
Cruise time ratio	93.40%		87.10%	80.10%	
Acceleration time ratio	0.90%		7.30%	10.10%	
Deceleration time ratio	5.50%		5.50%	9.70%	

Table 15 Real driving HV battery electric power consumption simulation results in different acceleration

Phase	Accel 0.625 m/s^2 Wh	Difference %	Accel 1.25 m/s^2 Wh	Accel 1.875 m/s^2 Wh	Difference %
Urban	837.90	2.14%	819.96	845.48	3.02%
Rural	954.56	3.23%	923.78	873.17	-5.80%
Highway	2030.40	-0.34%	2037.31	2032.40	-0.24%

3.5. Influence of Maximum Vehicle Speed on Energy Consumption

In order to analyze the effect of maximum vehicle speed on energy consumption using simulation, the SpeedFactor parameter of SUMO, which the base was 0.80 for urban, 1.15 for rural, and 0.97 for highway, was changed by 10% increase and decrease. After changing the SpeedFactor parameter, the simulation was run and the energy consumption was calculated and shown in Fig. 10 to Fig. 12. The average speed, time, idle time ratio, etc of each area from the simulation results can be seen in Table 16 to Table 18.

In urban, as can be seen in Fig. 10, energy consumption increased by 0.67% when the maximum vehicle speed decreased by 10%. The reason for this small difference is because the stop amount at traffic lights is increased to 14 as can be seen in Table 16 and during low vehicle speed, the adjusted motor efficiency map showed low efficiency, the electric motor consumes higher electric power to run the vehicle. However, the air resistance is decreased due to lower average vehicle speed. The difference in total electric power consumption can be seen in Table 19 is small, the total electric power consumption increased by 0.72%. When the maximum vehicle speed is increased by 10%, energy consumption is increased by 6.73%. The reason is because the air resistance is increased. The electric motor consumes higher electric power to run the vehicle as can be seen in Table 19, the total electric power consumption is increased by 6.68%.

In rural, as can be seen in Fig. 11, decreased maximum vehicle speed by 10% will improve energy consumption by 7.14%. The reason for this difference because the air resistance is lower and the electric motor doesn't need to consume higher electric power to run the vehicle as can be seen in Table 19, the total electric power consumption is decreased by 7.76%. Energy consumption improved by 1.18% when the maximum vehicle speed increased by 10%. Even though, the vehicle needs to overcome air resistance, the motor efficiency of the vehicle numerical model shows higher efficiency. As can be seen in Table 19, the total electric power consume by electric motor decreased by 1.42%.

In highway, as can be seen in Fig. 12, energy consumption is improved by 13.34% when the maximum vehicle speed is decreased by 10%. The reason for this difference because the air resistance is lower and the electric motor doesn't need to consume higher electric power to run the vehicle as can be seen in Table 19, the total electric power consumption is decreased by 13.57%. The energy consumption is increased by 12.42% when the maximum vehicle speed is increased by 10%. The reason is because the vehicle need to overcome higher air resistance. The electric motor is consumed higher electric power to run the vehicle as can be seen in Table 19, the total electric power consume by electric motor increased by 12.20%.

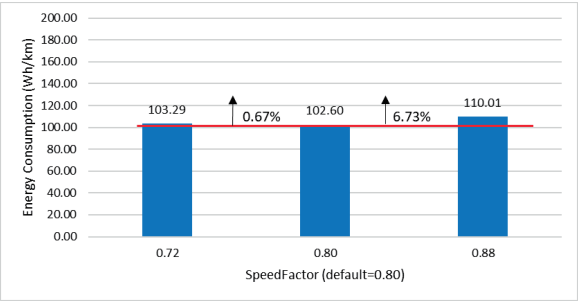

Fig. 10 Influence of Maximum Vehicle Speed on Energy Consumption in Real Driving Urban

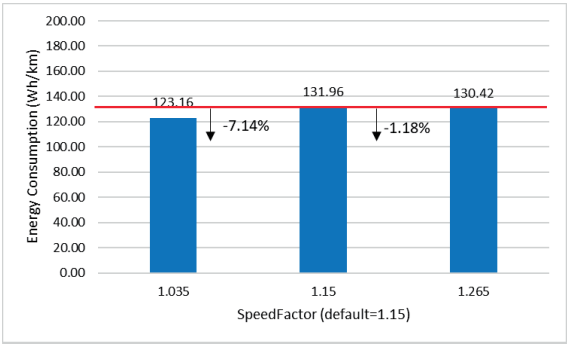

Fig. 11 Influence of Maximum Vehicle Speed on Energy Consumption in Real Driving Rural

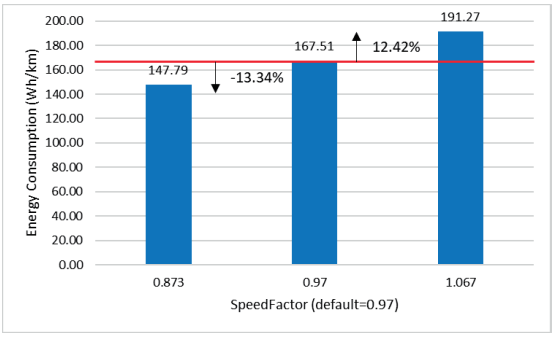

Fig. 12 Influence of Maximum Vehicle Speed on Energy Consumption in Real Driving Highway

Table 16 Real driving urban simulation results in different maximum vehicle speed

	Speed Factor 0.72		Speed Factor 0.80	Speed Factor 0.88	
Energy Consumption (Wh/km)	103.29	0.67%	102.60	110.01	6.73%
Average Vehicle Speed (km/h)	18.76	-14.63%	21.51	20.02	-7.41%
Time (Sec)	1487.00	13.99%	1279.00	1371.00	6.71%
Stop amount at traffic light	14		11	12	
Idle time ratio	25.70%		21.00%	30.60%	
Cruise time ratio	55.80%		59.10%	46.50%	
Acceleration time ratio	10.10%		10.90%	12.30%	
Deceleration time ratio	8.40%		9.10%	10.60%	

Table 17 Real driving rural simulation results in different maximum vehicle speed

	Speed Factor 1.035		Speed Factor 1.15	Speed Factor 1.265	
Energy Consumption (Wh/km)	123.16	-7.14%	131.96	130.42	-1.18%
Average Vehicle Speed (km/h)	34.44	-4.85%	36.10	35.30	-2.27%
Time (Sec)	684.00	4.53%	653.00	662.00	1.36%
Stop amount at traffic light	6		6	6	
Idle time ratio	15.30%		11.47%	11.16%	
Cruise time ratio	52.10%		45.72%	45.70%	
Acceleration time ratio	19.00%		24.30%	23.50%	
Deceleration time ratio	13.60%		18.50%	19.60%	

Table 18 Real driving highway simulation results in different maximum vehicle speed

	Speed Factor 0.873		Speed Factor 0.97	Speed Factor 1.067	
Energy Consumption (Wh/km)	147.79	-13.34%	167.51	191.27	12.42%
Average Vehicle Speed (km/h)	75.71	-10.66%	83.78	91.15	8.09%
Time (Sec)	562.00	9.43%	509.00	467.00	-8.99%
Idle time ratio	0.20%		0.20%	0.20%	
Cruise time ratio	88.30%		87.10%	83.80%	
Acceleration time ratio	6.60%		7.30%	9.20%	
Deceleration time ratio	5.00%		5.50%	6.80%	

Table 19 Real driving HV battery electric power consumption simulation results in different maximum vehicle speed

Phase	SpeedFactor Decreased by 10%		Difference %	SpeedFactor Base value		SpeedFactor Increased by 10%		Difference %
	SpeedFactor	Wh		SpeedFactor	Wh	SpeedFactor	Wh	
Urban	0.72	825.92	0.72%	0.80	819.96	0.88	878.67	6.68%
Rural	1.035	857.22	-7.76%	1.15	923.78	1.265	910.80	-1.42%
Highway	0.873	1793.86	-13.57%	0.97	2037.31	1.067	2320.4	12.20%

4. CONCLUSION

The BEV numerical model was constructed using simulation and the accuracy was verified. Furthermore, in combination with SUMO, the actual driving of the vehicle was reproduced by simulation, and as a result of changing the acceleration and maximum vehicle speed, the following was found.

1. The vehicle numerical model shows good results and accuracy of energy consumption in the steady speed and WLTC test since the difference between experiment and simulation is under 5%. Therefore, for the WLTC test in an Urban area, a decent result was obtained from simulation.
2. The real driving test results in an urban area of Driver A and Driver B in energy consumption, showed a difference above 5% between experiment and simulation. The concern comes from the motor efficiency map, which is calibrated only using the steady speed test data of motor speed and torque, all columns in the motor efficiency map can't be calibrated. In highway areas, the simulation doesn't calculate the gradient resistance and consumes less electric power compared to the experiment result. The calculated energy of gradient resistance has been added to the HV battery electric power of simulation result. The result of the electric power difference between experiment and simulation in the highway is under 5%.
3. As the result of changing acceleration in the real driving test of simulation, increasing the acceleration by 50% in rural areas will improve energy consumption by 5.57%.
4. As a result of changing the maximum vehicle speed in the real driving test of simulation, in rural areas, decreasing maximum vehicle speed by 10%, improved the energy consumption by 7.14%, and in highway areas, decreasing maximum vehicle speed by 10%, improved the energy consumption by 13.34%. So, by not unnecessarily increasing vehicle speed would effectively improve energy consumption in rural and highway areas.

For the eco-driving of BEV as an energy efficiency improvement method, in rural areas increasing acceleration and not unnecessarily increasing vehicle speed will improve energy consumption. In highway areas, not unnecessarily increasing

vehicle speed in high-speed driving would be effective to improve energy consumption.

REFERENCES

(1) Tomomori Niisato : Powertrain for Passenger Cars in 2030, Society of Automotive Engineers of Japan Spring Meeting Forum (2019)
(2) The 26th UN Climate Change Conference of the Parties (COP26) in Glasgow, https://ukcop26.org, Accessed April 3, 2023
(3) Yasuko Kameyama : COP26 Closing: What Was Decided at the First COP of "Decisive 10 Years", https://www.nies.go.jp/social/navi/colum/cop26.html, Accessed 23 January 2023
(4) Qu Yiqi, Glenn Hizkia A., Akira Kato : Study on Fuel Consumption on Real Road by using Traffic Flow Simulation, JSAE Kanto, International Conference of Automotive Technology for Young Engineers (2021)
(5) Glenn Hizkia A., Qu Yiqi, Akira Kato : Study of Fuel Efficiency Improvement Method for Small Passenger Cars using Traffic Flow Simulation, Second Report: Hybrid Electric Vehicle, JSAE Kanto, International Conference of Automotive Technology for Young Engineers (2022)
(6) Simulation of Urban Mobility, https://www.eclipse.org/sumo/, Accessed July 27, 2021
(7) Michael Melkior K., Yuta Nakane, Otsuki Taizo, Akira Kato : Investigation of Energy Consumption Measurement Method for Electric Vehicles Using External Diagnosis Tool, Japan Society of Mechanical Engineers Kanto Branch Tochigi Block Research Exchange Meeting (2022)
(8) Mathworks: Powertrain Blockset Automotive Powertrain System Modeling and Simulation, https://www.mathworks.com/products/powertrain.html, Accessed 23 January, 2023
(9) Ministry of Land, Infrastructure, Transport and Tourism : National Road and Street Traffic Situation Survey, https://www.mlit.go.jp/road/census/h27/, Accessed July 27, 2021
(10) Yuki Okuda, Takashi Okada, Kazuhiko Sato, Yoshiharu Sugiyama : Proposal of Fuel Economy Function Integrated Speed Planning Control Method for Automated Driving and Advanced Driver Assistance, Proceeding of Autumn Meeting of the Society of Automotive Engineers of Japan, (2019)

ACKNOWLEDGEMENT

This research was supported by Ono Sokki Co., Ltd., which conducted the CD test. We would like to express our gratitude for the valuable advice and suggestion from Ono Sokki Co., Ltd. for our research work.

講演番号	053

文献番号	20235053

Study of BEV ECO-Driving Methods using Mode and Real Driving Tests

- Actual Road Power Consumption Assessment and Characteristics -

Michael Melkior Kanugroho[1)] Yuta Nakane[2)] Taizo Otsuki[2)] Akira Kato[2)]

1) Teikyo University, Graduate School of Science and Engineering, Division of Integrated Science and Engineering
Toyosatodai 1-1, Utsunomiya City, Tochigi Prefecture 320-8551, Japan
2) Teikyo University, Department of Mechanical Precision Systems Engineering, Faculty of Science and Engineering
Toyosatodai 1-1, Utsunomiya City, Tochigi Prefecture 320-8551, Japan

ABSTRACT: With the goal of achieving carbon neutral by 2050, passenger vehicles are shifting from Internal Combustion Engine (ICE) vehicle to Battery Electric Vehicle (BEV). However, BEV has issues, such as limited range, long charging time, lack of charging stations, and high cost. In this study, we conducted a mode tests on Chassis Dynamometer (CD) and real driving tests in Utsunomiya city using a BEV under outside air temperature conditions of 5°C, 20°C, and 35°C with or without an Air Conditioner (AC). The purpose of this study is to analyze the effects of different outside air temperatures and whether AC used or not used to the energy consumption of BEV on actual road. Therefore, the energy consumption characteristic from experiment will be investigated and analyzed, and the eco-driving of BEV will be presented as an energy efficiency improvement method.

KEY WORDS: **EV and HV systems, state of charge (SOC), real drive emission (A3)**

1. INTRODUCTION AND RESEARCH PURPOSE

Nowadays, the world has to deal with three matters such as air pollution, global warming, and energy crisis(1). Concerning global warming, GHG (Green House Gasses) emissions reduction in transportation sector such as automobiles is necessary(2). In addition, to minimize the harmful effects of climate change. The Paris Agreement in 2015 aimed to maintain the earth temperature rise to be below 2°C, but allowing the temperature rise below 2°C would still be insufficient to reduce the harmful effects of climate change. COP26 in 2021, agreed to maintain the earth temperature rise below 1.5°C and to achieve it, the realization of carbon neutral in 2050 is necessary, passenger vehicles are shifting from ICE vehicle to BEV(3). However, BEV has issues, such as limited range, long charging time, lack of charging stations, and high cost(4).

In previous studies, experiment was conducted using gasoline vehicle and 2 Motor Hybrid Vehicle (2MHV). For gasoline vehicle, in real driving of urban and rural areas, increasing cruise time frequency and decreasing acceleration time frequency are effective to improve fuel consumption. On real driving of highway areas, it is effective to improve fuel consumption by not increasing vehicle speed unnecessarily during high-speed driving(5). For 2MHV, in real driving on highway area, it is possible to improve fuel consumption by reducing vehicle speed as at high-speed driving(6).

In addition, the simulation model of BEV was constructed and the energy efficiency improvement method for BEV on real driving using vehicle numerical modeling and traffic flow simulations (SUMO, Simulation of Urban Mobility) was proposed. For the eco-driving of BEV as an energy efficiency improvement method, in rural area increasing acceleration and not unnecessarily increasing vehicle speed will improve energy consumption. In highway area, not unnecessarily increasing vehicle speed in high-speed driving would be effective to improve energy consumption. By decreasing the maximum vehicle speed in rural and highway areas, the travel distance of BEV increased by 23 km and a difference of 8.90% from the calculated WLTC travel distance(7).

In this study, we conducted a mode tests on CD and real driving tests in Utsunomiya City using a BEV under outside air temperature conditions of 5°C, 20°C, and 35°C with or without an AC. The purpose of this study is to analyze the effects of different outside air temperatures and whether AC used or not used to energy consumption of BEV on actual road. Therefore, energy consumption characteristic from experiment will be investigated and analyzed, and the eco-driving of BEV will be presented as an energy efficiency improvement method. The eco-driving method results from experiment will be compare and analyzed with simulation results from previous study. The differences of eco-driving method from experiment and simulation will be presented.

2. EXPERIMENT METHOD

2.1. Test Vehicle

BEV as the specifications in Table 1 is chosen to use in the experiment. The chosen test vehicle (Nissan Leaf ZE1) has been sold approximately 167,000 units in Japan since December 2010 and is a representative of domestic BEV.

Table 1 Vehicle Specifications

Drive system	FF
Length (m)	4.48
Width (m)	1.79
Full height (m)	1.54
Vehicle weight (kg)	1,530
Battery type	Lithium-ion-battery
Battery capacity (kWh)	40
Motor model code	EM57
Motor maximum output (kW/rpm)	110/3283~9795
Motor maximum torque (N・m/rpm)	320/0~3283
Energy consumption (Wh/km)	155 (WLTC mode)
	120 (JC08 mode)
Travel distance per full battery (km)	322 (WLTC mode)
	400 (JC08 mode)

2.2. Chassis Dynamometer Tests

Mode tests of steady speed and WLTC tests were conducted using CD. In addition, an external diagnostic device (HDM9000 made by Hitachi Astemo) is used for real-time measurement method, it is connected to OBD port of test vehicle. Measured parameters such as High-Voltage (HV) battery voltage, HV battery amphere, logging time, and travel distance are used to calculate energy consumption of BEV. We calculate energy consumption of BEV by using Eq. 2.1 to 2.2.

According to WLTC regulations, the vehicle weight + 100kg + luggage weight multiplied by loading ratio (15% for passenger cars, 28% for small trucks) are set as weight of the test vehicle. However, in this CD tests, the vehicle weight + 110 kg (weight assuming two passengers) used in the JC08 mode tests were set as weight of the test vehicle.

$$P_T = \sum_{i=1}^{n} (V_i \times A_i \times Int_i) \quad (2.1)$$

$$E_1 = \frac{P_T}{L_T} \quad (2.2)$$

n : Amount of data measured by external diagnosis device
P_T : Total electric power (Wh)
V : HV battery voltage (V)
A : HV battery current (A)
Int : Logging time interval (h)
L_T : Total travel distances (km)
E_1 : Energy consumption (Wh/km)

2.2.1. Steady Speed Test

Steady speed tests were conducted at specific vehicle speed of 40 km/h, 60 km/h, 80 km/h, 100 km/h, and 120 km/h. As shown in Table 2, tests were conducted under temperature conditions of 5°C, 20°C, and 35°C while maintaining specific vehicle speed.

The test vehicle was run on a CD for about 1 minute with a total of 15 patterns of AC on and off. For AC on, the target temperature inside the cabin was set to 25°C, and the vehicle will adjust the temperature inside the cabin automatically.

Table 2 Steady Speed Tests

Outside air temperature (°C)	AC	Vehicle speed (km/h)				
		40	60	80	100	120
5	ON	•	•	•	•	•
	OFF					
20	ON	•	•	•	•	•
	OFF					
35	ON	•	•	•	•	•
	OFF					

2.2.2. WLTC Tests

The WLTC tests in Japan are divided into Low, Medium, and High. Low assumes driving in urban areas where traffic lights and traffic jams occur, Medium assumes rural areas that are not much affected by traffic lights, and High assumes driving on highways. In this test, outside air temperature was set to 5°C, 20°C, and 35°C with AC system on (set to 25°C) and off at each outside air temperature.

2.3. Real Driving Tests

The real driving tests were conducted on three different driving roads such as urban, rural, and highway around Utsunomiya City (shown in Fig. 1) with two different drivers (Driver A and B). The real driving tests were conducted in summer, autumn, and winter. In summer and winter, AC system is used, and target temperature is 25°C, the vehicle will adjust temperature inside the cabin automatically. In autumn, AC system is not used. An external diagnosis tool (HDM9000) was used during experiment for real-time measurement and energy consumption calculation is same as CD tests.

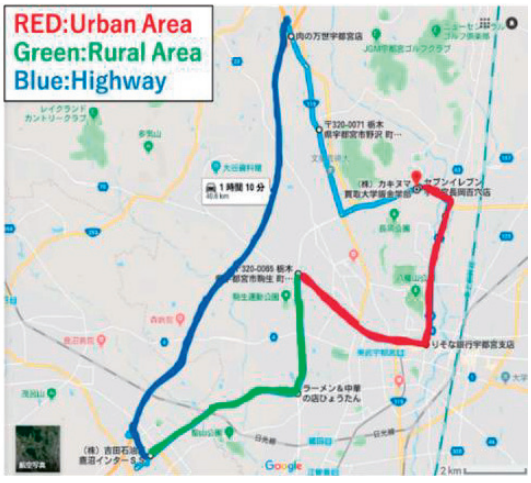

Fig. 1 Real Driving Road Test in Utsunomiya City

3. EXPERIMENT RESULT

3.1. Steady Speed Tests

Table 3 shows energy consumption results of steady speed tests. At each outside air temperature, higher the vehicle speed, energy consumption is increased. The lowest energy consumption result is 74 Wh/km, when outside air temperature is 35°C, the vehicle speed is 40 km/h, and AC off. The highest energy consumption result is 268 Wh/km, when outside air temperature is 5°C, the vehicle speed is 120 km/h, and AC on. Comparing energy consumption when using AC system, the results show that energy consumption is higher when using AC on heating mode (outside temperature is 5°C) rather than when using on cooling mode (outside temperature is 35°C) at all vehicle speeds.

Table 3 Energy Consumption of Steady Speed Tests

Outside air temperature (°C)	5		20		35	
AC	OFF	ON	OFF	ON	OFF	ON
Vehicle speed						
40 km/h (Wh/km)	92	148	81	85	74	128
60 km/h (Wh/km)	120	146	106	106	95	125
80 km/h (Wh/km)	154	168	137	138	126	149
100 km/h (Wh/km)	198	209	181	179	169	189
120 km/h (Wh/km)	257	268	241	240	232	248

3.2. WLTC Tests

Table 4 shows energy consumption results of the WLTC tests. In urban area with an outside air temperature of 35°C, the lowest result for energy consumption is 109 Wh/km when AC off and the highest result is 201 Wh/km when use AC on cooling mode. In urban area with an outside air temperature of 20°C, the energy consumption is 118 Wh/km rather AC on or off, which was a same result.

Comparing energy consumption in all areas, when AC off, the lowest results of energy consumption are obtained when outside air temperature is 35°C, and the highest results are obtained when outside air temperature is 5°C. This is thought to be caused by rolling resistance of tires increased due to the temperature drop. The temperatures drop also effect battery and motor temperature, more electric power was used for temperature adjustment.

Table 4 Energy consumption of WLTC Tests

Outside air temperature (°C)	5		20		35	
AC	OFF	ON	OFF	ON	OFF	ON
Urban（Wh/km)	120	190	118	118	109	201
Rural（Wh/km)	128	151	115	120	110	151
Highway（Wh/km)	148	164	136	138	141	156
Combine（Wh/km)	135	165	126	128	119	164

3.3. Real Driving Tests

Table 5 shows energy consumption for Driver A and B of real driving tests in summer with AC on (cooling mode). Table 6 shows energy consumption for Driver A and B of real driving tests in autumn with AC off. Table 7 shows energy consumption for Driver A and B of real driving tests in winter with AC on (heating mode). The outside air temperature data was obtained from information published by Japan Meteorological Agency[8].

Regarding energy consumption, the lowest result is 102 Wh/km at rural area of Driver B in autumn. The highest result is 189 Wh/km at highway area for Drivers A and B in winter.

Table 5 Energy Consumption of Real Driving Tests on Summer with AC On

Date	2022/8/8	2022/8/22	Average
Driver	A	B	
Weather	Cloudy	Cloudy	
Outside Air Temperature (°C)	32.1	28.3	30.2
Urban (Wh/km)	187	171	179
Rural (Wh/km)	159	148	154
Highway (Wh/km)	166	163	165

Table 6 Energy Consumption of Real Driving Tests on Autumn with AC Off

Date	2022/10/31	2022/11/1	Average
Driver	A	B	
Weather	Sunny	Cloudy	
Outside Air Temperature (°C)	18.1	18.2	18.2
Urban (Wh/km)	124	128	126
Rural (Wh/km)	105	102	104
Highway (Wh/km)	143	181	162

Table 7 Energy Consumption of Real Driving Tests on Winter with AC On

Date	2022/12/26	2022/12/27	Average
Driver	A	B	
Weather	Cloudy	Cloudy	
Outside Air Temperature (°C)	6.5	9.1	7.8
Urban (Wh/km)	158	152	155
Rural (Wh/km)	128	120	124
Highway (Wh/km)	189	189	189

4. DISCUSSION

4.1. Average Vehicle Speed and Energy Consumption

In conducting analysis, the unit of energy consumption was converted from Wh/km to km/kWh by using Eq. 4.1, following fuel efficiency unit of gasoline vehicles.

Fig. 2 shows relationship between average vehicle speed and energy consumption in each area of WLTC and real driving tests

with AC off. We set correlation coefficient at ±0.5, positive correlation is 0.5 or more and negative correlation is -0.5 or less. From Fig. 2, the correlation coefficient between BEV energy consumption and average vehicle speed ranges in urban and rural areas is 0.74, indicating a positive correlation. In addition, the coefficicent correlation in rural and highway areas is -0.98, indicating a negative correlation. From these results, it was found that BEV energy consumption improves as average vehicle speed increases in urban and rural areas. Energy consumption increased as vehicle speed increases at high speed driving in highway area.

From above, it is found that driving in urban and rural areas at an average vehicle speed of around 30 to 40 km/h is effective in improving energy consumption of BEV, and lowering vehicle speed in highway area is effective to improve energy consumption.

$$E_2 = \frac{L_T \times 1000}{P_T} \quad (4.1)$$

E_2 : Energy consumption (km/kWh)
P_T : Total electric power (Wh) from Eq. 2.1
L_T : Total travel distances (km)

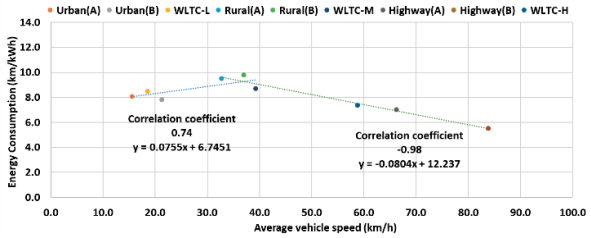

Fig. 2 Energy Consumption of WLTC and Real Driving Tests

4.2. Driving Condition and Energy Consumption

The relationship between acceleration and deceleration time frequency and energy consumption is analyzed. Acceleration and deceleration judgement value is set to 0.3 m/s^2, when vehicle acceleration is 0.3 m/s^2 or more, vehicle is accelerates. When it is -0.3 m/s^2 or less, vehicle is decelerates. When brake switch is on and vehicle speed is 0 km/h was defined as idling. Acceleration within -0.3 to 0.3 m/s^2 with vehicle speed over 1 km/h was defined as cruising. Tables 8 to 13 show time frequencies of acceleration, deceleration, idle, and cruise in WLTC and real driving tests.

Fig. 3 shows the correlation coefficients between time frequency of acceleration, cruising, and idling, to the energy consumption of BEV, and fuel consumption of gasoline vehicle and 2MHV in WLTC and real driving tests with AC off in urban and rural areas.

Regarding the correlation between acceleration time frequency, energy consumption, and fuel consumption, the correlation coefficient for gasoline vehicles is -0.65, indicating a negative correlation, but no correlation for 2MHV and BEV. The reason for this is thought to be the frequency of regenerative braking increases relatively with increase in acceleration time frequency in 2MHV and BEV, and electric power is regenerated during deceleration.

Regarding the correlation between deceleration time frequency, energy consumption, and fuel consumption, the correlation coefficient for gasoline vehicle is -0.75, indicating a negative correlation, while the correlation coefficient for BEV is 0.57, indicating a positive correlation. For 2MHV, the correlation coefficient is 0.29 as there is no correlation. From this, it was found that regenerative braking of BEV has a stronger effect on energy consumption compare to 2MHV on fuel consumption.

Regarding the correlation between idling time frequency, energy consumption, and fuel consumption, there are no correlation for gasoline vehicles and 2MHV, but the correlation coefficient for BEV is -0.85, indicating a strong negative correlation. The reason for this is presumed to be that electric power was used to adjust the temperature of the battery and motor while vehicle was stopped.

Regarding the correlation between cruise time frequency, energy consumption, and fuel consumption, there was no correlation for 2MHV, but the correlation coefficient for gasoline vehicles is 0.74 and for BEV is 0.91, indicating a positive correlation between gasoline vehicle and BEV.

Comparing with previous study, for gasoline vehicle, in real driving of urban and rural areas, increasing cruise time frequency and decreasing acceleration time frequency are effective to improve fuel consumption. For BEV, it was found that reducing idling time frequency, and increasing cruise time frequency are effective to improve energy consumption in urban and rural areas.

Table 8 Time Frequency of WLTC Tests at 5°C

Temp.	AC	Phase	Acceleration (%)	Deceleration (%)	Idle (%)	Cruise (%)
5°C	AC OFF	WLTC-L	19.0	18.8	24.2	38.0
		WLTC-M	22.0	20.4	10.8	46.7
		WLTC-H	18.2	16.7	2.7	62.4
	AC ON	WLTC-L	19.0	18.5	24.2	38.4
		WLTC-M	22.2	20.3	10.8	46.7
		WLTC-H	18.2	17.6	2.1	62.1

Table 9 Time Frequency of WLTC Tests at 20°C

Temp.	AC	Phase	Acceleration (%)	Deceleration (%)	Idle (%)	Cruise (%)
20°C	AC OFF	WLTC-L	21.6	15.4	24.0	39.0
		WLTC-M	22.3	22.2	10.5	44.9
		WLTC-H	17.9	16.2	2.0	63.9
	AC ON	WLTC-L	18.4	18.9	23.8	39.0
		WLTC-M	23.2	21.1	10.8	45.0
		WLTC-H	18.3	17.7	6.8	57.2

Table 10 Time Frequency of WLTC Tests at 35°C

Temp.	AC	Phase	Acceleration (%)	Deceleration (%)	Idle (%)	Cruise (%)
35°C	AC OFF	WLTC-L	19.0	18.9	24.4	37.7
		WLTC-M	21.6	20.4	10.7	47.3
		WLTC-H	18.5	17.4	2.0	62.1
	AC ON	WLTC-L	18.4	19.4	25.0	37.2
		WLTC-M	22.0	20.3	10.8	46.9
		WLTC-H	18.3	16.7	3.3	61.6

Table 11 Time Frequency of Real Driving Tests on Summer

Driver	Phase	Acceleration (%)	Deceleration (%)	Idle (%)	Cruise (%)
A	Urban	17.5	14.9	32.7	34.9
	Rural	13.9	14.2	19.6	52.2
	Highway	4.7	5.8	0.1	89.5
B	Urban	16.3	14.8	35.0	33.8
	Rural	19.2	14.8	22.3	43.7
	Highway	9.5	15.1	0.1	75.4

Table 12 Time Frequency of Real Driving Tests on Autumn

Driver	Phase	Acceleration (%)	Deceleration (%)	Idle (%)	Cruise (%)
A	Urban	14.4	12.3	37.7	35.6
	Rural	20.6	19.1	13.0	47.3
	Highway	3.2	4.5	1.4	90.9
B	Urban	15.6	13.1	32.6	38.7
	Rural	15.0	16.7	10.1	58.1
	Highway	7.5	6.6	1.2	84.6

Table 13 Time Frequency of Real Driving Tests on Winter

Driver	Phase	Acceleration (%)	Deceleration (%)	Idle (%)	Cruise (%)
A	Urban	18.3	15.1	34.1	32.4
	Rural	18.3	17.5	27.9	36.3
	Highway	7.1	8.9	0.8	83.2
B	Urban	16.3	14.6	35.6	33.4
	Rural	13.1	11.8	27.3	47.8
	Highway	10.2	8.0	1.1	80.7

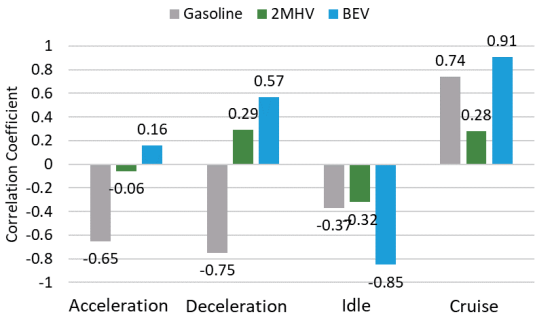

Fig. 3 Comparison of Gasoline, 2MHV, and BEV Correlation Coefficient in Urban and Rural Areas

4.3. Effect of Using AC on Energy Consumption

Fig. 4 shows the relationship between the reduction rate of energy consumption and the outside air temperature. The WLTC tests energy consumption result with AC off at an outside air temperature of 20°C in each area is choosed as a reference. In WLTC tests, the highest reduction rate in energy consumption when using AC on cooling mode is 41% in urban area with an outside air temperature of 35°C (shown in Table 14). The highest reduction rate in energy consumption when using AC on heating mode is 38% in urban area with an outside air temperature of 5°C (shown in Table 14). The reduction rate of energy consumption of BEV when using AC on cooling and heating mode is almost the same. It was found that the reduction rate in energy consumption due to the use of AC in urban area is greater than in the rural and highway areas. The reduction rate in energy consumption when using AC on cooling mode from the highest are urban, rural, and highway.

Working principles of AC system on heating mode of gasoline and Hybrid Electric Vehicle (HEV) are different compared to BEV. Heating system of gasoline and HEV are using released heat from engine coolant to warm the vehicle cabin. However, in BEV different characteristics was shown. When AC system of BEV is used for heating mode, the PTC heater works simultaneously in addition with AC compressor. AC compressor and PTC heater of BEV are directly used electric power from HV battery, it can effect energy consumption and travel distance results.

The travel distance on a single charge is calculated from the energy consumption result of the WLTC tests using Eq. 4.2. The travel distance results are shown in Fig. 5 for an outside air temperature of 5°C, Fig. 6 for an outside air temperature of 20°C, and Fig. 7 for an outside air temperature of 35°C. The longest travel distance on a single charge is 367 km in urban area with an outside air temperature of 35°C and AC off.

Comparing the reduction rate in travel distance on single charge in all WLTC areas (combination), when use AC on heating

mode (outside air temperature is 5°C), the reduction rate is 17.7% and when use AC on cooling mode (outside air temperature is 35°C), the reduction rate is 27.4%. It was found that the reduction rate of the travel distance is higher when use AC on cooling mode rather than when use AC on heating mode.

$$Travel\ Distance\ (km) = \left(\frac{BEV\ Battery\ Capacity\ (40\ kWh)}{Energy\ Consumption\ (^{Wh}/_{km})}\right) \quad (4.2)$$

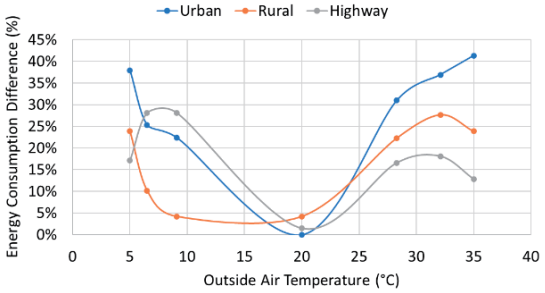

Fig. 4 Energy Consumption Reduction Rate Using AC in WLTC and Real Driving Tests

Table 14 Energy Consumption of WLTC Tests at Difference Outside Air Temperature with AC On and Off

Outside air temperature (°C)	5	Difference	20	Difference	35
AC	ON	→	OFF	←	ON
Urban (Wh/km)	190	-38%	118	-41%	201
Rural (Wh/km)	151	-24%	115	-24%	151
Highway (Wh/km)	164	-17%	136	-13%	156
Combine (Wh/km)	165	-24%	126	-23%	164

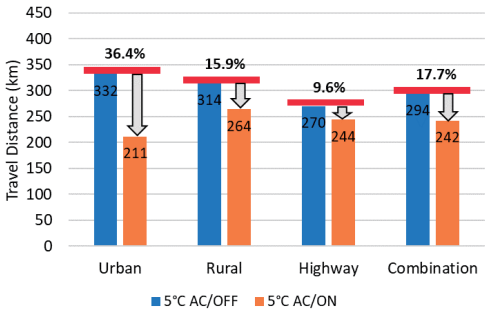

Fig. 5 Travel Distance of WLTC Tests at 5°C

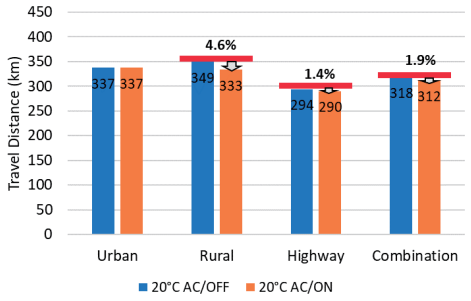

Fig. 6 Travel Distance of WLTC Tests at 20°C

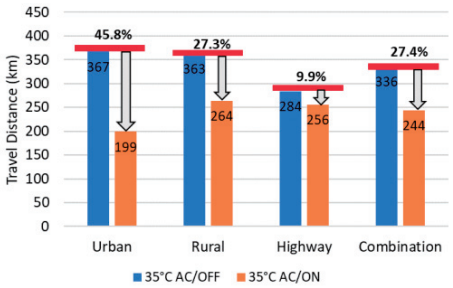

Fig. 7 Travel Distance of WLTC Tests at 35°C

4.4. Comparison of BEV ECO-Driving Method between Experiment and Simulation

4.4.1 Average Vehicle Speed and Energy Consumption

Regarding the relationship between average vehicle speed and energy consumption of WLTC and real driving tests with AC off in urban and rural areas. For experiment results, it was found that in BEV, when average vehicle speed increases except for high speeds driving, energy consumption improves. Therefore, for eco-driving method of BEV as energy efficiency improvement method, it is effective to increase vehicle speed in urban and rural areas.

The experiment results are different compare to the simulation results. In simulation results, it is effective to improve the energy consumption by reducing vehicle speed in rural areas. The different is though to be the vehicle numerical model which is run in traffic flow simulation have tendency to cruising, meanwhile in experiment, vehicle speed is always changed.

4.4.2 Vehicle Acceleration and Energy Consumption

Regarding the relationship between acceleration frequency and energy consumption of WLTC and real driving tests with AC off in urban and rural areas. For experiment results, there is no correlation in BEV between acceleration time frequency and energy consumption.

The experiment results are different compare to the simulation results. In the simulation results, the energy consumption is improved during high acceleration in rural area. In rural area during high acceleration, the electric motor from vehicle numerical model in simulation has a tendency to operate at high efficiency areas in motor efficiency map. The vehicle consumed lower electric power to run.

5. CONCLUSION

As a result of conducting mode and real drivng tests using BEV, the following things were found.

1. Regarding the correlation between average vehicle speed and energy consumption in WLTC and real driving tests with AC off in urban and rural areas, it was found that in BEV,

increases vehicle speed in urban and rural areas, will improves energy consumption.

2. Regarding the correlation between acceleration time frequency and energy consumption in WLTC and real driving tests with AC off in urban and rural areas, there is no correlation in BEV between acceleration time frequency and energy consumption. The reason for this is thought to be that BEV uses regenerative braking relatively more frequently when acceleration frequency increases, similar to 2MHV.
3. Regarding the correlation between deceleration time frequency and energy consumption in WLTC and real driving tests with AC off in urban and rural areas, the correlation coefficient between deceleration time frequency and energy consumption for BEV is 0.57, indicating a positive correlation. From this, it was found that regenerative braking of BEV has a strong effect on energy consumption.
4. Regarding the correlation between idle time frequency and energy consumption in WLTC and real driving tests with AC off in urban and rural areas, the correlation coefficient in BEV between idle time frequency and energy consumption is -0.85, showing a strong negative correlation. The reason for this is presumed to be that electric power was used to adjust the temperature of the battery and motor while the vehicle is stopped.
5. Regarding the reduction rate of energy consumption due to outside air temperature and use of AC system in WLTC tests, the highest reduction rate on energy consumption in urban area when using AC on cooling mode (outside air temperature of 35°C) is 41% and AC on heating mode (outside air temperature of 5°C) is 38%. The reduction rate of energy consumption of BEV when using AC on cooling and heating mode is almost the same. In addition, the working principles of AC system on heating mode of gasoline and HEV are different compared to BEV. In BEV, AC compressor and PTC heater are directly used electric power from HV battery, it can effect energy consumption and travel distance results.
6. For the travel distance on a single charge of WLTC tests, comparing the reduction rate in travel distance on single charge in all WLTC areas (combination), when use AC on heating mode (outside air temperature 5℃), the reduction rate is 17.7%, the travel distances decrease by 52 km, from 294 km (AC off) to 242 km (AC on). When use AC on cooling mode (outside air temperature 35℃), the reduction rate is 27.4%, the travel distances decrease by 92 km, from 336 km (AC off) to 244 km (AC on).

Therefore, for the eco-driving method to improve energy efficiency of BEV using mode and real driving tests, in urban and rural areas, it is effective to increase vehicle speed and reduce idle time frequency. In highway area, lowering vehicle speed is effective to improve energy consumption. It is also effective to refrain from using AC system to improve energy consumption.

REFERENCES

(1) Tomonori Niizato : Powertrain for Passenger Cars in 2030, JSAE Annual Congress (Spring), https://tech.jsae.or.jp/paperinfo p/en/content/fty201902.04/, (Accessed, 4 August 2023).
(2) European Commission : The EU Transport Sector and It's Contribution to Reaching Climate Neutrality, https://www.climate.ec.europa.eu/eu-action/transport-emissions _en, (Accessed, 6 August 2023).
(3) Yasuko Kameyama : COP26 Closing, What Was Decided at the First COP of "Decisive 10 Years", https://www.nies.go.jp /social/navi/colum/cop26.html (Accessed, 4 August 2023).
(4) Prabuddha Chakraborty, Et al., : Addressing the range anxiety of battery electric vehicles with charging en route, https://www.nature.com/articles/s41598-022-08942-2, (Accessed, 6 August 2023).
(5) Hiroyasu Morohoshi, Et al., : Study on Fuel Consumption of Passenger Car by Mode and Actual Driving Tests, JSAE Kanto, International Conference of Automotive Technology for Young Engineers, (2019).
(6) Nobuyuki Ishii, Et al., : Study on Fuel Consumption of Hybrid Vehicle in Real Road Driving: Actual Road Fuel Consumption of Two-Motor Hybrid Vehicle, JSAE Kanto, International Conference of Automotive Technology for Young Engineers, (2020).
(7) Michael Melkior Kanugroho, Et al., : Study of Fuel Efficiency Improvement Method for Small Passenger Cars using Traffic Flow Simulation, JSAE Annual Congress (Spring), (2023).
(8) Meteorological Agency, Utsunomiya Meteorological Observatory, https://www.data.jma.go.jp/obd/stats/etrn/index.php, (Accessed, 4 August 2023).

研 究 ノ ー ト

黒沢良夫

A11 C34 D44 D45

ヴァイオリンの有限要素モデル化と粒子速度計測結果について

○大塚　駿　　黒沢　良夫
（帝京大）　　（帝京大）

3D printed top plate creation and finite element analysis of violin

Shun Otsuka　Yoshio Kurosawa
(Teikyo Univ.)　(Teikyo Univ.)

ヴァイオリンの振動音響解析を有限要素法で行うため，木材の材料データ（ヤング率，密度など）の同定や，3D スキャナで１つ１つのパーツの形状データの取得を行い，有限要素モデルを作成した．また，習得した形状データから 3D プリンタを用いてヴァイオリンを作成した．木製と 3D プリンタ製のヴァイオリンの振動計測結果や FE モデルの振動解析結果との比較等を紹介する．また，粒子速度プローブによる実験結果を紹介する．

Key words: 木質系材料，固有モード，実験解析，モード解析，

1. はじめに

現在製作されているヴァイオリンは職人の手によって作られているものが多い．職人の勘と経験によって製作・調整されているため，ヴァイオリンの板厚等は一つ一つの楽器で異なっており，弾いた際に鳴る音も当然異なる．そのため，構造（形状や板の厚さ）・材料をどのように変更したら音（振動）にどのような影響が出るか，楽器の違いによる音色の違いを実験計測や数値計算を用いて研究[1][2]し，将来的には，ヴァイオリンの製作技術・調整技術を数値化することを目標としている．

本研究では，3D スキャナで１つ１つのパーツの形状データの取得を行い，有限要素モデルを作成した．材料の木材（spruce，maple）について，ヴァイオリンの部品を作成した端材から梁を作り，振動実験と有限要素モデルの計算結果から材料データを同定した．また，習得した形状データから 3D プリンタ（Formlabs 製 Form3L）を用いてヴァイオリンを作成した．木製と 3D プリンタ製のヴァイオリンの振動計測結果や FE モデルの振動解析結果との比較等を紹介する．また，粒子速度プローブによる実験結果を紹介する．

2. 木材の材料データの同定

初めに，ヴァイオリンの部品を作成した端材から梁(図 1，図 2)を作り，振動実験を行った．なお製作した梁は木目方向と等しいもの，木目に直角なもの(年輪方向)，そして端材側面の木目方向と年輪方向の計 4 方向の梁を 2 本づつ製作した．梁の下側の中心を加振し，梁の 4 点の振動をレーザードップラー振動計を用いて計測した．実験で得られた伝達関数を用いて，モーダル解析を行い，一次曲げ，一次ねじり，二次曲げの梁の周波数を同定した．

Altair HyperMesh にて，梁の FE モデルを作成し，論文[3][4]から得た spruce，maple の剛性値から計算を行った．maple のヤング率 Ex は論文[5]より，12.6GPa を用いた．spruce に関しては，論文[6]に記載されている式(1)を用いて Ex を求めた．

$$E = \frac{48\pi^2 l^4 \rho {f_n}^2}{h^2 \theta_n^4} \tag{1}$$

f_n[Hz]：共振または反共振周波数，l[m]：試験片の対応する長さ，h [m]：厚さ，ρ [kg/m^3]：密度，θ_n：振動モードとモード次数によって決定する係数である．

FE モデルの計算結果と，実験結果との合わせ込みを行い，spruce, maple の剛性値の同定を行った．合わせ込みにより同定した剛性値の比を表 1 に示す．maple の剛性値の比は，ポアソン比を除く全ての値が文献値より大きくなった．spruce に関しては，計算で得た比と文献値がおおむね一致した．

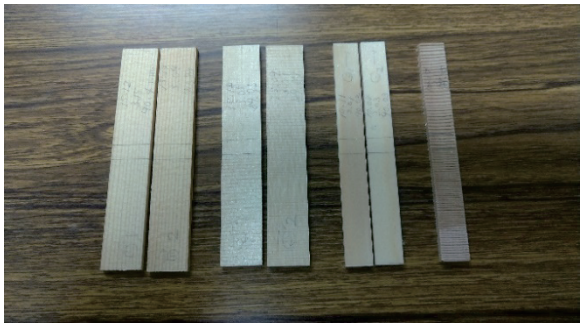

Fig.1 Spruce beams

Fig.2 Maple beams

Table.1 Stiffness value and Poisson's ratio of maple and spruce

Property		maple	spruce
Young's module	E_y/E_x	0.147	0.078
	E_z/E_x	0.072	0.043
Rigidity modulus	Gxy/Ex	0.124	0.064
	G_{yz}/Ex	0.023	0.003
	Gxz/Ex	0.091	0.052
Poisson's ratio	μxy	0.424	0.372
	μyz	0.774	0.435
	μxz	0.476	0.467

3. 有限要素モデルの作成

ヴァイオリンの各パーツを 3D スキャナ(Gom core 200 5M)にて読み込み(図 3), 3D 形状を取得し, Altair HyperMesh で表板(図 4), 裏板(図 5), 側板(図 6), ネック・指板(図 7)等の FE モデルを作成した. これらを組み合わせることで, 有限要素モデルのヴァイオリンとした(図 8).

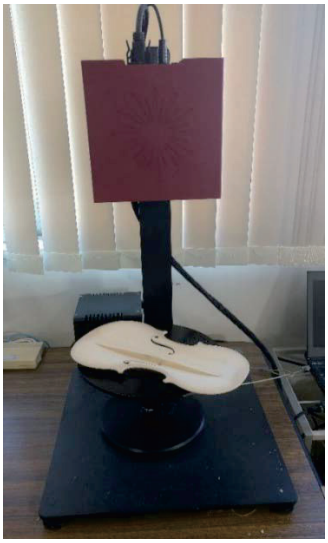

Fig.3 3D scanner (top plate)

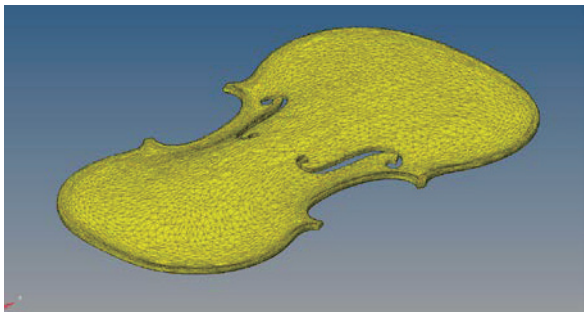

Fig.4 FE model of violin top plate

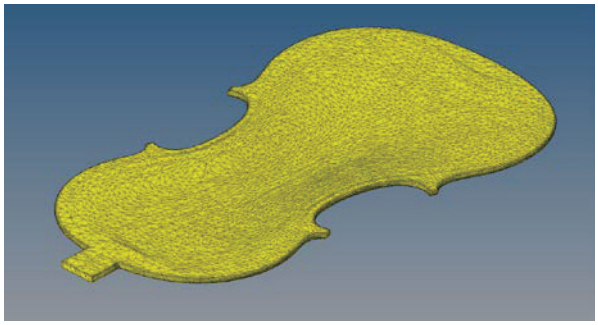

Fig.5 FE model of violin back plate

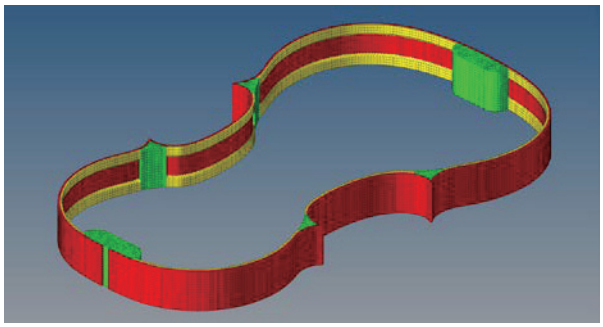

Fig.6 FE model of violin side plate

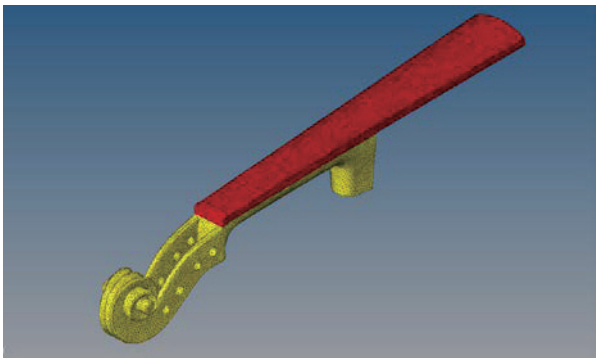

Fig.7 FE model for neck and figure board

Fig.8 FE model for violine

4.　実験結果と計算結果の比較

図 9 に，作成した有限要素モデルの計算結果と実験結果の振動加速度伝達関数の比較を示す．表板，裏板などニカワで接着された部分はばね要素でモデル化した．駒中央を表板向きに加振し，テールピースの 20mm 横付近（図 10 赤丸参照）の振動応答を計算・計測した．2000Hz まで計算し，おおよそ近い値となった．

図 10 に，栃木県産業技術センターの 3D プリンタ(formlabs 製 Form3L)を用いて，Clear Resin v4 を材料として作成したヴァイオリンの振動計測の様子を示す．Clear Resin v4 は等方性材料とし，ヤング率は 2.8GPa，密度は 1183.3kg/m^3 である．spruce の密度は 397.8 kg/m^3，maple の密度は 615.9kg/m^3 であり，形状は木製のヴァイオリンと同じだが，重量は 458g→ 814g と重くなった．木製ヴァイオリンの材料データを Clear Resin v4 の値に変更し，図 9 同様に伝達関数の計算結果と実験結果の比較結果を図 11 に示す．こちらもおおよそ計算結果は実験結果を再現できた．

図 12 に，木製ヴァイオリンと Clear Resin v4 ヴァイオリンの伝達関数計測結果の比較を示す．400Hz 以上で，振動レベルが小さくなっており，剛性・密度の影響と考えられる．図 13 に FE モデル同士の比較結果を示す．おおよそ図 12 と同様の結果が得られた．

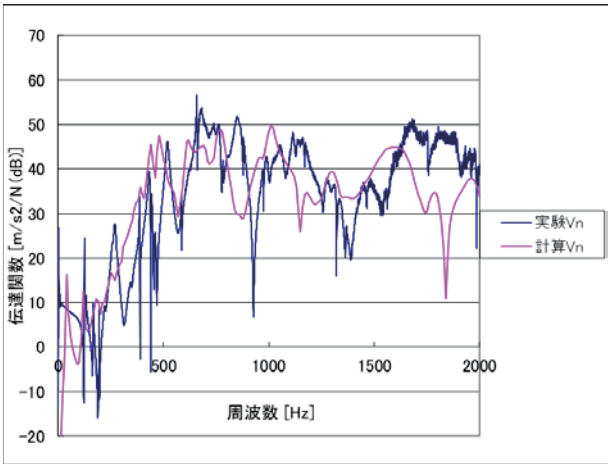

Fig.9 Comparison of experimental and calculated results for transfer function of wooden violin

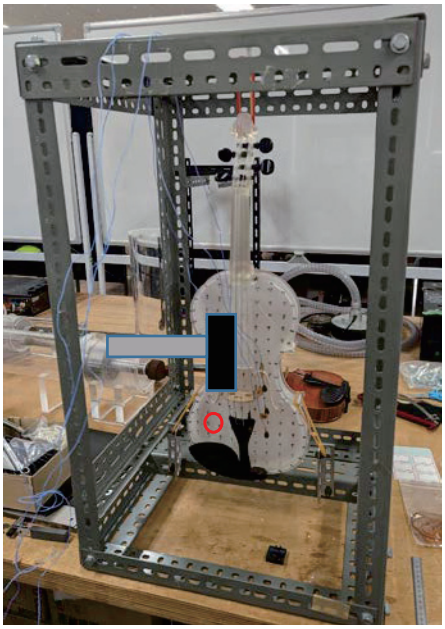

Fig.10 Setup of clear resin violin

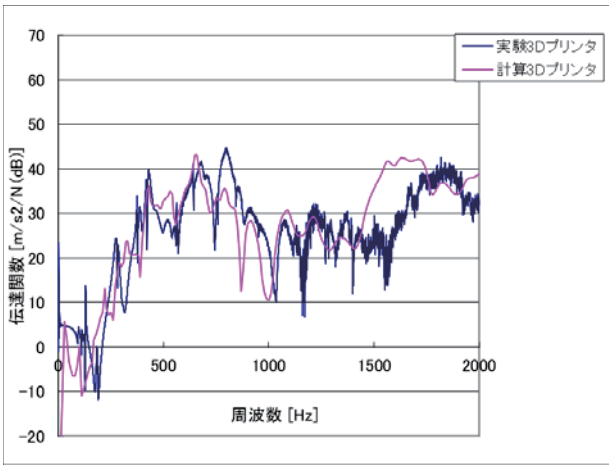

Fig.11 Comparison of experimental and calculated results for transfer function of clear resin violin

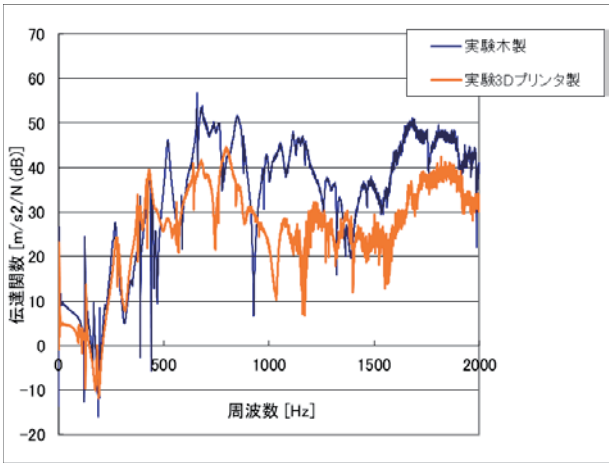

Fig.12 Comparison of transfer functions of wooden violin and clear resin violin (experimental results)

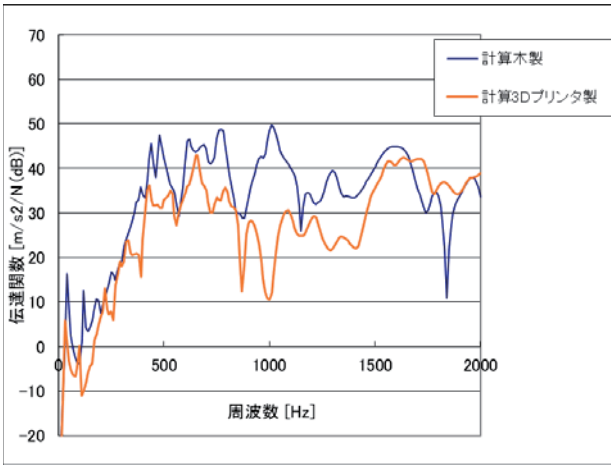

Fig.13 Comparison of transfer functions of wooden violin and clear resin violin (calculated results)

5. 粒子速度プローブを用いた実験結果

粒子速度プローブ(図 14)を用いて，木製のヴァイオリンと 3D プリンタ製のヴァイオリンのそれぞれ表板 12 か所の粒子速度計測を実施した．図 15 に G 線の開放弦を演奏時のそれぞれの楽器の計測結果を示す。材料の違いにより音の広がり方に変化が見られた。

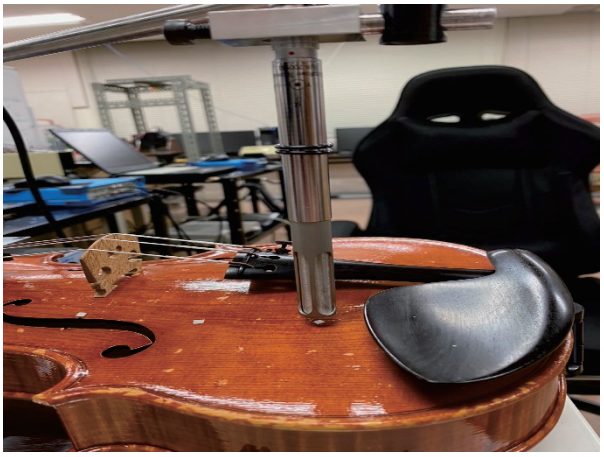

Fig.14 Setup of particle velocity probe

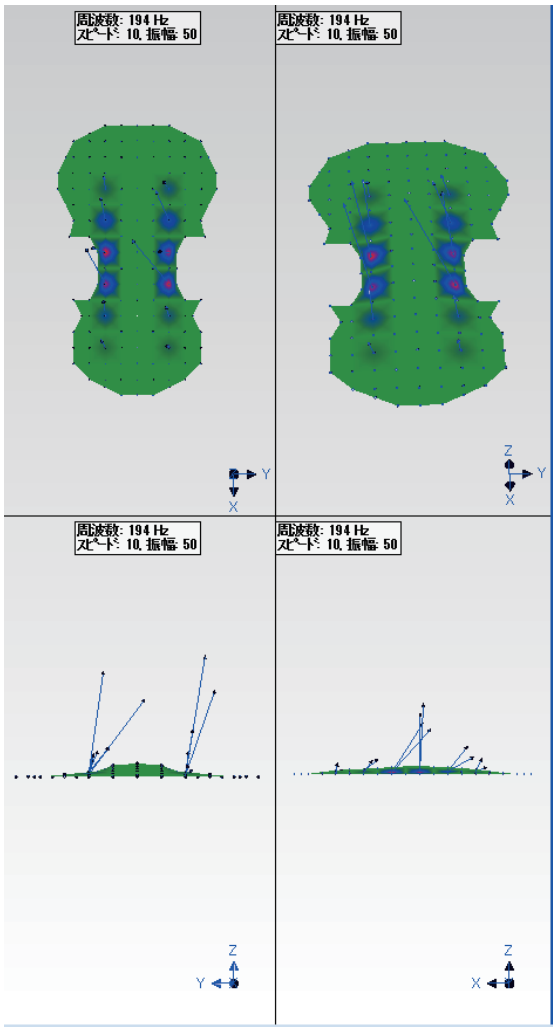

a. wooden violin

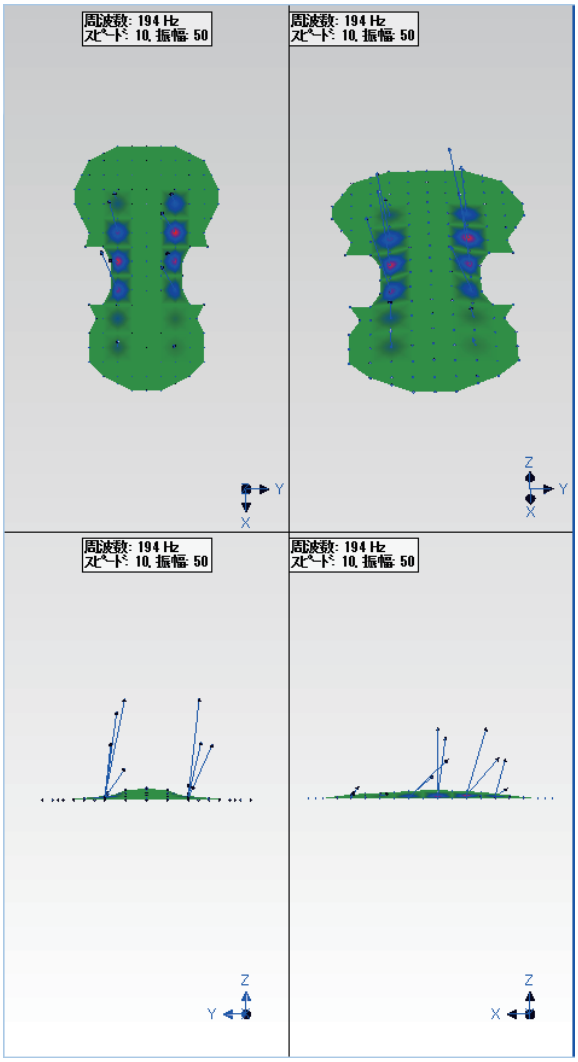

b.　Clear Resin v4

Fig.15 Particle velocity probe measurement results (G strings)

6.　おわりに

ヴァイオリンの有限要素モデルを作成した．実際のヴァイオリンの伝達関数計測結果と FE モデルの計算結果は近い値となった．また，3 D プリンタにてヴァイオリンを製作し，同形状で材質が異なった場合の伝達関数を比較した．その結果，密度や剛性値の違いで伝達関数が大きく異なることが確認できた．

また，粒子速度プローブを用いて木製のヴァイオリンと 3D プリンタ製のヴァイオリンの比較実験を行った．

謝　辞

今回実験に使用したヴァイオリンは，伊藤丈晃ヴァイオリン工房に作成頂いた．深く感謝いたします．

文　献

(1) 黒沢良夫，ヴァイオリンのバスバー有無による 振動・音への影響，制振工学研究会 2017 技術交流会資料集 SDT17023.
(2) 黒沢良夫，ヴァイオリンネックの振動解析，制振工学研究会 2021 技術交流会資料集 SDT21004.
(3) 横山真男ほか，日本音響学会音楽音響研究会資料 Vol.39，No.5, MA2020-27.
(4) Gough,C.E. ”A violin shell model: vibrational modes and acoustics” The Journal of the Acoustical Society of America137.3(2015):1210-1225.
(5) Green,D.W., Winandy, J.D., and Kretschmann, D.E. "Mechanical properties of wood. Wood handbook: wood az an engineering material” Madison, WI:USDA Forest service, Forest Products Laboratory,1999. General technical report FPL; GTR-133: (1999): 4.1-4.45, 133.
(6) 岸田雄太郎ほか，　クラシックギターの数値モデルの構築(構成部材における材料特性の実験的同定)，日本機械学会 D&D2021, No.311.
(7) 岡本朋也，黒沢良夫，3D プリンタによる表板作成とヴァイオリンの有限要素解析，制振工学研究会 2022 技術交流会資料集 SDT22007.

※制振工学研究会 2023 技術交流会原稿より
制振工学研究会事務局の承認を得て掲載

C34 C35 D46 E53

音響メタマテリアルにフェルトとゴム層を積層した防音材の遮音解析

○岩井　大地（帝京大）　黒沢　良夫（帝京大）　福井 一貴（寿屋フロンテ）　原山　和也（寿屋フロンテ）　荏原　裕典（寿屋フロンテ）

Sound insulation analysis of soundproofing materials made by laminating felt and rubber layers on acoustic metamaterials

Daichi Iwai (Teikyo Univ.)　Yoshio Kurosawa (Teikyo Univ.)　Kazuki Fukui (Kotobukiya Fronte Co.,Ltd.)　Kazuya Harayama (Kotobukiya Fronte Co.,Ltd.)　Ebara Hironori (Kotobukiya Fronte Co.,Ltd.)

PP をハニカム構造に加工したものの上下にフィルムを貼り，膜振動による吸音効果を持つ音響メタマテリアルを作成した．さらにフィルム部分に小さな穴を開け，ヘルムホルツ共鳴による吸音効果を追加した．自動車トリムへの適用を考慮し，本構造にフェルトとゴム層を積層した. 本構造を有限要素法でモデル化し, 透過損失の計測結果・計算結果について報告する.

Key words: Acoustic, Sound insulation, CAE, FEM, Metamaterial

1. 緒　　言

近年，自動車の快適性が重視され，車内騒音の低減（車内静粛性の向上）がすすんでいる．環境問題への対応から，電気自動車やハイブリッド車の割合が増えてきている．これらの自動車では，エンジン騒音が減った分，風切り音やタイヤ騒音が目立つ結果となり，対策が必要となってきている．ドアミラー，ピラー形状，車両外観等の風切り音の音源対策やタイヤ単体での騒音対策にも限界があり，コスト・重量も考慮すると車体側での対策が重要である．また，日本では国連の車外騒音規制への対応もあり設計構想段階から低騒音化が求められている．新たな車外騒音規制では，従来と走行条件が異なり，車外騒音に対するタイヤのパターンノイズの寄与が大きくなっている．そのため，これらの騒音を音響メタマテリアルを用いて低減することを考えた.

メタマテリアルとは人工的に作られた物質という意味であるが，音響で用いる場合は，膜振動や共鳴を持つ小型の微細構造を周期的に配置するものが多い. 本研究では 1 枚の PP（ポリプロピレン）のシートを折りたたみ，六角形の断面形状のハニカムの繰り返し構造を作る．そこに PP や PE（ポリエステル）からなる薄いフィルムを接着することにより，フィルムの面外振動により音響エネルギーを吸音する音響メタマテリアルを用いた[1]. 本論文では，フィルムに穴を開けることでヘルムホルツ共鳴による吸音効果を付与した構造[2]のテストピースについて，自動車トリムへの適用を考慮し，本構造にフェルトを積層したテストピースを作成した. テストピースの最上部にゴム，音響メタマテリアルの上面，下面，両面にフェルトを積層した場合，それぞれ穴なし，上面穴あり，下面穴あり，両面穴ありの場合に遮音性能にどのように影響があるか計測結果を比較した．また，有限要素法を用いてモデルを作成し，遮音性能の解析を行った．計測結果との比較等を報告する.

2. テストピースの計測結果と計測結果

2・1　計算手法

波長に対して極端に狭い空間では，空気の有する粘性により壁面境界近傍において粘性減衰が生じる．また，音の伝播過程において膨張・圧縮により発生した熱は，空気の熱容量に比して大きい壁面材料に伝達し散逸する．そのため，微小な空間を伝播する音波については，微小振幅を仮定して線形化した Navier-Stokes 方程式，熱伝導方程式，質 量保存則および状態方程式の 4 つの式を基本支配方程式として考えるのが一般的である（3）.

変位・圧力・密度・温度の変動を微小として方程式を線形化すると式（1）~式（3）を得る.

$$\rho_0 j\omega \boldsymbol{v} = -\nabla p + \mu\nabla^2 \boldsymbol{v} + \frac{1}{3}\mu\nabla(\nabla\cdot\boldsymbol{v}) \quad (1)$$

$$\kappa\nabla^2\tau = j\omega\rho_0 C_p\tau - j\omega p \quad (2)$$

$$\nabla\cdot\boldsymbol{v} + j\omega\left(\frac{\delta}{\rho_0} - \frac{\tau}{T_0}\right) = 0 \quad (3)$$

ρ_0：空気の密度，j：虚数単位，ω：角周波数，p：音圧変動，μ：粘性係数，v：速度変動，κ：熱伝導率，τ：温度変動，Cp：定圧比熱，δ：密度変動である．

2・2　テストピースと FE モデル

図 1 に今回計測で用いた音響メタマテリアルのテストピースを示す．1 辺 150㎜ の正方形にくり抜いたものを準備した．ハニカムは 1 辺の長さが 4.342㎜ の 6 角形で，高さは約 10㎜ である．図中赤枠で囲った部分はヘルムホルツ共鳴による吸音効果を付与するためのフィルムの穴を示す．今回は穴なし，上面（音が入射するのと反対側）に直径 0.7㎜ の穴，下面（音が入射する側）に直径 0.7㎜ の穴，両面に 0.7㎜ の穴の 4 種類のテストピースを作成した．円形の穴を開けたが実際は若干小さめの楕円形となった（図 1 右図）．

図 2 に今回用いた音響メタマテリアルの断面図を示す．図中上下の黒い線は PP，PE，PP からなるフィルムを示す．厚さは約 0.065㎜ である．黄色い部分は PP からなるハニカムを示す．ハニカムの厚さは約 0.15㎜ である．青い部分は空気である．1 枚の PP のシートからハニカム構造を作成するため，音が入射する下面はフィルムのみの部分とフィルム＋PP の部分が交互にあるのが特徴である．

図 3 に今回作成した有限要素モデルを示す．図 3a. が音響メタマテリアル単体(図中青色)で，1 列おきに交互に中央に 0.7㎜ の穴が開いている．図 3b. は厚さ 0.8㎜ のパネル（図中茶色）の上に厚さ 10㎜ のフェルト（図中白色）を積層し，その上にメタマテリアル，ゴム(図中緑色：以下 HL)の順に積層したモデルである．図 3c. は，パネルの上に音響メタマテリアルを積層し，その上にフェルト，ゴムの順に積層したモデルである．図 3d. は，パネルの上にフェルトを積層し，その上に音響メタマテリアルを積層し，その上に同じフェルト，ゴムの順に積層したモデルである．それぞれ，穴なし，上面穴，下面穴，両面穴モデルを作成したので，計 12 種類のＦＥモデルを作成した．両面にフェルトを積層したモデルで約 47 万要素である．下側からホワイトノイズを入力し，透過損失を計算した．

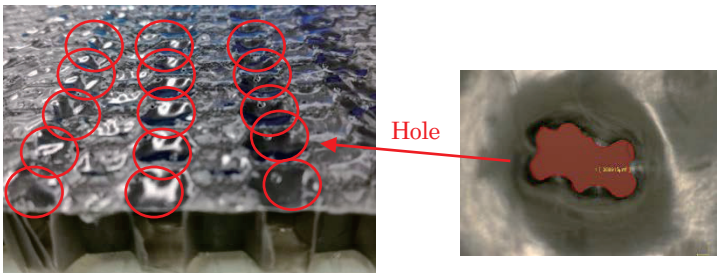

Fig.1 Test piece of acoustic metamaterial

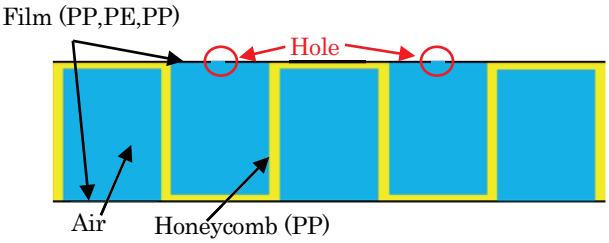

Fig.2 Sectional drawing of test piece

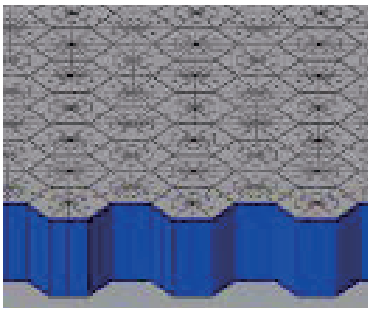

a. Metamaterial

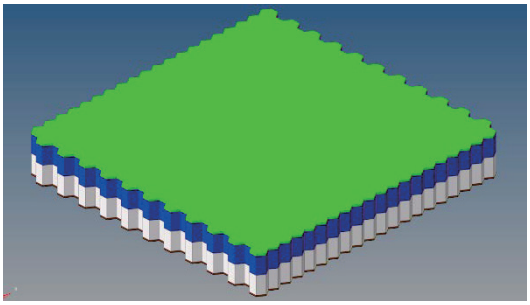

b. Panel + Felt + Metamaterial + HL

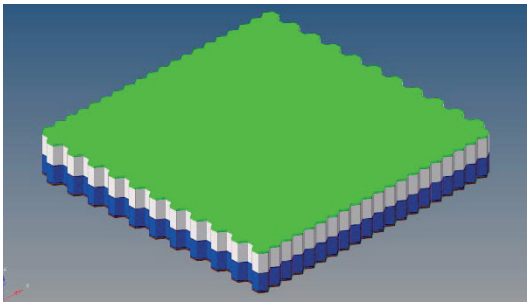

c. Panel + Metamaterial + Felt + HL

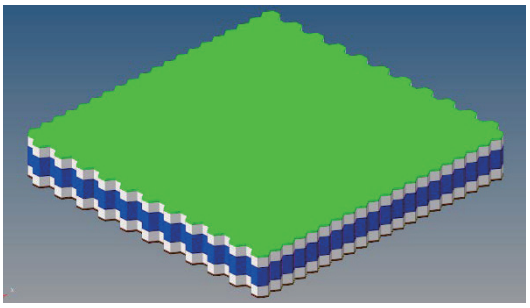

d. Panel + Felt + Metamaterial + Felt +HL

Fig.3 FE model for test piece

3.　計測結果と解析結果

3・1　同じフェルトの積層位置で穴構造の違いによる比較

図 4 に厚さ 0. 8㎜ のパネルの上に厚さ 10㎜ のフェルトを積層し，その上に音響メタマテリアル, ゴムの順に積層したテストピース（図 3b. ）の透過損失の計測結果と計算結果を示す．穴なし（図中青線），上面（音が入射するのと反対側）に直径 0. 7㎜ の穴（図中黄色線），下面（音が入射する側）に直径 0. 7㎜ の穴（図中オレンジ線），両面に 0. 7㎜ の穴（図中灰色線）の 4 種類の比較を行った．計測結果（図 4a. ）では 1250～3150Hz バンドで穴なしと下面穴の計測結果に透過損失の落ち込みがあり，同様に計算結果（図 4b. ）では 1000～3150Hz で差がみられた．

図 5 にパネルの上に音響メタマテリアルを積層し, その上にフェルトを積層したテストピース（図 3c. ）の透過損失計の計測結果を示す. 計測結果（図 5a. ）では 1250～3150Hz バンドで穴なしと上面穴の計測結果に落ち込みがあり,計算結果（図 5b. ）では 1600～3150Hz で差がみられた．穴がない面とパネルが積層されているテストピースであり下面に穴を開けるほうが高性能になった.

図 6 にパネルの上にフェルトを積層し，その上に音響メタマテリアルを積層し，その上に同じフェルトを積層したテストピースの透過損失の計測結果を示す．計測結果（図 6a. ）では低周波域である 800～2000Hz において穴による変化がみられたが, 計算結果（図 6b. ）では穴の有無による性能の変化は見られなかった.

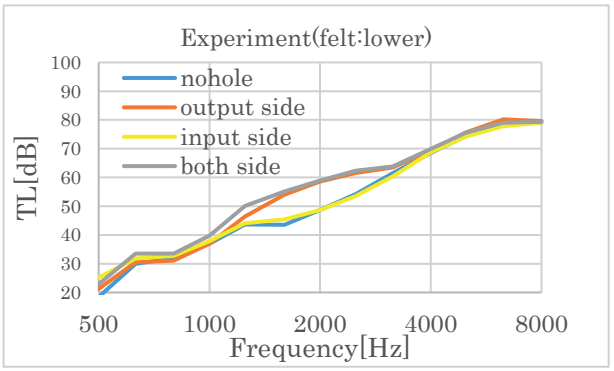

a. Experimental results

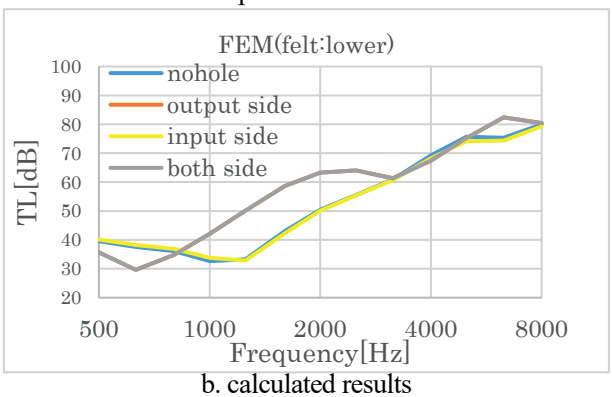

b. calculated results

Fig.4 Comparison of experimental results and calculated results for transmission loss by lower felt

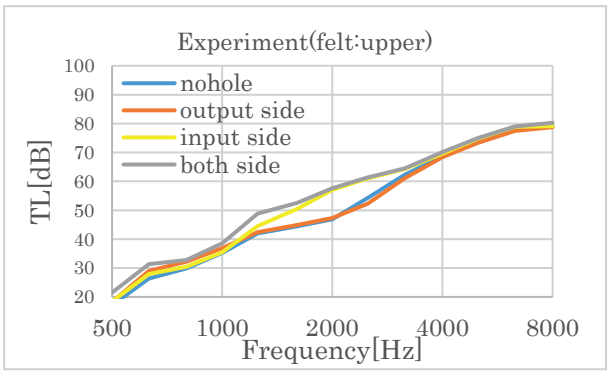

a.　Experimental results

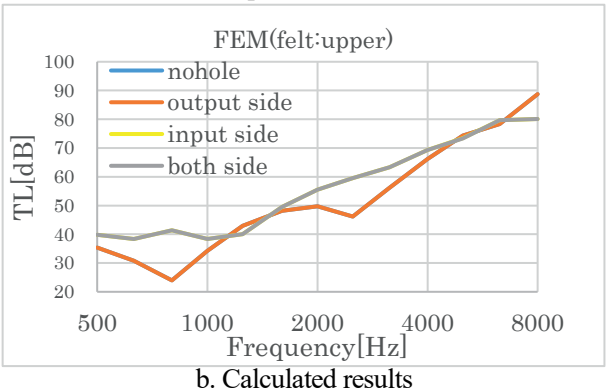

b. Calculated results

Fig.5 Comparison of experimental results and calculated results for transmission loss by upper felt

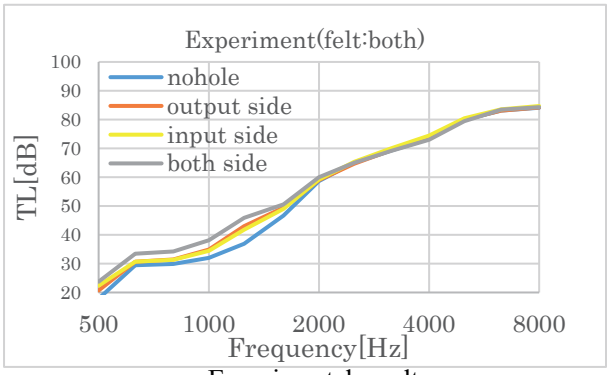

a. Experimental results

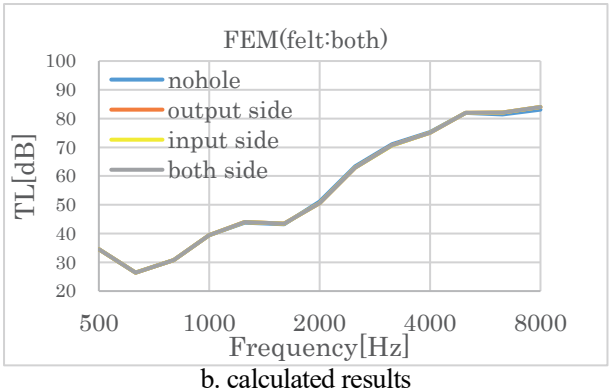

b. calculated results

Fig.6 Comparison of experimental results and calculated results for transmission loss by both felt

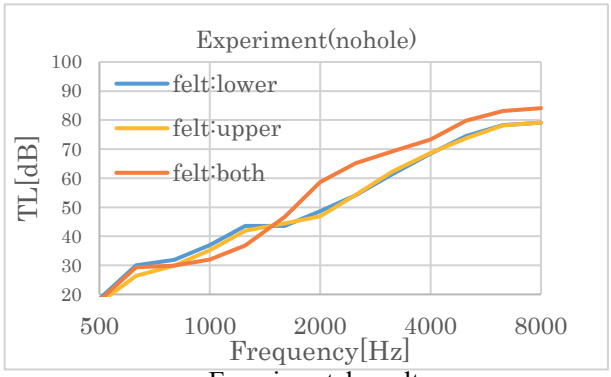

a. Experimental results

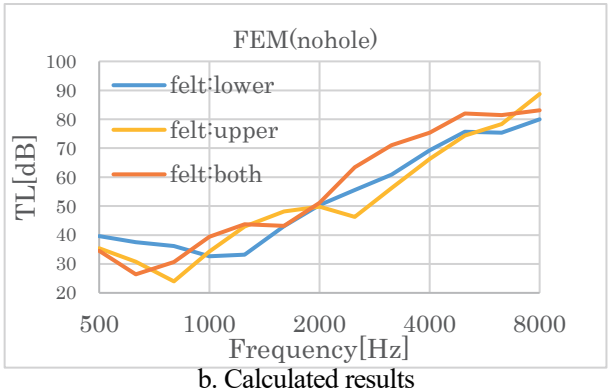

b. Calculated results

Fig.7 Comparison of experimental results and calculated results for transmission loss by no hole

3・2　同じ穴構造でフェルトの積層位置の違いによる比較

図 7 に穴なしの音響メタマテリアルの透過損失の計測結果（図 7a.）と計算結果（図 7b.）の比較を示す．下フェルト（図 5b.　参照：図中青線），上フェルト（図 5c. 参照：図中黄色線），上下フェルト（図 5b. 参照：図中オレンジ線）の 3 つで比較すると，計測結果・計算結果とも下フェルトと上フェルトはおおよそ同程度の性能で，上下フェルトの性能が高周波域において高くなっている．透過損失の計算結果はおおよそ計測結果の傾向を再現している．

図 8 に上面穴，図 9 に下面穴，図 10 に両面穴の音響メタマテリアルの透過損失の計測結果と計算結果の比較を示す．穴なしと同様の傾向で，計算結果はおおよそ計測結果の傾向を再現している．

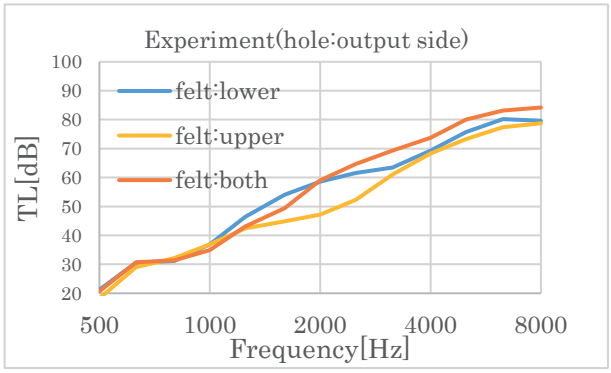

a. Experimental results

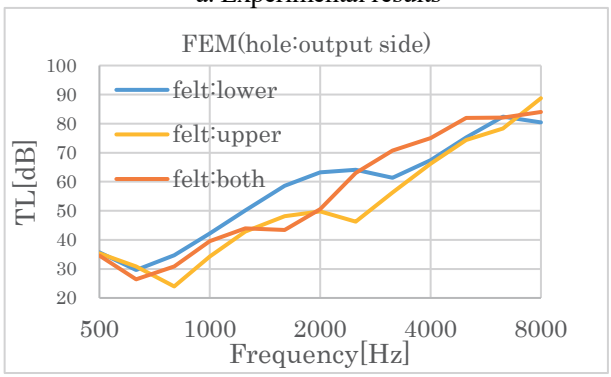

b. Calculated results

Fig.8 Comparison of experimental and calculated results for transmission loss by output side holes

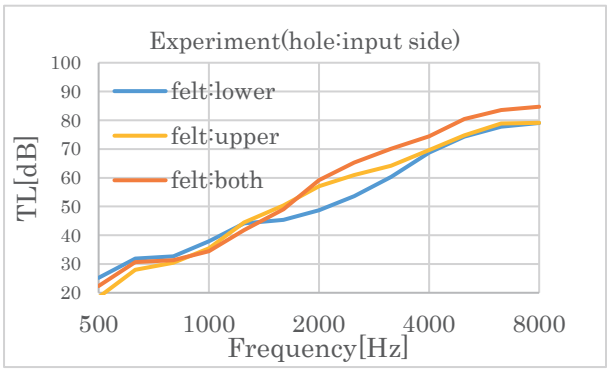

a. Experimental results

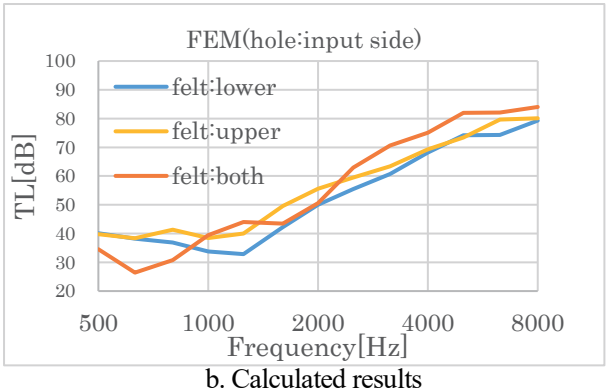

b. Calculated results

Fig.9 Comparison of experimental and calculated results for transmission loss by input side holes

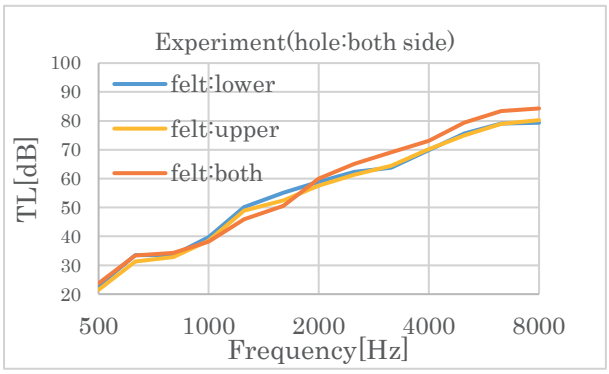

a. Experimental results

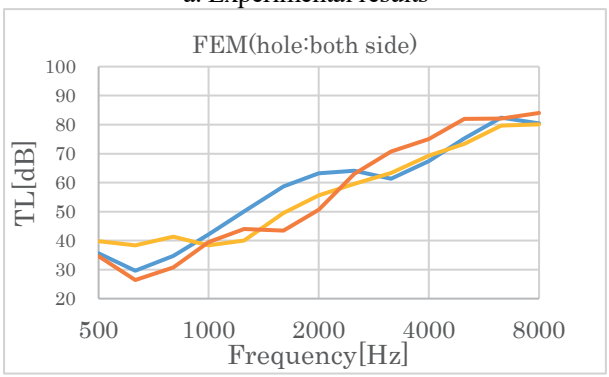

b. Calculated results

Fig.10 Comparison of experimental and calculated results for transmission loss by both side holes

3・3　同じ穴構造・フェルトの積層位置でゴム層の有無の違いによる比較

図 11 に下面フェルトにおける両面穴の音響メタマテリアルの透過損失の計測結果（図 11a.）と計算結果（図 11b.）の比較を示す．ゴムあり（図中青線），ゴムなし（図中黄色線）の 2 種類の比較を行った．下面フェルトでは 6300Hz における透過損失が計測結果（図 11a.）で 59. 2dB から 79. 05dB と約 20dB ゴムありの性能がよく，計算結果（図 11b.）では 64. 5dB から 82. 41dB と計測結果同様に約 20dB の性能向上がみられた．

図 12 に上面フェルトにおける両面穴の音響メタマテリアルの透過損失の計測結果（図 12a.）と計算結果（図 12b.）の比較を示す.計測結果に比べて計算結果の性能上昇幅が小さいのは,計算結果におけるゴムなしの解析精度が不十分だと考えられる．

図 13 に上下面フェルトにおける両面穴の音響メタマテリアルの透過損失の計測結果（図 13a.）と計算結果（図 13b.）の比較を示す.下面フェルト同様に計測結果,計算結果ともに約 20dB の性能向上がみられた．

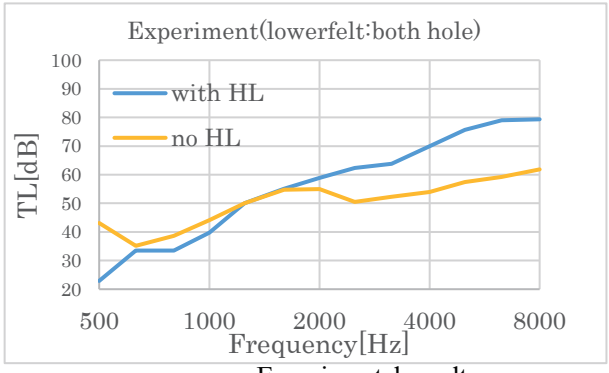

a. Experimental results

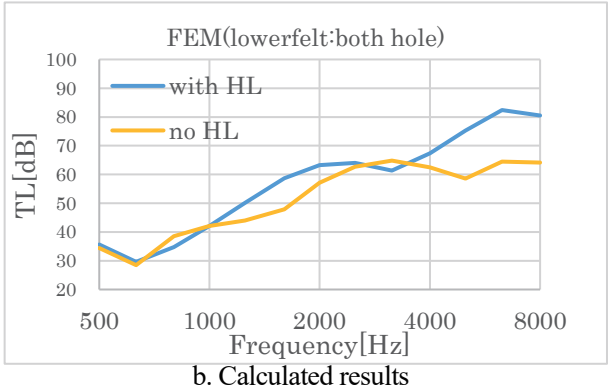

b. Calculated results

Fig.11 Comparison of rubber ants and no rubber with both side holes by lower felt

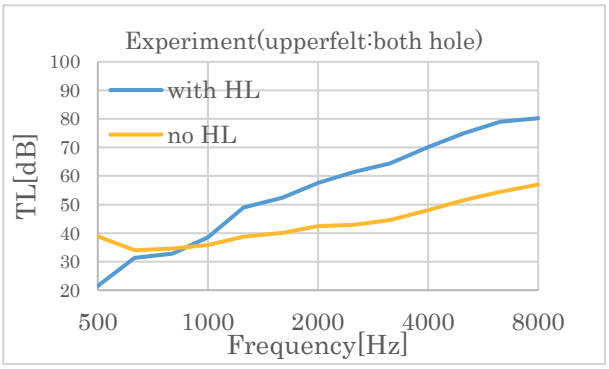

a.Experimental results

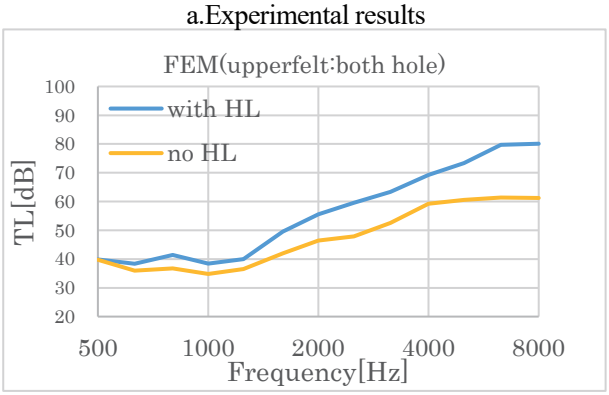

b.Calculated results

Fig.12 Comparison of rubber ants and no rubber with both side holes by upper felt

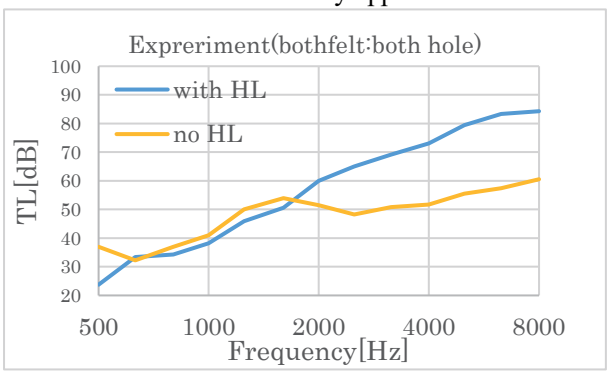

a.Experimental results

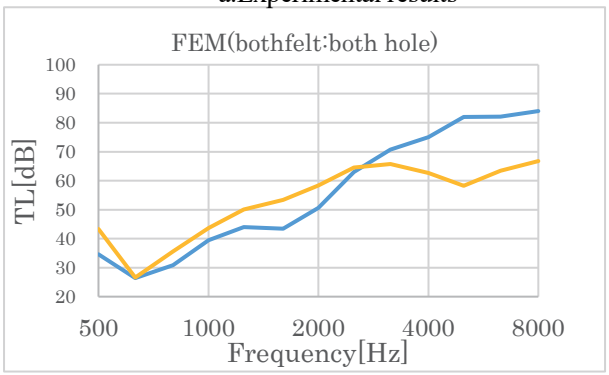

b.Calculated results

Fig.13 Comparison of rubber ants and no rubber with both side holes by both felt

4. まとめ

自動車用防音材として用いる，PP をハニカム構造に加工したものの上下にフィルムを貼り，4 種類のパターン（穴なし，上面，下面，両面）でセルの中央に穴を開けた音響メタマテリアルのテストピースを作成し，3 種類の積層パターン（パネル＋フェルト＋メタマテリアル，パネル＋メタマテリアル＋フェルト，パネル＋フェルト＋メタマテリアル＋フェルト）と組み合わせて，最上部にゴムを積層した計 12 種類の透過損失の計測を行った．

ゴムを最上部に置くことにより，すべてのモデルで遮音性能が大きく向上した．下面フェルトでは，約 1250～3150Hz において穴なし，下面穴と上面穴，両面穴で差が生じ，上面フェルトでは約 1250～3150Hz において穴なし，上面穴と下面穴，両面穴で差が生じ，下面に穴を開ける方が高性能になった．上下面フェルトでは計測結果において 1250Hz 付近で穴径による差がみられた．

また，テストピースと同様の FE モデルを作成し，透過損失を計算した．計算結果は下面フェルト，上面フェルトでは計測結果をおおよそ再現できた．上下面フェルトの計測結果における穴位置による透過損失の違いを FE モデルで再現することが今後の課題である．

文　　献

(1) 黒沢良夫，福井一貴，“メタマテリアルの吸音解析”日本機械学会 Dynamics and Design Conference 2019, No.337(2019) , p.1-6.

(2) 次橋一樹，田中俊光，草苅樹宏，“多孔板を含む音場の数値解析法に関する研究（第 2 報：多孔板の音響連成振動を考慮する場合）”，日本機械学会論文集 C 編，Vol. 78, No. 789 (2012), pp.535-545.

(3) Kampinga, W. R., Wijnant, Y. H. Boer, A., “Performance of several viscothermal acoustic finite elements, *Acta Acustica united with Acustica*, Vol. 96 (2010), pp.115-124.

(4) Beltman, W. M., Hoogt, P. J. M., Spiering, R. M. E. , Tijdeman, H., “Implementation and experimental validation of a new viscothermal acoustic finite element for acoust-elastic problems”, Journal of Sound and Vibration, Vol.216 (1998), pp.159-185.

(5) Beltman, W. M., “Viscothermal wave propagation including acousto-elastic interaction, partI, Theory”, Journal of Sound

and Vibration, Vol.227 (1999), pp.555–586.
(6) Beltman, W. M., “Viscothermal wave propagation including acousto-elastic interaction, partII, Application”, Journal of Sound and Vibration, Vol.227 (1999), pp.587-609.
(7) 山本崇史，黒沢良夫，“微小音響空間の粘性減衰と熱散逸を考慮したモデル化と等価特性の検討”，日本機械学会論文集，Vol. 81, No. 830 (2015), pp.1-16.
(8) 岩井大地, 黒沢良夫, 福井一貴,原山和也，“音響メタマテリアルにフェルトを積層した防音材の遮音解析”,制振工学研究会 2022 技術交流会.

※制振工学研究会 2023 技術交流会原稿より
制振工学研究会事務局の承認を得て掲載

研 究 ノ ー ト

蓮田裕一

4th International Symposium on Engineering and Technology Innovation（ISBENS2023）

Practice and Effects of Manufacturing Education through the Challenge to Testing Skill Proficiency of Machining at Universities

Masanori TAKANO[a], Gai KANEDA[a], Koichi MURO[a], Yuta FUKUSHIMA[a], Yuichi HASUDA[a*]

[a] School of Science and Engineering, Teikyo University

1-1 Toyosatodai, Utsunomiya,Tochigi, Japan

* hasuda@ics.teikyo-u.ac.jp

Abstract

Production technology that produces high-quality products is essential for the continuation of Japan's development, and for this reason, it is important to systematically train young engineers with high technical skills. Therefore, it is very meaningful for science and engineering university students to experience the machining of machine parts during practical training and graduation research while they are in school. At Teikyo University Faculty of Science and Engineering, teacher offer classes on the design and processing of mechanical parts. We hope to improve the technical skills of the students and develop human resources with high technical skills. Therefore, in order to acquire the skills to process complex parts, teachers at Teikyo University educated students on machining techniques in classes and after-school circle activities, and students learned how to use machine tools. We are challenging the skill proficiency test based on the technology.

The mechanical skill proficiency test not only contributed to the improvement of students' processing skills through manufacturing. For example, students make full use of the skills they have acquired in the machining process to create autonomous robots, which have achieved great results in global robot contests. It is one of the factors that made it possible to demonstrate the achievements of these world-class robots is the ability to process robot parts with high precision. Efforts for skill proficiency tests have also had a tremendous effect on career education. The students who participated in the certification exam were able to tell the recruiting staff of the company specifically what they had done during their school days in job hunting, so they were able to get a job at a company with a higher ranking than other students. It is also a big advantage that you can decide to find a job earlier.

Student’s ability to work in groups and communicate is also a great appeal to Japanese companies. This is because it will be a great advantage when interviewing and clarifying your motivation. Many students who have taken the skill proficiency test have shown the surprising effect of finding employment. In this study, we report the practice and effect of manufacturing education through the skill proficiency test of machining in Teikyo University Mechanical Engineering Department.

Keywords: testing skill proficiency, manufacturing education, lathe, autonomous robot

1. Introduction

Japan, which has few resources, has become one of the world's leading economies by manufacturing highly reliable industrial products with its excellent industrial technology. Production technology that produces high-quality products is essential for the continuation of Japan's development, and for this reason, it is important to systematically train young engineers with high technical skills [1]. Therefore, it is very meaningful for science and engineering university students to experience the machining of machine parts during practical training and graduation research while they are in school. It is necessary to provide technical education in which students actually experience the operation of CAD/CAM and machine tools, in addition to the conventional design and production centered on classroom lectures at universities. Furthermore, the placement of excellent faculty members who guide these students and the establishment and practice of technical instruction methods will lead to the improvement of the educational capabilities of the university itself.

At Teikyo University Faculty of Science and Engineering, the Department of Mechanical and Precision Systems Engineering and the Robot and Mechatronics Course of the Department of Information and Electronic Engineering offer classes on the design and processing of mechanical parts. In addition, among the student circle activities, there are circles that build robots and formula cars, and there are many students who are highly interested in manufacturing. Many of these activities involve machining, and by designing and manufacturing the parts designed by the students themselves, we hope to improve the technical skills of the students and develop human resources with high technical skills. can have Therefore, in order to acquire the skills to process complex parts, teachers at Teikyo University educated students on machining techniques in classes and after-school circle activities [2], and students learned how to use machine tools. We are challenging the skill proficiency test based on the technology [3・4]. In this study, we report the practice and effect of manufacturing education through the skill proficiency test of machining in Teikyo University Mechanical Engineering Department.

2. Skill proficiency test and mechanical education facilities practiced at Teikyo University Faculty of Science and Engineering

2.1 Skill proficiency test

skill proficiency test is "a national test system that tests the skills of workers according to certain standards and certifies them as a country of Japan"[3]. This skill proficiency test is conducted for 137 occupations, and those who pass the skill test receive a high evaluation at each workplace. Support for students is provided by 6 technical staff members and 1 professor belonging to the Department of Mechanical and Precision Systems Engineering and the Department of Information and Electronics Engineering. In addition, all of our technical staff are qualified as 1st grade machining technicians, and 3 of them are special

grade machining technicians. We also hold certification exams at our facilities. As a result of recent educational guidance for certification exams, 2 students passed the 3rd grade in 2020, 1 student passed the 3rd grade in 2021, and 1 student passed the 1st grade and 2 students passed the 2nd grade in 2022.

2.2 Educational facilities in mechanical training factories

The practical training factory of the Faculty of Science and Engineering of Teikyo University was established in 1989, and is mainly used for practical training using machine tools, classes such as experiments, graduation research, and the production of samples and parts for student circles. Figure 1 shows the main machining equipment. We have approximately 30 machine tools, including machining centers, NC lathes, and ultra-precision surface grinders, and we can use the CAD/CAM system to provide consistent education for students, from design to production.

(a) NC lathe

(b) Engine lathe

(c) Milling machine

(d) Machining center

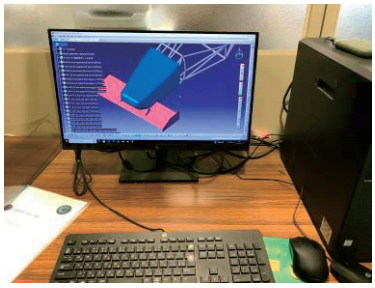

(e) CAD/CAM

(f) Welding machine

Fig. 1: Machine tools and equipment that support educational activities

3. Practice of manufacturing education through Skill Proficiency test of machining

3.1 Description of lathe mechanism and processing principles

Some of the students who take the skill proficiency test of machining have experienced machining at technical high schools, but for most students it is almost their first time machining. Therefore, teachers started to teach the types and mechanisms of NC lathes and ordinary lathes, as well as applications such as machining examples (see Fig. 2 and 3). After that, as shown in Fig. 3, students actually experience machining such as simple outline cutting and end face cutting, and learn the basic operation method of the lathe.

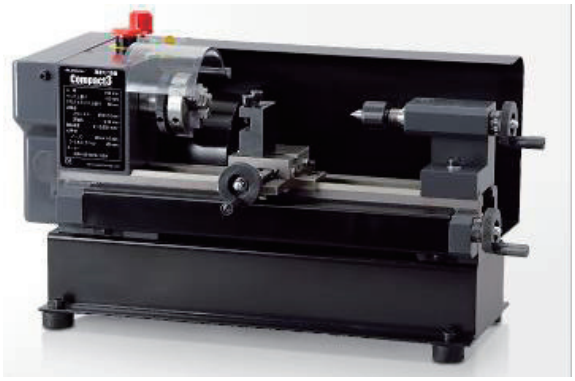

Fig. 2: Simple Engine lathe in the Department of Information and Electronics Engineering

Fig. 3: Machining experience such as contour cutting and end face cutting using Engine lathe

3.2 Guidance on handling measuring instruments

One of the important factors in the skill proficiency test is how to use measuring instruments to complete products with higher processing accuracy. As shown in Fig. 4, in mechatronics classes, students learn basic measurement methods using vernier calipers, micrometers, and height gauges. Students who challenge the skill proficiency test experience how to use measuring instruments during machining, which is even more difficult.

When performing measurement in lathe work, the workpiece is clamped in the chuck, so the measurement is mostly done while bending down a little. Therefore, it is much more difficult than sitting in a chair and measuring in an easy-to-measure position, and measurement errors are more likely to occur. In fact, when the outer diameter and inner diameter are measured with a vernier caliper by tightening the workpiece on the lathe, there is a measurement error of 0.2 to 0.3 mm even though the same point is measured. When such errors occur, it is almost impossible for a student to process a product that passes the skill proficiency test.

Therefore, higher-dimensional measurement techniques are required for higher-precision machining. Students were instructed repeatedly to measure the outer diameter, inner diameter, depth, etc. according to the situation. Fig. 5 shows the state of measurement with a vernier caliper with the workpiece mounted on the lathe. From Fig. 5, it can be seen that it is difficult to measure due to the influence of the measurement posture and space

(a) Measurement with vernier calipers and micrometer

(b) Basic measurement with height gauge

Fig. 4: Basic measurement methods for vernier calipers and height gauges

(a) Measurement with vernier calipers

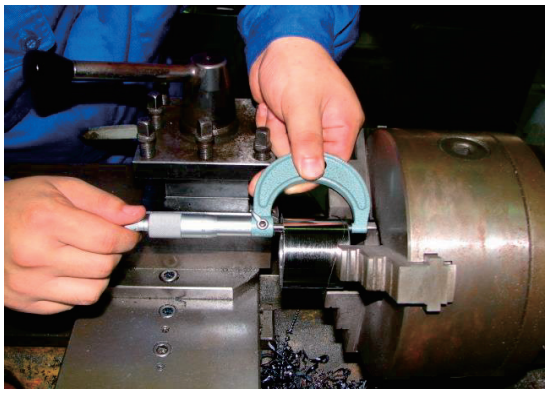

(b) Measurement with a micrometer

Fig. 5 : Accurate measurement of the workpiece attached to the lathe

4. Guidance plan for examination tasks

4.1 Important teaching method for passing

In order to pass the test, students learn not only how to use measuring instruments, but also the machining process, selection of tools, cutting conditions, conditions of the material to be processed, and placement of tools. The time limit for the certification test is 3 hours for the 2nd grade and 2 hours for the 3rd grade, and the product must be manufactured with the required accuracy within these time. Therefore, it is important to make quick measurements, operate machine tools quickly, select appropriate cutting conditions, and reduce the number of times workpieces are clamped, and select and replace tools. The important point is to shorten the time when not cutting. If that time can be shortened, it will be possible to carefully process areas with strict dimensional tolerances, and more accurate processing will be possible.

4.2 Creation of processing process chart

Since it is difficult to create a processing process chart for the 2nd grade skill proficiency test,

a staff member who is qualified as a 1st grade skill proficiency technician provided materials, and the students created it themselves. By creating the process chart by themselves, students will be able to simulate the processing of test assignments. There is a limit to the machining time, and when machining is performed to meet the required accuracy, it is important to know how to perform machining efficiently and how to perform machining effectively. Students are free from hesitation when moving to the next process, which greatly reduces thinking time and shortens work time.

4.3 Test subjects and their guidance

Students will be guided by an experienced teacher in understanding the tasks of the certification exam and in the actual processing experience. Fig. 6 shows the manufacturing drawing of the 3rd grade skill proficiency test of Lathe.

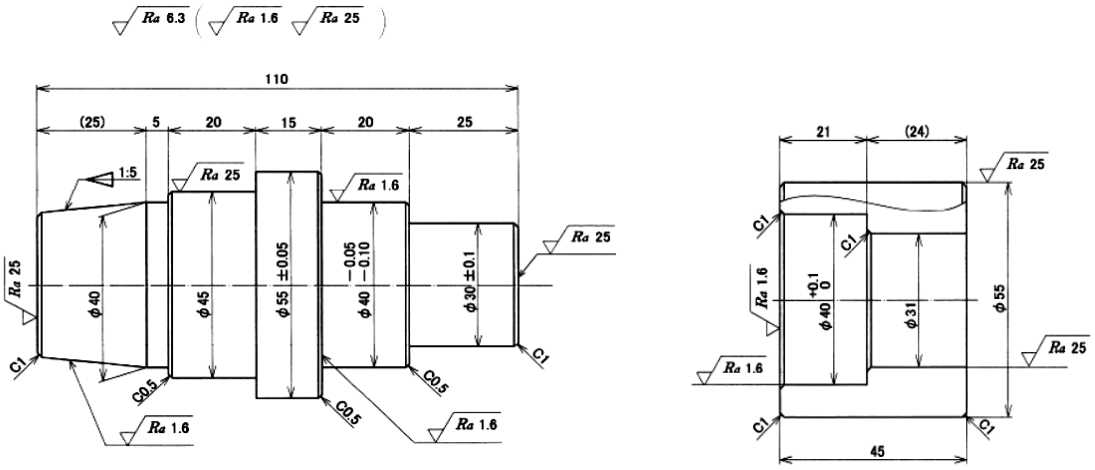

Fig. 6: Manufacturing drawing of the 3rd grade skill proficiency test of Lathe.

Using a Engine lathe, perform cutting such as inner/outer diameter cutting, taper cutting, thread cutting, knurling, and eccentric cutting for one ϕ60×150mm S45C material and one ϕ65×80mm S45C material. Perform the work test with a standard time of 3 hours and 30 minutes and a cut-off time of 4 hours.

In 2nd grade skill proficiency test of machining (Engine lathe work), machining is performed based on the manufacturing drawing shown in Fig. 7. Using a Engine lathe, perform cutting such as inner/outer diameter cutting, taper cutting, thread cutting, and eccentric cutting for one S45C material of ϕ60×150mm and one S45C material of ϕ60×57mm. The standard time was 3 hours, and the censoring time was 3 hours and 30 minutes.

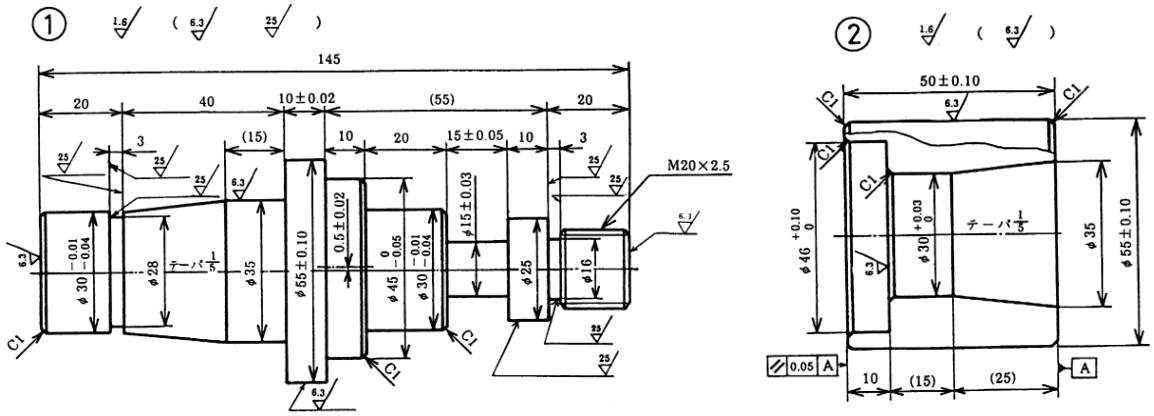

Fig. 7: Production drawing of skill proficiency test lathe 2nd grade

In the initial stage of machining instruction, the instructor instructed students one-on-one, explaining the flow of the process chart and making them memorize the tools to be used, cutting conditions, etc. When the students reached the stage where they could understand the order of processing, we measured the time used for processing. In 2022, it took about 5 hours 2nd grade skill proficiency test and about 3 hours for 3rd grade skill proficiency test. After that, the students were instructed to think about important methods for shortening the time and to process the assignment several times [5] (see Fig. 8).

(a) Teaching 3rd grade skill proficiency test tasks

(b) Teaching 2nd grade skill proficiency test tasks

Fig.8: Guidance for skill proficiency test lathe work

At the point when the skills were cultivated through the students' own efforts, the skills of the students improved dramatically by showing them how the skilled staff processed the examination tasks within the time limit. While the students themselves strongly felt what was necessary to clear the examination tasks, the educational effect of increasing their understanding and motivation was obtained. Gradually, all the students were able to

complete the machining within the time limit in the machining practice, and it was thought that the education on machining was able to be put into practice. Fig. 9 shows the works for the 2nd and 3rd grade skill proficiency test produced by the students who received systematic guidance from the teacher.

(a) 2nd grade skill proficiency test assignments

(b) 3rd grade skill proficiency test assignments

Fig. 9: 2nd and 3rd grade skill proficiency test tasks

5. Educational effects of trade skill proficiency tests on other fields

The mechanical skill proficiency test not only contributed to the improvement of students' processing skills through manufacturing. For example, students make full use of the skills they have acquired in the machining process to create autonomous robots, which have achieved great results in global robot contests. The student robot circle supervised by Professor Yuichi HASUDA, one of the authors, participated in the Youth Manufacturing Competition [6, 7] and the robot division of the Skills Competition for the first time in Japan as a student [8] (Fig. 10). See (a)), World Robot Olympiad (WRO) Japan representative from 2015 to 2018 and 2020 to 2022 won the Japanese tournament and has also participated in the world tournament [9]. Placed 10th at WRO 2015 Qatar, the first time it participated, 3rd at WRO 2017 Costa Rica (see Fig. 10(b)), and 6th at WRO 2019 Hungary (see Fig. 10(c)). It is one of the factors that made it possible to demonstrate the achievements of these world-class robots is the ability to process robot parts with high precision.

Another educational effect of the skill proficiency test is the jump-up award in the 2019 Japan competition and the design award in 2022 at the Japanese Formula Car Championship (see Fig. 10 (d)). It is the result of applying machining technology to the design and production of formula cars while making use of group work and communication skills.

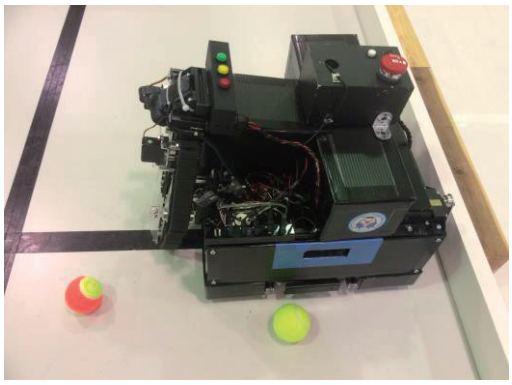

(a) Design and manufacture of automatic transport robots

(b) WRO 2017 Costa Rica　3rd place

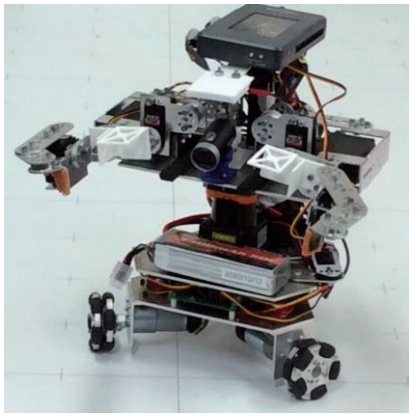

(c) WRO2017 Hungary 9th Place Robot

(d) Making parts for formula cars

Fig. 10: Educational effect of skill proficiency test

Efforts for skill proficiency tests have also had a tremendous effect on career education. The students who participated in the certification exam were able to tell the recruiting staff of the company specifically what they had done during their school days in job hunting, so they were able to get a job at a company with a higher ranking than other students. It is also a big advantage that you can decide to find a job earlier.

While making formula cars and autonomous robots, student's ability to work in groups and communicate is also a great appeal to Japanese companies. This is because it will be a great advantage when interviewing and clarifying your motivation. In Japan, job hunting begins in the latter half of the third year of university, and many students who have taken the skill proficiency test have shown the surprising effect of finding employment by the end of their third year.

6. Summary and outlook

In the 2022 certification exam, unfortunately, there were no passers for the 2nd grade skill proficiency test, but all 4 students passed the 3rd grade skill proficiency test. By taking on

the skill test, the students learned the necessity of communicating and working together, which seems to have played a major role in improving their qualities as engineers [10]..As an instructor, we realized how difficult it is to teach an amateur student who has never used a lathe from scratch, and how difficult it is to find the right points in the flow of instruction.

In the future, we would like to make efforts to provide more efficient guidance and support to students who wish to take the skill proficiency test. We will pursue the following four items. Specifically, i) improve work process charts and check sheets, and effectively check and instruct students on processing skills using the PDCA cycle, ii) film processing work and use videos Easy-to-understand explanations for beginners, analysis of students' skills, and safety education, iii) Efficient guidance for dealing with written exams, iv) Guidance that leads students to grow as engineers as human beings rather than results. In addition, we are planning to extend the guidance to skill proficiency tests in the fields of electrical/electronic and mechatronics in the PBL subjects, in addition to the mechanical technology test [11,12].

7. References

[1] Hajime NAKAMURA and Kenichi TAKANO (2014), A study of the policy for the expect skill succession, *Journal of Social Technology Research*, Vol.11, pp82-95.

[2] Minoru Hoshino, Akito Katou, Ikuya Hasegawa, Ryouhei Hasegawa, Kazushige Matsumoto and Kohei Tsubota (2015), Project Type Production System through Club Activities, *TRANSACTIONS OF JASVET, VOL. 31, NO. 1 2015*, pp32-41.

[3] Tochigi Vocational Ability Development Association (2022), http://www.tochi-vada.or.jp

[4] Masanori TAKANO, Yoichi SHIRASAWA, Ybshihisa INOUII, Makoto INOHARA and Toshiaki FURUSAWA (2006), *Tochigi block lecture of the Japan Society of Mechanical Engineers*, pp123-124,2006.

[5] Takefumi Oku, Norio Irikura (2015), Quantitative Evaluation and Decomposition of Lathe Skill Learning Process between Skill Elements, *TRANSACTIONS OF JASVET, VOL. 31, NO. 1* 2015, pp68-73.

[6] Yusaku NAGANO and Yoshihiro HIDAKA (2014), Current Conditions and Challenges Affecting Training of Highly Skilled Technical High School Students～Focus on the Japanese Mechatronics Youth Skills Competition～, *TRANSACTIONS OF JASVET, VOL. 30, NO. 1 2014*, pp35-41.

[7] Yoshihiro Hidaka and Yuusaku Nagano (2016), A Basic Study of Learning Effect of Highly Skilled in Technical High School- Focusing on the Japanese ‘Mechatronics’ Youth Skills Competition -, *TRANSACTIONS OF JASVET, VOL. 32, NO. 1 2016*, pp107-111.

[8] Minami TAMAKAKE, Keita HIRAYAMA, Yuki ARAI, and Yuichi HASUDA (2019), Design and Production of the Robot for National Skills in Japan and Participation in the Competition, *International Conference on Education, Economics, Psychology and Social Studies（ICEEPS2019）*,pp.93-200.

4th International Symposium on Engineering and Technology Innovation（ISBENS2023）

[9] Yukiko Hattori , Daichi Takahashi , Yuki Arai and Yuichi Hasuda (2019), Design and Production of the Robot for WRO International Competition, *International Conference on Education, Economics, Psychology and Social Studies（ICEEPS2019）*,pp.209-217.

[10] Kazuhachi Okui and Tsuyoshi Ouchi (2014), Human resource development using skill competitions -Improving Skills by Utilizing the Youth Manufacturing Competition-, *Abstracts of the 27th Kyushu Branch Conference of the Japan Society of Technology Education*, pp.69-70 (2014).

[11] N.Hoshino & Y.Arai & Y.Hasuda (2018),Investigation of the Accuracy of the Sensors used for Educational Robots and Effective Exemplification of the Use, *Annual Conference on Engineering and Applied Science 2018*, pp134-144.

[12] Y.Arai & K.Zamora & Y.Takagi & Y.Hasuda (2018),The Practice and Achievement of Creativity Education through Problem-Solving Classes, *Annual Conference on Engineering and Applied Science 2018*, pp148-152.

4th International Symposium on Engineering and Technology Innovation（ISBENS）委員会の承認を得て掲載

8th International Scientific Conference on Engineering and Applied Sciences

Development of Teaching Materials on Autonomous Driving of robots using Deep Learning

Norito NIKI , Justin Lee , Koichi MURO, Yuta FUKUSHIMA and Yuichi HASUDA*
Department of Information and Electronic Engineering,
Teikyo University Tochigi prefecture Utsunomiya city
toyosatodai 1-1, Japan
* hasuda@ics.teikyo-u.ac.jp

Abstract

Automatic driving technology, where systems control cognitive processes, judgments, and operations performed by humans during driving, is rapidly becoming more prevalent and familiar to our world. The system drives automatically by analyzing the surrounding information collected by cameras and sensors. Deep learning is essential for collision avoidance and safe autonomous driving. In order for university students to experience these technologies in their lectures, it is necessary to introduce teaching materials on autonomous using simple models. In this study, we developed teaching materials on autonomous driving of robots using Deep Learning with AI, then verified its functionality in lectures and contests.

In this study, we tried to develop teaching materials on autonomous driving of robots using Deep Learning. Using Raspberry Pi 4 as the controller and implementing Deep Learning programming with Python, the prototype teaching material was able to recognize and avoid the two types of obstacles used while driving through the obstacle course. The prototype was able to accurately recognize the randomly placed obstacles on the 3m x 3m obstacle course and avoid them by turning left or right without making any contact with the obstacles.

Keywords: Deep Learning, Autonomous Driving ,Teaching Material, AI, robots

1. Introduction

Automatic driving technology, where systems control cognitive processes, judgments, and operations performed by humans during driving, is rapidly becoming more prevalent and familiar to our world[1.2]. The system drives automatically by analyzing the surrounding information collected by cameras and sensors. [3-5] · In Japan, under the guidance of the Ministry of Economy, Trade, and Industry, the three major car manufacturers, Toyota, Nissan, and Honda conducted public road demonstrations and experiments showcasing their autonomous driving technologies back in 2013. Deep learning is essential for collision avoidance and safe autonomous driving. In order for university students to experience these

technologies in their lectures, it is necessary to introduce teaching materials on autonomous using simple models. Therefore, in this study, we developed teaching materials on autonomous driving of robots using Deep Learning with AI, then verified its functionality in lectures and contests.

2. Prototype of Autonomous Driving Model teaching material using myRIO

Figure 1 shows the prototype of the robot used as teaching material. The design incorporates a steering mechanism on the front wheels and involves analyzing images sent from the camera located at the front of the robot to the myRIO controller. The ultimate objective is for the robot to identify the shapes and colors of the obstacles, enabling the robot to avoid them autonomously. [6] (Refer to Figure 2). Ultrasonic sensors are installed on both sides of the vehicle's main frame to prevent collisions with walls.

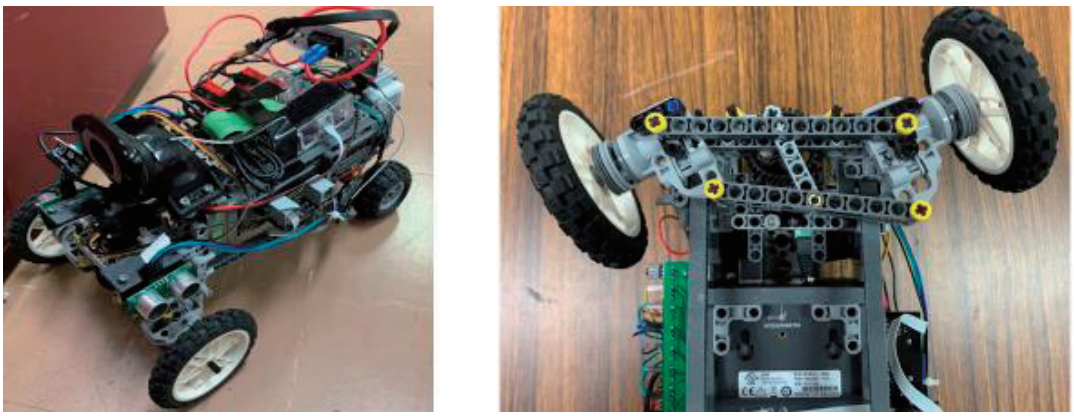

(a) Overview of the model car (b) Steering of the model car

Fig.1: Overview of the model car and the steering installed on the front wheels

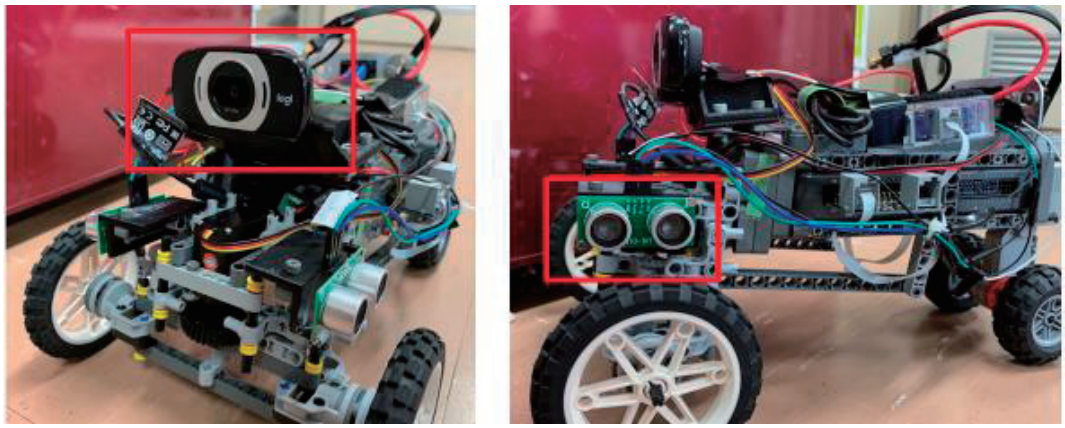

(a) Camera in front of the model car (b) Ultrasonic sensor on the side

Fig.2: Camera and Ultrasonic sensor installed to the model car

As shown in Figure 3, the obstacle models are square columns with dimensions of 50mm width, 50mm length, and 100mm height, in green and red. Images of these obstacles were pre-trained and programmed using LabVIEW to avoids obstacles by turning left when encountering a green obstacle and turning right when encountering a red obstacle[7] (Refer to Figure 4).

The prototype teaching materials were able to recognize and avoid two types of obstacles using Deep Learning while driving through the obstacle course. The robot was able to recognize obstacles and avoid collisions using both myRIO and LabVIEW, albeit at a low speed[8]. However, the production cost of a single unit amounted to approximately 200,000yen, which is relatively high. The vehicle weight also exceeded 2.5kg. We concluded that it is necessary to supply the teaching materials inexpensively.

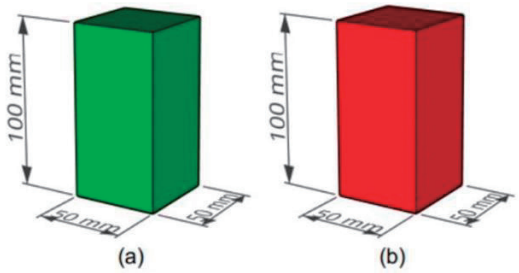

Fig.3: The two types of obstacle models used on the course

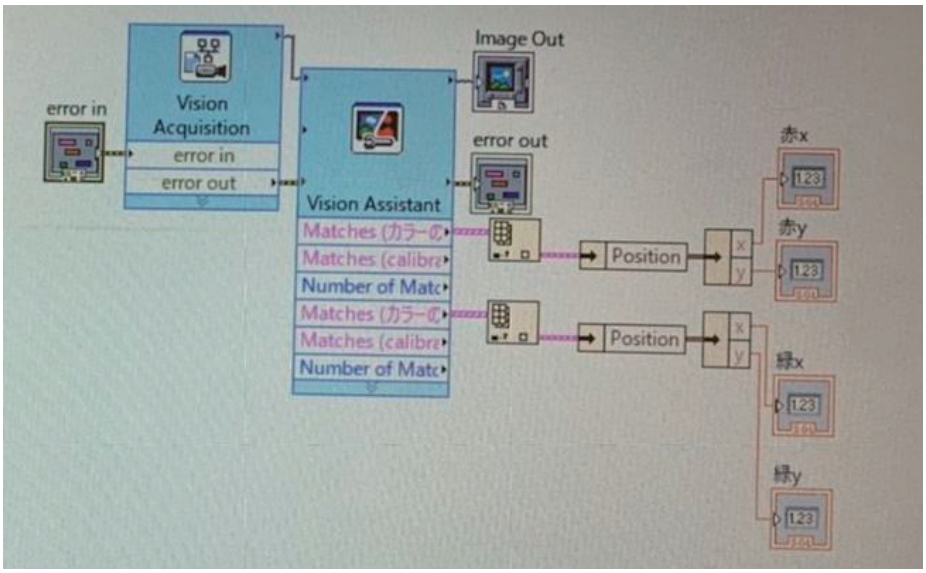

Fig.4: LabVIEW used in programs

3. Development of Teaching materials on Autonomous Driving Robot using RaspberyyPi4

3.1 Overview of the Autonomous Driving robot

In order to reduce the overall production cost of the teaching material, Raspberry Pi 4 was used as the controller (Refer to Figure 5). The Raspberry Pi 4 analyzes the images sent from the camera at the front of the robot. Based on the analysis, the Raspberry Pi 4 determines the positions and colors of the obstacles and enables the robot to avoid them according to their characteristics. This approach allows for cost reduction while maintaining the functionality required for obstacle avoidance.

By using Raspberry Pi 4 as the controller and optimizing the design, it was possible to reduce the production cost for one unit to approximately 30,000 yen, which is a cost reduction of about six times compared to the original prototype. The motor and steering are also reduced to two. Furthermore, instead of attaching ultrasonic sensors to both sides of the car's body, only one is attached at the left side of the car to prevent collisions with walls. The weight of the robot has been reduced from myRIO-type' s 2.5kg to 0.8kg, which is less than one-third of the original weight.

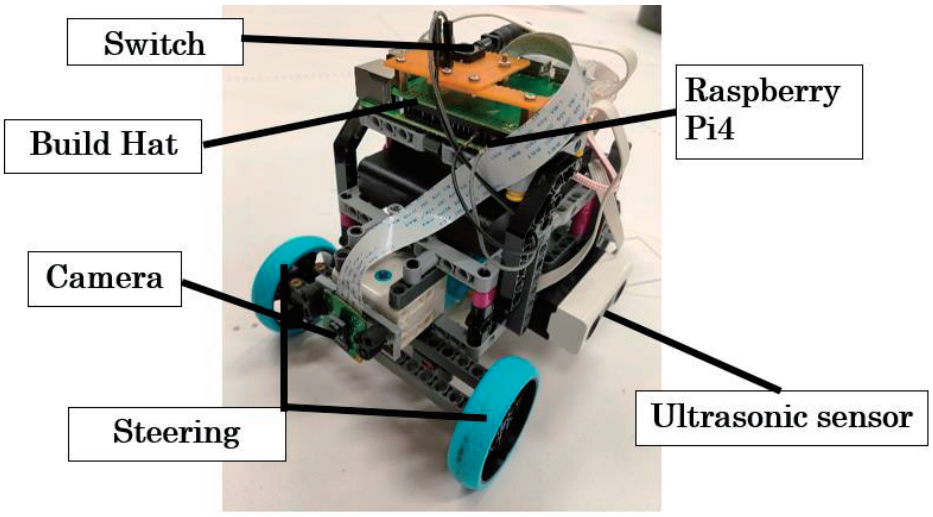

Fig.5: Autonomous driving robot teaching material

3.2 Formula and Equation

By using OpenCV, the robot was pre-trained using the obstacle model shown in Figure 3. The robot is programmed to avoid obstacles by turning left when encountering a green obstacle and turning right when encountering a red obstacle. The image recognition program was created using Python's OpenCV to process the images sent from the camera. The robot was able to obtain information about the obstacles by performing binary thresholding on the

image with red and green colors. Figure 6 shows the program for binary thresholding.

```
def binary_threshold(frame, color='red'):
    hsv = cv2.cvtColor(frame, cv2.COLOR_BGR2HSV)
    if color == 'red':
        lower_red = np.array(lower_R)
        upper_red = np.array(upper_R)
        lower_red2 = np.array(lower_R2)
        upper_red2 = np.array(upper_R2)

        mask1 = cv2.inRange(hsv, lower_red, upper_red)
        mask2 = cv2.inRange(hsv, lower_red2, upper_red2)

        mask = mask1 + mask2
    else:  # green
        lower_green = np.array(lower_G)
        upper_green = np.array(upper_G)
        mask = cv2.inRange(hsv, lower_green, upper_green)

    return mask
```

Fig.6: Program for binary thresholding

When binary thresholding is being performed, noise due to light reflection, which could hinder the process. Therefore, additional processing to remove objects within a certain area is added (Figure 7).

```
def remove_small_objects(mask, min_size):
    num_labels, labels, stats, _ = cv2.connectedComponentsWithStats(mask, connectivity=8)
    for i in range(1, num_labels):
        if stats[i][-1] < min_size:
            mask[labels == i] = 0
    return mask
```

Fig.7: Program to remove small area

The object's center coordinates, area, and minimum value of Y-axis is calculated from the binary threshold image. It is possible for multiple contours to exist within the image. Therefore, information is obtained from the object with the largest area from the binary threshold image (Figure 8).

```
def get_largest_object_center(mask):
    contours, _ = cv2.findContours(mask, cv2.RETR_EXTERNAL,
                                   cv2.CHAIN_APPROX_SIMPLE)
    bottom_most = (0, 0)
    if contours:
        l_contour = max(contours, key=cv2.contourArea)
        moments = cv2.moments(l_contour)
        if moments['m00'] != 0:
            center = int(moments['m10'] / moments['m00']),
            int(moments['m01'] / moments['m00'])
        else:
            center = (160,0)
        max_area = cv2.contourArea(l_contour)
        # get the bottom most point
        bottom_most = tuple(l_contour[l_contour[:,:,1].argmax()][0])
    else:
        center = (160, 0)
        max_area = 0
    return center, max_area, bottom_most
```

Fig.8: Program to obtain the object's information

4. Deep Learning program

GoogleColaboratory, a cloud-based platform was used for the AI training process. Images and data of the objects are sent to the PC from Raspberry Pi 4 to create the training model. Figure 9 shows the system diagram for image analysis and autonomous driving.

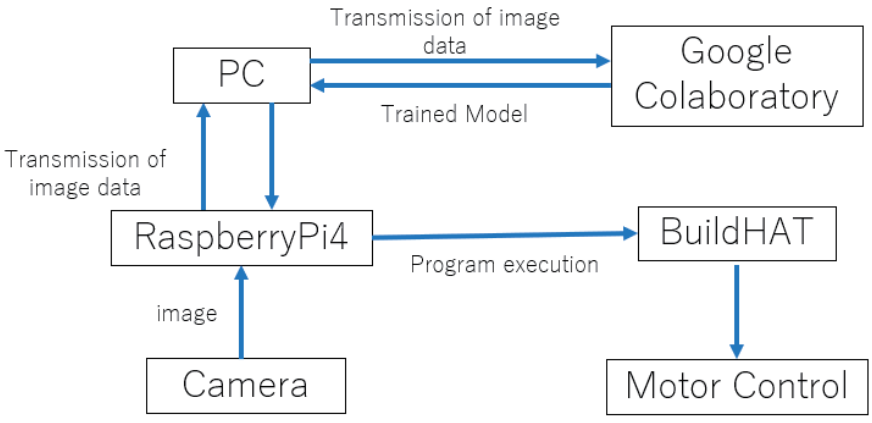

Fig.9: System diagram of image analysis and autonomous driving

In Deep Learning, it is necessary to adjust the parameters such as dropout rate, learning rate, weight decay, mini-batch size, and number of epochs before starting the training process. Figure 10 shows the configuration values used for the training process and results obtained from the process.

Dropout rate	0.5
Learning rate	0.01
Weight decay	0.000001
Mini-batch size	64
Number of epochs	100

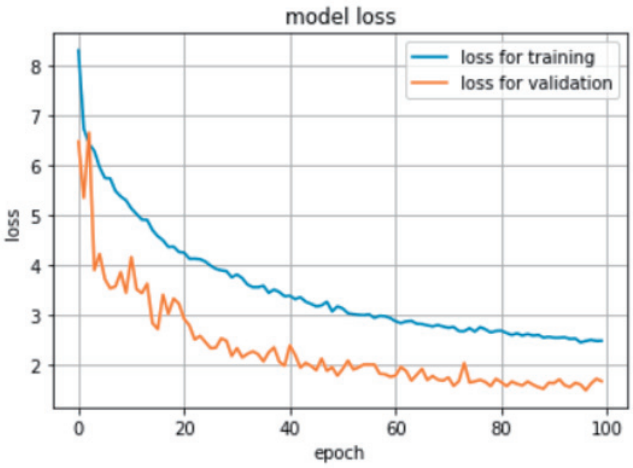

(a) Configuration values　　(b) Leaning result

Fig.10: Deep Learning results

The horizontal axis of the graph represents the number of training iteration, while the vertical axis represents the error between the predicted values generated by the training model and the actual values. As the number of training iterations increases, the data error decreases, allowing for the development of a more accurate training model.

5. Conclusion

In this study, we tried to develop teaching materials on autonomous driving of robots using Deep Learning. Using Raspberry Pi 4 as the controller and implementing Deep Learning programming with Python, the prototype teaching material was able to recognize and avoid the two types of obstacles used while driving through the obstacle course. The prototype was able to accurately recognize the randomly placed obstacles on the 3m x 3m obstacle course and avoid them by turning left or right without making any contact with the obstacles.

In the future, we aim to enhance the capabilities of the robot to include features such as parking assistance, detecting potential dangers and slowing down or stopping accordingly and implementing automatic deceleration before collisions. The goal is to improve the robot to a level where it can be practically introduced and used in educational settings in lectures.

6. References

[1] Daisuke FUJIMOTO (2019) ,A security on the Sensing process, Institute of Electronics, Information and Communication Engineers (IEICE), Fundamental reviews Vol.13,No.2,pp.142-150.

[2] Adrian Zlocki, Julian Bock, Lutz Eckstein (2017), Database of relevant traffic scenarios for highly automated vehicles, Autonomous vehicle Test & Development symposium, 2017

[3] Kishikawa, Arai (2019), Ensuring the safely of autonomous driving through inverse Deep Learning. The 33rd Annual Conference of the Japanese Society for Artificial Intelligence 2019, pp.1-4.

[4] Sugimoto, Uchida, Kurashige (2021), Evaluation of Indoor Mobile Robot Path Planning Algorithm Using Deep Reinforcement Learning, Journal of Industrial Application Engineering Society Vol. 9, No. 2, pp. 118-124.

[5] Hiroaki Agatsuma, Current Status and Issues of Driver Assistance and Autonomous Driving Technology Using Artificial Intelligence, Instrumentation and Control, Vol.54, No.11, November 2015, pp.808-815.

[6] Yukiko HATTORI, Daichi TAKAHASHI, Yuki ARAI, and Yuichi HASUDA (2019),esign and Production of the Robot for WRO International Competition, International Conference on Education, Economics, Psychology and Social Studies (ICEEPS2019) 209-217.

[7] Yuichi Hasuda, Keita Hirayama (2021), Development and Usability Test of Pesticide Spraying Robot for Greenhouse,International Journal of Engineering Research & Technology (IJERT) 10(5) 116-121.

[8] Yuichi Hasuda, Keigo Ozaki(2022), The Pesticide Spraying Robot Moving in A Greenhouse with A Line-Trace, International Journal of Engineering Research & Technology (IJERT) 11(1) 304-307.

8th International Scientific Conference on Engineering and Applied Sciences 委員会の承認を得て掲載

4th International Symposium on Engineering and Technology Innovation（ISBENS2023）

Development of a robot that wipes and sanitizes handrails in medical facilities

Justin Lee[a,*], Kosuke SUGAYA[b], Koichi MURO[b], Yuta FUKUSHIMA[b],Yuichi HASUDA[b,*]

[a] Department of Information and Electronic Engineering, Teikyo University, Malaysia

* justinrenyilee@gmail.com

[b] Department of Information and Electronic Engineering, Teikyo University, Japan

* hasuda@ics.teikyo-u.ac.jp

Abstract

Handrails at public places have been one of the objects that help spread COVID-19. Touching handrails alone does not lead to virus contraction. However, if people touch their faces or eyes, without washing their hands between them, they are at high risk of contracting the virus. This therefore highlights the importance of sanitizing handrails, especially in hospitals or medical facilities, where sick or elderly people often visit. Our study aims to help sanitize handrails in medical facilities, by creating an autonomous mobile robot that can sanitize handrails efficiently while minimizing the cost of production. We want to make sure that the handrails are always sanitized even when humans are too occupied to sanitize them.

The sanitizing robot has several components, including a brush to sanitize the handrails along with a container supplying alcohol-based disinfectant to the brush, magnetic sensors for navigation, NFC tags for location verification, and a camera for real-time tracking. By reading the NFC tags, users are able to access a screen displaying the robot's current location along with the footage of the camera through a smartphone or computer. The robot was able to sanitize a handrail that had been marked by a non-permanent marker without leaving any stains. We equipped our robot with brushes to sanitize handrails instead of spraying disinfectants or UV sterilizations. This is because spraying disinfectants when someone is nearby, especially children, is very dangerous if the disinfectant enters their eyes, while UV sterilizations might harm the human body and is very costly. By introducing our robot, we hope we are able to reduce healthcare worker's burden and ensure cleanliness of medical facilities.

Keywords: virus contraction, autonomous mobile robot, sanitizing robot, handrail

1. Introduction

Due to the global spread of COVID-19, cases of infections and death are still occurring even to this day [1], and measures to prevent further spread of COVID-19 are being reconsidered by medical institutions and research facilities across the world [2,3]. It is important to maintain a hygienic environment in places where elderly people and people with underlying health conditions often visit, such as hospitals or care facilities. Handrails, in particular, are very likely

to become a medium to spread COVID-19 as they are frequently held by countless people every day. The virus can survive on hard surfaces such as plastic and stainless steel for up to 72 hours, if not sanitized properly [4]. Therefore, regular sanitizing of handrails is necessary [3]. In hospitals where patients have contracted COVID-19, healthcare workers require protective suits, most commonly PPE (Personal Protective Equipment) to protect themselves while working, which is quite troublesome and time consuming. Besides, due to the cluster infection, the number of available healthcare workers may decrease, which can affect regular tasks such as sanitizing handrails. Shortage of healthcare workers has become a major issue in the healthcare industry because healthcare workers themselves are also getting infected by COVID-19 [5-7]. Hospitals are becoming overcrowded because of the lack of hospital beds, and are unable to allocate healthcare workers to properly carry out sanitization throughout the hospital. Therefore, the need to develop robots that are able to sanitize the environment automatically in place of healthcare workers has become necessary.

Various companies have been developing robots for sanitization [8-11], but the robots are only able to spray the disinfectant instead of a wiping mechanism [12-14]. It is dangerous for the robot to spray the disinfectant especially when the disinfectant is highly flammable, just like alcohol-based disinfectants. In this study, we have devised a robot that sanitizes handrails by wiping them with alcohol-based disinfectant. We aim to reduce the burden of healthcare workers by designing a robot that is able to patrol while sanitizing handrails.

2. Development of the sanitizing robot

2.1 Overview of the sanitizing robot

Figure 1 shows the robot that we have developed. The robot is 870mm tall, 260mm long and 250mm wide. The upper part of the robot consists of the sanitizing brush and the DC motor. We also use omni wheels so that the robot will be able to move freely across hospital hallways. We also used aluminum alloy to ensure the robot's structural components are light and rigid for sanitizing. We have installed an ESP32 microcontroller to control the movement of the DC motor and the sanitizing brush. ESP32 is capable of connecting to Wi-Fi, so we can pinpoint the robot's exact location in the hospitals by reading IC tags installed in the hallways.

The sanitizing brush installed at the upper part of the robot grip and wipe the handrails. The container filled with sanitizing alcohol is installed in the center of the robot. The alcohol inside the container is supplied to the brush through a hose by pumping air into the container [14]. It is necessary to design the brushes used for sanitizing to fit the shape of the handrails because there are different shapes and types of handrails used by various hospitals. Therefore, we used a 3D printer to create designs that are not only made up of lightweight materials but can fit the size and shape of the handrails. The sanitizing brush has 10 holes in it, allowing the brushes to be soaked by the alcohol pumped through the hose from the alcohol container to sanitize the handrails (Refer to Figure 2).

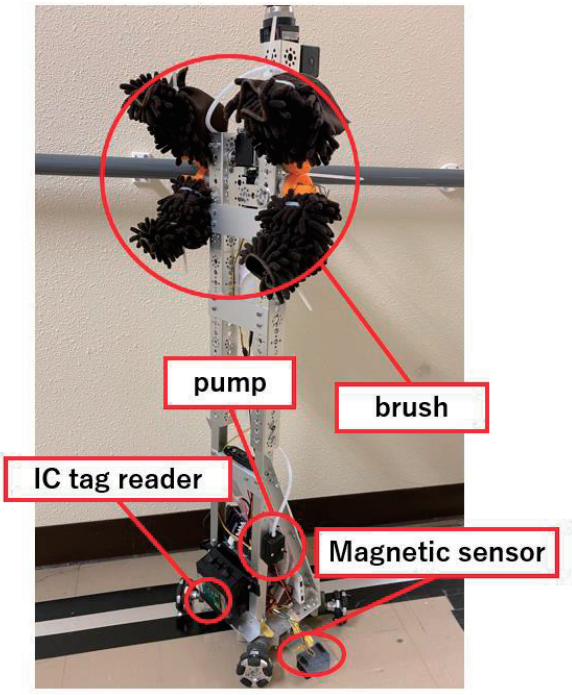

Figure 1: The sanitizing robot

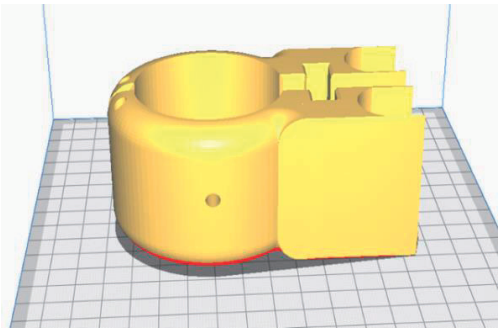

Figure 2: Design of the sanitizing brush

2.2 Movement around the hospital hallways

The robot must move precisely along the handrails to sanitize them efficiently. To make sure the robot is able to move precisely even in areas where handrails are intermittent such as bathrooms, we have placed magnetic tapes directly under the handrails so that the robot is able to move accordingly by line tracing. In hospitals, white tiles are commonly used to maintain cleanliness, so using light sensors for navigation can be problematic due to changes in floor color and light reflection, which can affect line tracing. Therefore, through the combination of magnetic tape (Refer to Figure 3) and magnetic sensors, the robot is able to navigate through the hallways regardless of floor color or time of day.

The magnetic sensors might not be able to recognize the magnetic field if there is a distance of more than 3mm between the magnetic sensor and the magnetic tape. To address this issue, we designed a mechanism to maintain proper distance between the magnetic sensor and the floor by placing springs to allow the sensor to move up and down to accommodate uneven surfaces (Refer to Figure 4). We also used the 3D printer to design a mount for the magnetic sensor so that we can fix the sensor onto the robot.

Figure 3: Magnetic tapes on the floor

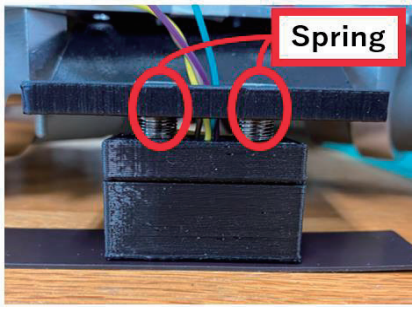

Figure 4: Sensor mount

2.3 Location verification system

As mentioned previously, it is necessary to accurately grasp the location of an autonomous mobile robot navigating through hospital hallways. Therefore, we have installed a Sony RC-S620/S NFC tag reader in front of the robot [10-12]. The robot is able to acquire and transmit its location by reading the NFC tags attached to the walls as shown in Figure 5. The medical staff are able to check the robot's current location while staying inside the reception or nurse station through this location verification system. As shown in Figure 6, by looking at the images captured by the camera attached to the robot, the medical staff are able to check the surroundings of the robot.

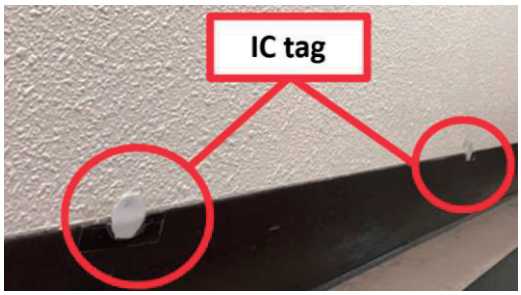

Figure 5: IC tags attached on the walls to pinpoint the robot's location

Figure 6: Display of the robot's current location

3. Software design of the sanitizing robot

3.1 Libraries and the programs used by the sanitizing robot

Figure 7 shows libraries of the servomotor used to control the robot's brush opening and closing, the DC motor for the robot's movement, and the NFC tag to track the robot's location. Table 1 shows the details of each library used.

Figure 7: Libraries and functions used

Table 1: Details of libraries

Library name	Details
PRIZM.h	TETRIX motor controller
Wire.h	connection with the motor controller
Servo.h	servomotor's control
RCS620.h	NFC tags' reading

We used Arduino to program the sanitizing robot's line tracing and turning movements. Line tracing, turning and other actions are based on the values obtained from the magnetic sensor and the NFC tag reader. Since the two magnetic sensors return values when they detect magnetic fields, if one of the sensors does not return a value, the robot will correct its direction. The NFC tags will not have the same number because they are assigned unique numbers of their own. Therefore, NFC tags are attached onto the walls of places where turning is required, such as the bathrooms and patient rooms. We can then check whether the number on the tag matches the predetermined number using the NFC tag reader.

3.2 Program of the location verification system

Figure 8 shows the transmission system of how the sanitizing robot sends the information of its location to its users. We can obtain the information on the robot's location by reading the NFC tags attached to the walls. The information obtained is then sent to the HTTP server in Raspberry Pi through ESP32. Users are then able to access the robot's location through smartphones or laptops by accessing a specified address[10-12]. We used P5.js, a JavaScript library specialized in animation to create animation on the robot's location screen on the web. We also created an Arduino program for sending and receiving the robot's location, and another program to display the web page.

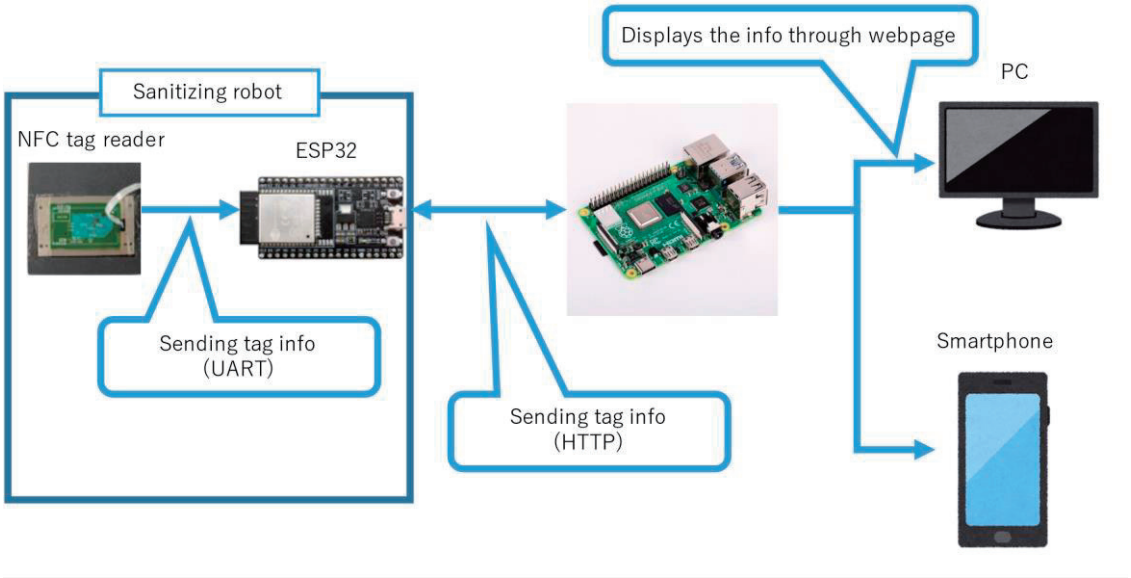

Figure 8: Details of the sending and receiving of the robot's location information

3.3 Experimental demonstrations

As shown in Figure 9, a circular handrail with an outer diameter of 32mm has been fixed at a height of 80mm in the hallway of our university to create a similar environment to that of a hospital or nursing facility. The robot is placed on the floor facing the handrail, and by reading a specified IC tag, the robot moves towards the magnetic tape attached to the floor directly under the handrail, then stops at a position suitable to start sanitizing the handrail. The brush opens up, and once the brush grips the handrail, the saniziting alcohol is pumped from the alcohol container. The brush and the handrail is soaked by the alcohol through holes in the inner part, then the robot moves along the handrail to begin saniziting the handrail. Afterwards, the robot continues to wipe and sanitize the handrail as it moves along the handrail (following the direction of the arrow), as shown in Figure 10.

During the sanitizing process, the robot reads a tag that indicates it is near a door, and issues an audio or visual warning to people in the room to alert them of its presence. This allows the

robot to avoid contact with people and mvoe safely along the hallways[2,8,10]. By reading IC tags while sanitizing handrails, the robot can turn and face the other handrail on the opposite side, autonomously performing a series of tasks without stopping. We used a non-permanent marker and marked the handrail, then observed if the robot was able to wipe and sanitize the handrail (Refer to Figure 11). We can confirm that the robot was able to clean the dirty handrail without leaving any stain (Refer to Figure 11(b)).

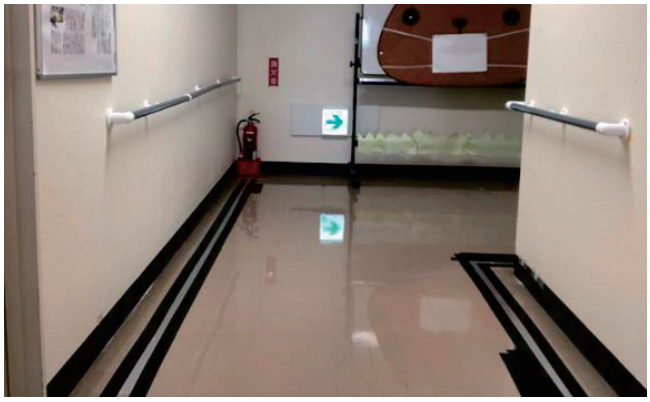

Figure 9: Handrails installed at the hallway

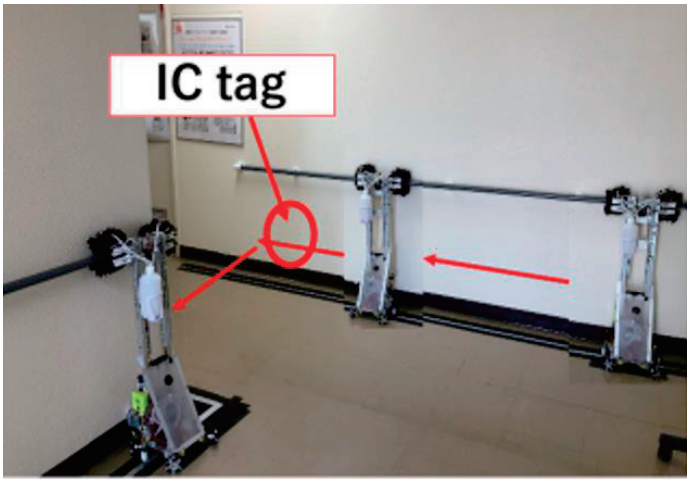

Figure 10: Movement of the robot saniziting the handrail

(a) Before sanitizing　　(b) After sanitizing

Figure 11: Verification of sanitization

4. Discussions and future prospects

In hospitals and nursing facilities, it is very important to maintain a hygienic environment because there are many elderly people and people with underlying medical conditions. This especially applies to handrails as they are frequently held by a large number of people every day, therefore becoming a medium to spread infectious disease. In this study, we have devised a system in which a robot wipes and sanitizes handrails with an alcohol-based sanitizer. Conventional sanitizing robots are usually unable to sanitize the inner handrails facing the wall. Ultraviolet light is also another method of sterilization [8-12,15], but this requires long exposure towards the targeted area, therefore takes a very long time for extensive sterilization [16]. Moreover, UV sterilization affects the human body negatively [3], so the time of usage is limited. However, while there are a few issues with using UV light for sanitizing, there are advantages of using it. For example, no power source or mechanism is required to spray volatile liquid, which helps lower the cost of sanitization and makes it easier to function.

When it comes to practical use in hospitals and nursing facilities, it is necessary to reduce the size of the robot due to factors such as the width of the hallways and the need to navigate around corners. In this study, we sought to achieve that by using a printed circuit board to construct the circuits more efficiently. In order to construct the printed circuit boards, we designed the circuit diagram (refer to Figure 12), placement of the components using the open-source board CAD software, KiCad.

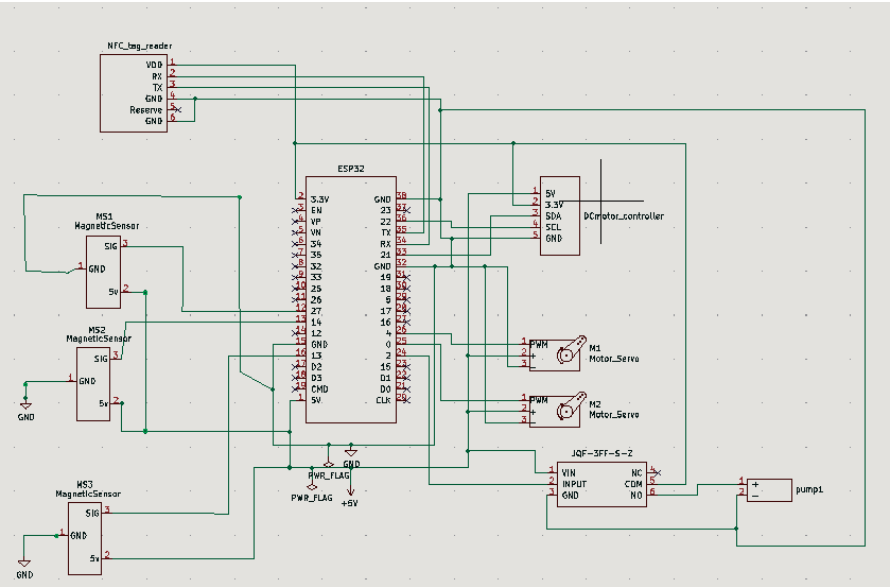

Figure 12: Circuit diagram

We aim to design a robot that autonomously patrols the hallways and sanitizes handrails, aiming to prevent the spread of infection and reduce the burden on healthcare workers. We have been working on practical applications by showing the robot and its videos to staff at

nearby hospitals,while gathering opinions from them. In the future, we plan to proceed with installations while considering factors such as individual rooms and bathrooms in actual facilities and bring it to the level where our robot can be practically implemented in medical institutions. Moreover, it is necessary to verify the effect of sanitization [9,11]. We plan to evaluate the sanitization effect by using the ATP swab test (A3 method), which is commonly used in medical facilities. Finally, a part of this research received the Chairman's Award, which is the highest award at the 2021 Invention and Innovation Contest for university students sponsored by The Japan Society of Technology Education and was presented at the 2022 Student and Corporate Research Presentation held in Tochigi Prefecture, Japan, where it received the "Kaname Creative Challenge Award".

5. References

[1] World Health Organization,Weekly Operational Update on COVID-19. Accessed: May 24 2021. [Online]. Available:https://www.who.int/publications/m/item/weekly-operational-updateon-covid-19—24-may-2021

[2] Akiko OGURA, Seiko NASU and Asako DOI, How Did the Nosocomial Outbreak of COVID-19 Occur, and How Was it Contained? Environmental Infection Record Vol. 36 no. 6, 2021, pp.307-314

[3] Ministry of Health, Labour and Welfare, Ministry of Economy, Trade and Industry, Consumer Affairs Agency special page, Sanitization methods for the novel coronavirus, https://www.mhlw.go.jp/stf/seisakunitsuite/ bu nya/syoudoku_00001.html,(Accessed: 3 November 2022)

[4] skynews, Coronavirus: How to avoid catching it - and whether you can touch handrails, https://news.sky.com/story/coronavirus-how-to-avoid-catching-it-and-whether-you-can-touch-handrails-11932158, (Accessed: 23 April 2022).

[5] Zhu N, Zhang D, Wang W, et al. A novel coronavirus from patients with pneumonia in China, 2019. N Engl J Med. 2020;382(8):727–33.

[6] Li Q, Guan X, Wu P, et al. Early Transmission Dynamics in Wuhan, China, of Novel Coronavirus-Infected Pneumonia. N Engl J Med. 2020;382(13):1199–207.

[7] Asahi Shimbun Cross-Search, (Novel coronavirus) Nabari Municipal Hospital suspends emergency admissions, infections increase, overnight rotations in the Iga region affecte/ Mie prefecture, https://www.asahi.com/articles/ASP1P76WGP1PIIPE00F.html, (Access: 2 December 2022)

[8] Yunzhou Fana, Yu Hua, Li Jianga, Qian Liua, Lijuan Xionga, Jing Panb, Wenlu Hub, Yao Cui, Tingting Chenb, Qiang Zhang, Intelligent disinfection robots assist medical institutions in controlling environmental surface disinfection, Intelligent Medicine 1 (2021) 19–23

[9] Pacharawan Chanprakon, Tapparat Sae-Oung,and W. Piyawattanametha, An Ultra-vi

olet sterilization robot for disinfection, 2019 5th International Conference on Engineering, Applied Sciences and Technology (ICEAST)

[10] Heeju Hong , WonKook Shin, Jieun Oh , SunWoo Lee , TaeYoung Kim , WooSub Lee, JongSuk Choi,SeungBeum Suh and KangGeon Kim, Standard for the Quantification of a Sterilization Effect Using an Artificial Intelligence Disinfection Robot, Sensors 2021, 21, 7776

[11] Akash Akolkar, Unmesh Supekar, Sourav Deshmukh, Pratiksha Dombale, Disinfection of Room using UV-C Sanitization Robot (UV-PAUS), International Journal of Science and Research (IJSR),pp.25-30.

[12] Aida Tatsuya, Wakai Hideki, Ito Yusuke, Hasegawa Mikio, Design and implementation of an unmanned sanitization system that reduces the cost of disinfectant by using an autonomous mobile robot, Report of the Institute of Electronics, Information and Communication Engineers(IEICE), vol. 121, no. 442, CCS2021-41, pp. 31-36, 2022.

[13] G Sundar raju, K Sivakumar, A Ramakrishnan, D Selvamuthukumaran and E Sakthivel Murugan5, Design and fabrication of sanitizer sprinkler robot for covid19 hospitals, Materials Science and Engineering, pp.1-7.

[14] Yu-Lin Zhao, Han-Pang Huang, Member, IEEE, Tse-Lun Chen, Pen-Chi Chiang, Yi-Hung Chen, Jiann-Horng Yeh, Chien-Hsien Huang, Ji-Fan Lin, and Wei-Ting Weng, A Smart Sterilization Robot System with Chlorine Dioxide for Spray Disinfection, IEEE SENSORS JOURNAL, VOL. 21, NO. 19, OCTOBER 1, 2021

[15] Sato Keiji, Introduction and operation of an ultraviolet irradiation robot that complements the accuracy of environmental disinfection in infection control, Newmed.co.jp 47(1), 108-113, 2020

[16] Copyright(c) nichiban Co., Ltd, Ministry of Health, Labour and Welfare sanitization test data,http://www.nb-nichiban.co.jp/sterilization_data/index.html,(Access: 2 December 2022)

編集後記

自動車技術センター年報 第２巻をお読みいただきありがとうございます。

センター発足から４年目であった2023年度も、多くの方々からのご協力をいただきながら、様々な活動を行うことができました。帝京大学学生への教育や県内企業への情報発信ができたのではないかと思います。中でも、NHK 解体キングダムの取材については大変貴重な経験であったと感じています。

最後になりますが、本書発刊に際してご協力いただいた皆様にお礼を申し上げます。そして今後ともよろしくお願いいたします。

（簾内 将景）

教員・スタッフ

センター長　加藤　彰　教授（理工学部 機械・精密システム工学科）
井上 秀明　教授（理工学部 機械・精密システム工学科）
黒沢 良夫　教授（理工学部 機械・精密システム工学科）
蓮田 裕一　教授（理工学部 情報電子工学科）
米田　洋　教授（理工学部 航空宇宙工学科）
牧田 匡史　准教授（理工学部 機械・精密システム工学科）
福田 直紀　助教（理工学部 機械・精密システム工学科）
小柳出 敏弘 助手（理工学部 機械・精密システム工学科）
白沢 洋一　助手（理工学部 機械・精密システム工学科）
簾内 将景　技術職員

帝京大学　自動車技術センター年報　第２巻

2024年8月30日発行

編集・発行　帝京大学自動車技術センター
〒320-8551　栃木県宇都宮市豊郷台1-1
帝京大学宇都宮キャンパス
電話　028-627-7010
Fax　028-627-7296
e-mail: autotech@teikyo-u.ac.jp
URL: https://www.teikyo-u.ac.jp/affiliate/laboratory/atc